Survey of Rotorcraft Navigation and Control

*Report No.*DU2SRI-2014-04-001

Jessica Alvarenga
Nikos I. Vitzilaios
Kimon P. Valavanis
Matthew J. Rutherford

April 2014

This work was supported in part by NSF CNS-1229236

Contents

This work was supported in part by NSF CNS-1229236

This work was supported in part by NSF CNS-1229236

NOMENCLATURE

Acronyms

ACAH	Attitude Command Attitude Hold
AHRS	Attitude Heading Reference System
DDP	Differential Dynamic Programming
DoF	Degrees of Freedom
NDI	Nonlinear Dynamic Inversion
EKF	Extended Kalman Filter
EOM	Equations of Motion
FLC	Fuzzy Logic Control
KF	Kalmn Filter
LTI	Linear Time Invariant
MAV	Micro-Aerial Vehicle
MIMO	Multi-Input Multi-Output
MLPID	Multi-Loop PID
MPC	Model Predictive Control
MTFC	Mamdani-Type Fuzzy Control
NLMPTC	nonlinear Model Predictive Tracking Control
NN	Neural Networks
PID	Proportional Integral Derivative
RCAH	Rate Command Attitude Hold
SISO	Single-Input Single-Output
TPP	Tip-Path Plane
UAS	Unmanned Aircraft System
UAV	Unmanned Aerial Vehicle
UKF	Unscented Kalman Filter

This work was supported in part by NSF CNS-1229236

Roman Symbols

P	Particle point mass
V	Volume
p^I	Inertial frame position vector
p^B	Body-fixed frame position vector
$d^P(t)$	Distance of particle from body center of mass
v^B	Translational velocity vector $[u\ v\ w]^T$
$\mathcal{F}_B = O_B,\ \vec{i}_B,\ \vec{j}_B,\ \vec{k}_B$	Body-fixed frame
$\mathcal{F}_I = O_I,\ \vec{i}_I,\ \vec{j}_I,\ \vec{k}_I$	Inertial frame
$\mathcal{F}_h = O_h,\ \vec{i}_h,\ \vec{j}_h,\ \vec{k}_h$	Main rotor hub frame
$Q = [q_0, q_1, q_2, q_3]$	Quaternion angle representation
$\vec{x}$	State vector
$\vec{y}$	Output vector
$\vec{u}_c$	Control input
p	Pitch rate, $\dot{\theta}$
q	Roll rate, $\dot{\phi}$
r	Yaw rate, $\dot{\psi}$
q_0	quaternion constant
q_i	quaternion parameters
R	Rotation matrix
g	Gravity
$\vec{f}$	Force vector $[X, Y, Z]$
m	Mass
F	Force
M^{CM}	Moments about the center of mass
G	Linear momentum
H^{CM}	Angular momentum
J_{xx}	Moment of inertia
J_{xy}	Product of inertia
J	Inertia matrix
$\mathcal{I}$	Inertia tensor

This work was supported in part by NSF CNS-1229236

a_0	Main rotor collective pitch
a_1	Longitudinal tilt of main rotor blade
b_1	Lateral tilt of main rotor blade
c_1	Longitudinal tilt of stabilizer blade
d_1	Lateral tilt of stabilizer blade
R_b	Main rotor blade length
c_b	Blade chord
$C_{l\alpha}$	Main rotor blade lift coefficient
C_D	Main rotor blade drag coefficient
u_i	Inflow velocity
U	Total air velocity on blade
U_T	U component $\parallel$ to the hub plane and $\perp$ to the blade
U_P	U component $\perp$ to the hub plane downward
U_R	U component radially outward from the blade
V_∞	Free stream velocity
N_{mb}	Number of main rotor blades
N_{tb}	Number of tail rotor blades
c_θ	$cos\theta$
s_θ	$sin\theta$
t_θ	$tan\theta$

This work was supported in part by NSF CNS-1229236

Greek Symbols

Θ	Attitude vector $\Theta = [\theta, \phi, \psi]$
ω	Angular rate vector $[p, q, r]$
υ	velocity
θ	Pitch angle
ϕ	Roll angle
ψ	Yaw angle
ψ_b	Blade azimuth angle, $\psi_b = \Omega t$
Ω	Blade angular velocity
τ	Moment vector $[L, M, N]$
$\lambda_i, i = 1, 2, 3$	Inflow dynamics
δ_{col}	Main rotor collective input
δ_{ped}	Tail rotor collective input
δ_{lat}	Lateral cyclic angle
δ_{lon}	Longitudinal cyclic angle
β	Blade flapping angle
ξ	Blade lead-lag angle
ζ	Blade pitch/feathering
ϕ_b	Inflow angle
α	Blade angle of attack
Θ_p	Blade pitch angle
α_{hb}	Blade α with respect to hub plane
α_b	Blade α with respect to U
ρ	Density
ρ_a	Air density

Sub- and Super-scripts

$\square^{CM}$	Center of mass
$\square^{p}$	Refers to a point
$\square_{N}$	Inertial navigation reference frame
$\square_{B}$	Body-fixed frame

Mathematical Operators and Symbols

$S(\cdot)$	Skew symmetric matrix
$\square^T$	Matrix transpose
$\square^{-1}$	Matrix inverse
$\square^{-T}$	Matrix inverse transpose
$\dot{\square}$	Time derivative
$\perp$	Perpendicular
$\parallel$	Parallel
$\times$	Cross-product
$\hat{x}$	Skew-symmetric matrix

This work was supported in part by NSF CNS-1229236

1 Introduction

Over the past decades, there has been an increasing interest in Unmanned Aircraft Systems (UAS) with autonomous capabilities for use in military and civilian applications. UAS include two basic vehicle configurations, fixed-wing unmanned aerial vehicles (UAVs) and rotorcraft[1] UAVs (RUAVs). Each type has its advantages and disadvantages, as well as specific applications. Fixed-wing UAVs are ideal for long flight and high payload applications. However, rotorcraft UAVs have the advantage of hovering capability, lending them to applications including, but not limited to, aerial surveillance, search and rescue, and reconnaissance in environments and terrain unreachable by fixed-wing UAVs.

Potential applications of RUAVs have grown to include further involvement in law enforcement, coast and border surveillance, road traffic monitoring, disaster and crisis management, agriculture and forestry, as well as search and rescue operations [86]. The ability to deploy an unmanned vehicle eliminates danger to an onboard human pilot as the craft may operate in dangerous situations or environments. For example, the ability of the rotorcraft to maneuver through complex terrain quickly would allow for several small-scale, unmanned helicopters fitted with state of the art vision systems to be deployed for search and location of lost hikers or campers. The rotorcraft would be capable of searching a larger area than a rescue group could. It could then return location information of the lost individuals to a base station.

A large amount of research has been performed and is ongoing in the area of unmanned aircraft systems, especially rotorcraft. Various rotorcraft platforms have been explored, most notably and popular being traditional main and tail rotor configuration helicopters, quadrotor vehicles, and micro air vehicles (MAVs).

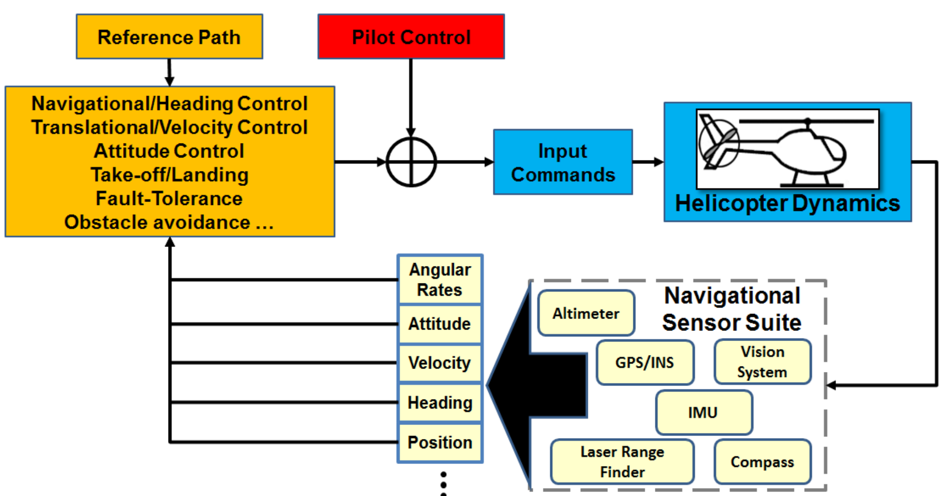

Figure 1: Typical helicopter control flow.

[1]In this report, rotorcraft, unmanned rotorcraft, unmanned helicopters or helicopter refer to the same thing.

This work was supported in part by NSF CNS-1229236

Several surveys on advances in RUAV systems [86], [137], [148], [194] have been published exploring the work done in the area of guidance, navigation, control, and perception techniques. These include work from over 25 institutions around the globe engaging in RUAV research. These surveys include vehicle platforms, control techniques, flight control system (FCS) design, vision systems, visual perception techniques, and includes a wide range of vehicles. However, very little detail is provided on the control architectures and navigation/control techniques themselves.

In 2004, *"Control and perception techniques for aerial robotics"*, [137],focusing mostly on perception techniques, reviewed various methods that have been applied to aerial robotics including different vehicle platforms, flight control hardware, and a very brief survey of control architectures and methods.

In 2008, *"A practical survey on the flight control system of small unmanned helicopter"*, [194], reviewed and compared a variety of control methodologies for unmanned helicopters, including linear, nonlinear, and model-free techniques. This survey provided diagrams of the control methodologies presented with some discussion of flight modes along with advantages and disadvantages of each approach.

In 2010, *"Autopilots for small unmanned aerial vehicles: a survey"*, [27], presented a survey of autopilot systems intended for use with small or micro UAVs. This survey focused heavily on the hardware involved in designing autopilots. There was no comparison of control methods presented.

In 2011, *Linear and nonlinear control of small-scale unmanned helicopters*, [148], presented a description of linear and nonlinear control techniques. Detailed models of both the nonlinear and linear dynamics of a small-scale helicopter were presented. A summary of control methodologies was also presented, giving details on the states used for modeling, vehicle platforms, and the application of the techniques.

In 2012, *"Survey of advances in guidance, navigation, and control of unmanned rotorcraft systems"*, [86], provided a detailed review of research involving RUAVs over the past 20 years, focusing on Guidance, Navigation and Control (GNC). The survey presented classifications of RUAVs, from full-scale optionally piloted helicopters down to MAVs. An in depth review was organized by institution, which included the class of vehicle platforms used, most recent research areas and projects, as well as major achievements and milestones. In addition, a characterization of levels of autonomy was presented, providing definitions and categorizations for levels of autonomy in GNC. A summary of advances in modeling and identification techniques was also provided. Flight control systems were classified into three main categories: linear, nonlinear, and learning-based controllers. A review of existing work was outlined, including the specific method (PID, $\mathcal{H}_\infty$, LQR, etc.), operating condition, and type of results, whether simulated or experimental. Little detail was provided on the exact structure of each approach or the states used and in the model design. This work focused on navigation systems, including hardware, vision techniques and algorithms, sensing technology, and work conducted with quadrotors and MAVs.

This work was supported in part by NSF CNS-1229236

1.1 Scope and Motivation

This research focuses on surveying existing control methods and modeling techniques with the objective of determining capabilities and effectiveness of algorithms for unmanned autonomous flight, navigation, obstacle avoidance, and performance of acrobatics. The surveyed control techniques can be fit into one of three categories: linear, nonlinear and model-free. After summarizing each controller, and its application, each control approach is categorized accordingly in the comparative table shown in Figure 2. The linear methods are divided into single-input single-output (SISO) methods and multi-input multi-ouput (MIMO) methods. Proportional-Integral-Derivative (PID) controllers fall under the SISO linear control category. MIMO linear controllers consist of linear feedback controllers, such as linear quadratic regulators (LQG) and linear quadratic Gaussian (LQG), $\mathcal{H}_\infty$ controllers, and gain scheduling controllers that may utilize synthesis techniques. Nonlinear methods are divided into linearized and fully nonlinear methods. Linearized techniques start with a nonlinear model, and utilize various techniques to linearize the system dynamics, including input/output feedback linearization. Other methods can then be applied, including adaptive control, model predictive control (MPC), and nested saturation loops. Lastly, backstepping control approaches utilize fully nonlinear models. Lastly, model free and learning-based methods include neural networks (NN), fuzzy logic, and human-based learning techniques. Human-based learning techniques include differential dynamic programming (DDP) and reinforcement learning.

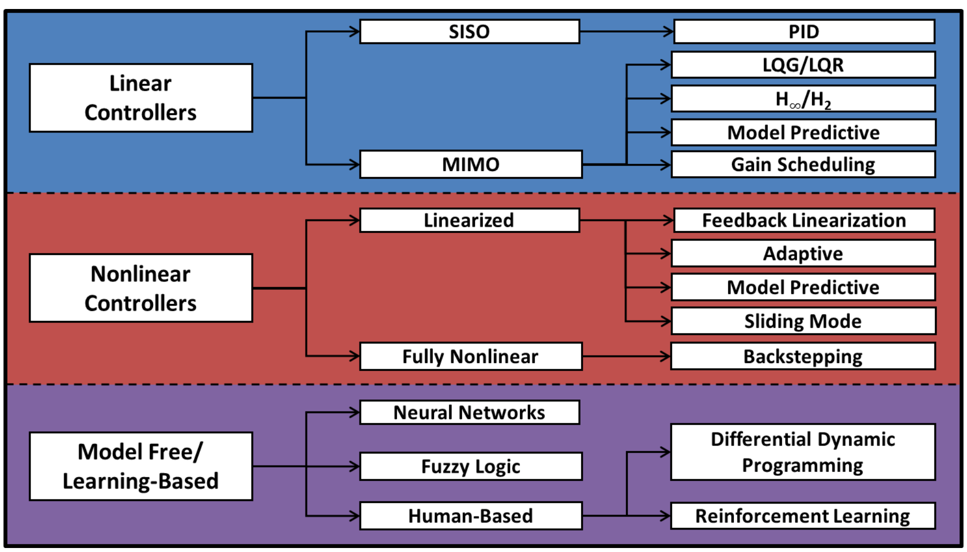

Figure 2: Control techniques

In order to provide the same reference point for comparison purposes, the following rationale is used:

- Helicopter model and platform
- Method of identification, including parameter estimation and system modeling

- Control technique and loop architecture
- Flight mode and maneuvers
- Types of results: theoretical, simulated, or experimental

2 Helicopter Dynamics

Rotorcraft have distinct advantages in maneuverability through the use of rotary blades. This design allows rotorcraft to produce the necessary aerodynamic thrust forces without the need of relative velocity. However, control of rotorcraft has inherent complications. These include the complexity of helicopter dynamics due to their heavy nonlinearity and significant dynamic coupling between the aerodynamic forces and moments. In addition to nonlinearity and dynamic coupling, helicopters are underactuated systems, since there are fewer control inputs than system states.

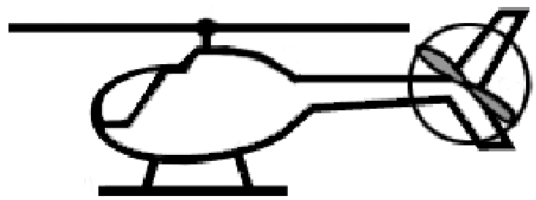

Figure 3: Basic helicopter configuration showing main and tail rotors.

Helicopter dynamics are generally governed by Six-Degrees-of-Freedom (6-DoF) rigid body kinematics and dynamics. The forces and moments that affect the vehicle dynamics are generated by the rotors, body, gravity and aerodynamics. These forces can be either controlled (e.g. rotor thrust) or uncontrolled (e.g. drag forces, wind gusts). The forces are modeled as functions of the vehicle states, pilot inputs, and environmental factors.

The modeling of aerodynamic forces is complicated and difficult. In order to achieve high-fidelity models of the aerodynamic properties of the vehicle, finite-element techniques are used. This, however, is time consuming and computationally complex. For the purposes of control design, the system may be divided into lumped-parameter models for each subsystem using simplified aerodynamics. With this method each subsystem of the helicopter is viewed separately in order to approximate the dynamics while considering certain assumptions. This approach can significantly reduce the state space of the system and the number of parameters describing its behavior. The most basic helicopter configuration consists of a single main rotor and tail rotor, as shown in Figure 3. In addition to the rotors, other helicopter components that affect the dynamics are typically lumped into the following subsystems for modeling purposes:

i Main rotor

ii Tail rotor

iii Fuselage body

iv Tail horizontal stabilizer (fin)

v Tail vertical stabilizer (fin)

vi Stabilizer or flybar

vii Engine

This work was supported in part by NSF CNS-1229236

viii Servo linkages and swashplate

ix Actuators or servos

Figure 4 depicts the typical structure of the helicopter dynamics. The forces and moments generated by each subsystem are determined and, then, combined into generalized forces and moments relative to a body-fixed coordinate system. These forces, ultimately, drive the helicopter's rigid body dynamics and kinematics equations, which ultimately define the helicopter dynamic model.

For navigational purposes, a fixed reference coordinate system is established. This is an Earth-fixed coordinate system defined by the designer of the navigational system, and fully dependent on where the vehicle will be operating. Typically, GPS (Global Positioning System) receivers are used for navigational feedback.

2.1 Helicopter Rigid Body Equations of Motion

For a 6-DoF rigid body, the motion of the helicopter is defined relative to an inertial reference frame in order for Newtonian mechanics to hold true. An inertial reference frame follows Newton's first law of motion, where an object is either at rest or moves at a constant velocity unless acted on by some external force. However, establishing a reference frame fixed to the helicopter body significantly simplifies the analysis of forces acting on the helicopter. In order to derive a set of equations describing the motion of the helicopter two Cartesian reference frames are established.

The first reference frame is chosen fixed to the helicopter body. In a body-fixed Cartesian frame, $\mathcal{F}_B = \{O_B, \vec{i}_B, \vec{j}_B, \vec{k}_B\}$; the origin is fixed at the helicopter center of mass. In this frame, the unit vector $\vec{i}_b$ points from the origin outward toward the helicopter nose. The unit vector $\vec{j}_B$ points from the origin to the right of the fuselage. The unit vector $\vec{k}_b$ points downward. The orientation of these vectors in relation to the helicopter body is seen in Figure 5.

The second reference frame is an inertial Earth-fixed Cartesian frame, which follows the North-East-Down directional convention. In this Earth-fixed frame, $\mathcal{F}_I = \{O_I, \vec{i}_I, \vec{j}_I, \vec{k}_I\}$. The unit vectors $\vec{i}_I$, $\vec{j}_I$, and $\vec{k}_I$, point North, East and down towards the center of the Earth, respectively, as shown in Figure 6.

Rigid body dynamics are governed by the Newton-Euler laws of motion given in (1) and (2). These equations ultimately provide information on translational and angular velocities as a result of forces acting on the rigid body.

$$F_{net} = \frac{d}{dt} G(t), \tag{1}$$

$$M_{net}^{CM} = \frac{d}{dt} H^{CM}(t). \tag{2}$$

The net external forces, F_{net}, are defined as the rate of change of the body's linear momentum, $G(t)$. The net external moments about the body's center of mass, M_{net}^{CM}, are

This work was supported in part by NSF CNS-1229236

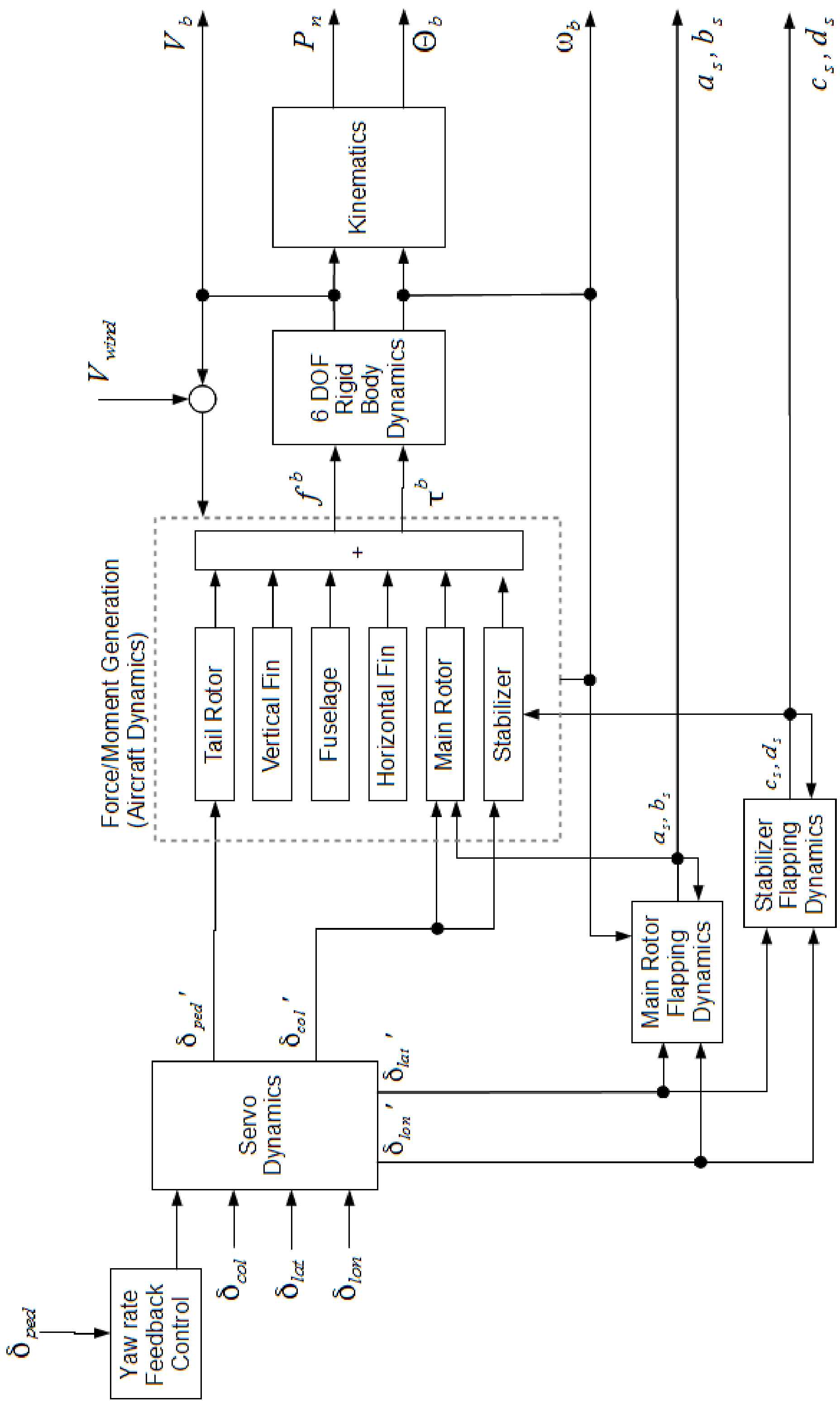

Figure 4: Helicopter dynamics.

This work was supported in part by NSF CNS-1229236

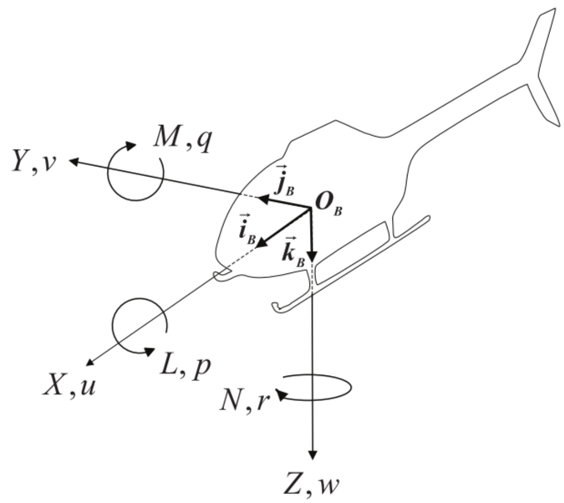

Figure 5: Body-fixed frame coordinate system, [148].

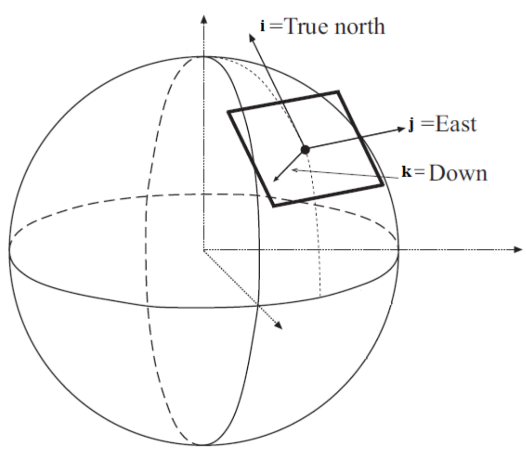

Figure 6: North-East-Down Earth-fixed reference frame, [41].

equal to the rate of change of angular momentum about the center of mass, H^{CM}. These moments are derived here for a rigid body following the procedure in [12].

For a point mass m with linear velocity v, the linear momentum is defined as:

$$G(t) = m(t)v(t). \tag{3}$$

The angular momentum of the point mass about a point is defined in (4), where d^P is the distance of the mass from the point.

$$H(t) = d(t) \times m(t)v(t). \tag{4}$$

For a rigid body, the linear momentum is defined as the sum of infinitesimal linear momentums of particles that make up an entire body. For each particle, the mass is defined as infinitesimally small, dm, for an infinitesimally small volume dV of density ρ. The total linear momentum is summed for each particle over the volume of the object:

$$G = \int_V vdm, \text{ where } dm = \rho dV. \tag{5}$$

The total angular momentum of the mass about some point is defined as a sum of infinitesimal angular momentums of particles:

$$H = \int_V d \times vdm. \tag{6}$$

The position of a particle P relative to the inertial reference frame, p_I^P is given as:

$$p_I^P(t) = p_I^{CM} + R(t)d_B^P \tag{7}$$

where p_I^{CM} is the position of the helicopter center of mass with respect to the inertial frame, $R(t)$ is a rotation matrix between the body-fixed frame and inertial frame, and d_B^P is the distance of the particle from the center of mass with respect to the body-fixed frame.

The translational velocity of the particle relative to the inertial reference frame is obtained through differentiation of (7) and is given as:

$$v_I^P(t) = v_I^{CM}(t) + \dot{R}(t)d_B^P \tag{8}$$

where v_I^{CM} is the translational velocity of the helicopter center of mass relative to the inertial reference frame. The linear momentum is found by evaluating the integral over the volume of the body:

$$G_I(t) = \int_V (v_I^{CM}(t) + \dot{R}(t)d_B^P)dm = v_I^{CM}(t)\int_V dm + \dot{R}(t)\int d_B^P dm. \tag{9}$$

The center of mass of an object is defined as:

$$\bar{d}^{CM} = \frac{1}{m}\int_V d^P dm. \tag{10}$$

Typically, the body-fixed frame origin is defined at the helicopter's center of mass. Since the center of mass from the body-frame origin coincides with the body-fixed frame origin, $\bar{d}_B^{CM} = 0$. By equating this with (10) and assuming mass is non-zero, then:

This work was supported in part by NSF CNS-1229236

$$\int_V d_B^P dm = 0. \tag{11}$$

Additionally, the total mass m is found through integration of the infinitesimal point masses over the entire volume of the body and is given as $m = \int_V dm$. Using these simplifications the final linear momentum equation becomes:

$$G_I(t) = mv_I^{CM}(t). \tag{12}$$

Next, using (8) the angular momentum about the helicopter's center of mass with respect to the inertial frame origin is evaluated as:

$$H_I^{CM}(t) = \int_V \{d_I^P(t) \times v_I^{CM}(t)\}dm + \int_V \{d_I^P(t) \times \dot{R}(t)d_B^P\}dm. \tag{13}$$

Here, d_I^P is the distance to the point from the center of mass with respect to the inertial reference frame. This distance may be defined with respect to the body-fixed frame as $d_I^P = R(t)d_B^P$, and is substituted into (13) as:

$$H_I^{CM}(t) = \int_V \{R(t)d_B^P \times v_I^{CM}(t)\}dm + \int_V \{R(t)d_B^P \times \dot{R}(t)d_B^P\}dm. \tag{14}$$

In order to further simplify the angular momentum equation, the following properties are used. First, the properties of cross products are defined as follows:

$$a \times b = -b \times a \tag{15}$$

$$\int \vec{u} \times \vec{v}dx = \vec{u} \times \int \vec{v}dx = (\int \vec{u}dx) \times \vec{v} \tag{16}$$

$$(Ax) \times (Ay) = (detA)\, A^{-T}\, (x \times y) \tag{17}$$

where for a 3×3 rotation matrix A, $det\ A = 1$ and $A^{-T} = A$. Second, the rigid body rotational kinematics, [170], are introduced and given as:

$$\dot{R}(t) = R(t)\hat{\omega}_B(t) \tag{18}$$

where $\hat{\omega}(t)$ is the skew-symmetric matrix of the angular velocity vector, $\omega(t)$, such that:

$$\hat{x} = \begin{bmatrix} 0 & -x_3 & x_2 \\ x_3 & 0 & -x_1 \\ -x_2 & x_1 & 0 \end{bmatrix}, \text{for } x = \begin{bmatrix} x_1 \\ x_2 \\ x_3 \end{bmatrix}^T, \tag{19}$$

$$x \times y = \hat{x}y, \tag{20}$$

$$x, y \in \mathbb{R}^3. \tag{21}$$

These assumptions in (15) – (17), (18), and (19) – (21) and the equality in (11) reduce the angular momentum in (14) to:

$$H_I^{CM} = \int_V R(t)\left[d_B^P \times \hat{\omega}_B(t)d_B^P\right]dm = \int_V R(t)\hat{d}_B^P\hat{\omega}_B(t)d_B^P dm. \tag{22}$$

This work was supported in part by NSF CNS-1229236

By defining $d_B^P = [x\ y\ z]^T$ and $\omega_B(t) = [p\ q\ r]^T$ it can be shown that $\hat{d}_B^P \times \hat{\omega}_B(t) d_B^P = \mathcal{I}\omega_B$, as shown in [12], where $\mathcal{I}$ is the inertial tensor of the rigid body. The inertia matrix for the rigid body is defined as $J = \int_v \mathcal{I} dm$. The final angular momentum is then given as:

$$H_I^C M(t) = R(t) \int_V \mathcal{I}\omega_B dm = R(t) J \omega_b(t). \tag{23}$$

The net external moments and forces in terms of the linear moments and angular momentum simplifications described in (12) and (23) are then applied to the Newton-Euler equations in (1) and (2) to find the forces and moments acting on the body with respect to the inertial frame and are given as follows:

$$F_I(t) = m \dot{v}_I^{CM}(t), \tag{24}$$

$$M_I^{CM} = \dot{R(t)} J \omega_B(t) + R(t) J \dot{\omega}_B(t). \tag{25}$$

Finally, the forces and moments can be expressed in the body-fixed frame following the procedure in [12] as:

$$F_B(t) = m \left(\omega_B(t) \times v_B^{CM}(t) + \dot{v}_B^{CM} \right), \tag{26}$$

$$M_B^{CM} = \omega_B \times J \omega_B(t) + J \dot{\omega}_B(t). \tag{27}$$

The helicopter equations of motion described in (26) and (27) are known as the Newton-Euler equations of motion for a rigid body, where $f_B = F_B^{CM}$ and $\tau^B = M_B^{CM}$, and are given below as:

$$\begin{bmatrix} mI_3 & 0 \\ 0 & \mathcal{J} \end{bmatrix} \begin{bmatrix} \dot{v}_B \\ \dot{\omega}^B \end{bmatrix} + \begin{bmatrix} \omega^B \times m v^B \\ \omega^B \times \mathcal{J} \omega^B \end{bmatrix} = \begin{bmatrix} f^B \\ \tau^B \end{bmatrix}. \tag{28}$$

The forces, moments, and translational velocity may be separated into components corresponding to each of the principal axes of the body-fixed frame as $f^B = [X\ Y\ Z]^T$, $\tau^B = [L\ M\ N]^T$, and $v_B^{CM} = [u\ v\ w]^T$, respectively. Transforming the gravity vector from the inertial frame, $g_I = [0\ 0\ g]^T$, to body-frame results in $g_B = R^T(t) g_I$, where:

$$R = \begin{bmatrix} R_{11} & R_{12} & R_{13} \\ R_{21} & R_{22} & R_{23} \\ R_{31} & R_{32} & R_{33} \end{bmatrix}. \tag{29}$$

The equations of motion with respect to the body-fixed frame are given as:

$$\begin{cases} \dot{u} = rv - qw + R_{31} g + X/m \\ \dot{v} = pw - ru + R_{32} g + Y/m \\ \dot{w} = qu - pv + R_{33} g + Z/m \\ \dot{p} = qr(J_{yy} - J_{zz})/J_{xx} + L/J_{xx} \\ \dot{q} = pr(J_{zz} - J_{xx})/J_{yy} + M/J_{yy} \\ \dot{r} = qp(J_{xx} - J_{yy})/J_{zz} + N/J_{zz} \end{cases} \tag{30}$$

This work was supported in part by NSF CNS-1229236

2.2 Position and Orientation Dynamics

For flight navigation, it is necessary to express the position and orientation of the helicopter with respect to an Earth-fixed inertial reference frame. To do so, a relationship between the body-fixed and inertial frames must be established in order to provide a method of describing the orientation of the frames relative to one another. This relationship is called the *rotation matrix* R that represents a series of rotations from the body-fixed frame to the final orientation of the inertial frame, [34, 170]. The rotation matrix is is typically expressed in terms of roll (ϕ), pitch (θ), and yaw (ψ) Euler angles. These rotations must occur in a specific sequence, . The first rotation moves the helicopter an angle of ϕ about the $\hat{k}$ axis, as seen in Figure 7. The second rotation moves the helicopter an angle of θ about the new $\hat{j}$ axis, as seen in Figure 8. Finally, the last rotation moves the helicopter an angle of ψ about the new helicopter $\hat{\imath}$ axis, as seen in Figure 9.

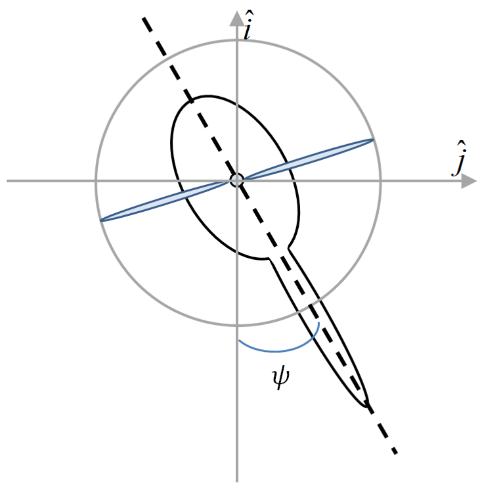

Figure 7: Helicopter yaw motion.

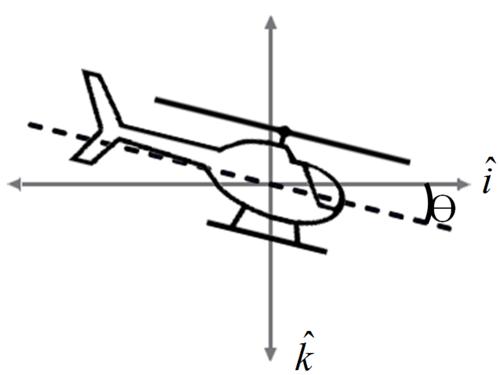

Figure 8: Helicopter longitudinal motions.

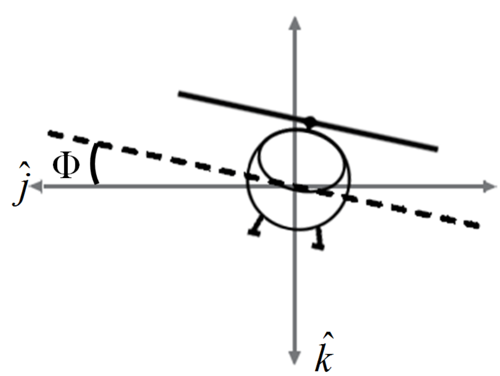

Figure 9: Helicopter lateral motions.

The final rotation matrix is obtained by multiplying the individual rotation matrices in (31) following the properties of transformations in [170]. This final rotation is given as

$R = R_\psi R_\theta R_\phi$ and is expanded in terms of Euler angles below as:

$$R_\psi = \begin{bmatrix} \cos\psi & \sin\psi & 0 \\ -\sin\psi & \cos\psi & 0 \\ 0 & 0 & 1 \end{bmatrix} \quad R_\theta = \begin{bmatrix} \cos\theta & 0 & -\sin\theta \\ 0 & 1 & 0 \\ \sin\theta & 0 & \cos\theta \end{bmatrix} \quad R_\phi = \begin{bmatrix} 1 & 0 & 0 \\ 0 & \cos\phi & \sin\phi \\ 0 & -\sin\phi & \cos\phi \end{bmatrix} \tag{31}$$

$$R(\Theta) = \begin{bmatrix} \cos\psi\cos\theta & \cos\psi\sin\phi\sin\theta - \cos\phi\sin\psi & \sin\phi\sin\psi + \cos\phi\cos\psi\sin\theta \\ \cos\theta\sin\psi & \cos\phi\cos\psi + \sin\phi\sin\psi\sin\theta & \cos\phi\sin\psi\sin\theta - \cos\psi\sin\phi \\ -\sin\theta & \cos\theta\sin\phi & \cos\phi\cos\theta \end{bmatrix} \tag{32}$$

In order to determine the orientation dynamics, the time derivative of the rotation matrix is determined and is given in Equation 33. The proof may be seen in [170]:

$$\dot{R} = R\hat{\omega}_B \tag{33}$$

Next, the time derivative of the rotation matrix in (32), and the relationship in (33), are used to find the orientation dynamics of the helicopter, given in Equations 34 and 35. Details on these derivations can be found in [132, 148, 170, 64]. Here, the Euler angles are denoted by $\Theta = [\phi\ \theta\ \psi]^T$:

$$\dot{\Theta} = \begin{bmatrix} \dot{\phi} \\ \dot{\theta} \\ \dot{\psi} \end{bmatrix} = \Psi(\Theta)\omega^B \tag{34}$$

$$\Psi(\Theta) = \begin{bmatrix} 1 & \sin\phi\tan\theta & \cos\phi\tan\theta \\ 0 & \cos\phi & -\sin\phi \\ 0 & \sin\phi/\cos\theta & \cos\phi/\cos\theta \end{bmatrix} \tag{35}$$

The position and velocity dynamics together with the orientation dynamics form the complete helicopter equations of motion in terms of the helicopter's body-fixed frame forces and moments and are given in below as:

$$\begin{cases} \dot{p}^I = v^I \\ \dot{v}^I = \frac{1}{m}Rf^B \\ \dot{R} = R\hat{\omega}^B \\ I\dot{\omega}^B = -\omega^B \times (I\omega^B) + \tau^B \end{cases} \tag{36}$$

Here p^I and v^I denote the position and linear velocity of the helicopter center of gravity (CG) with respect to an earth-fixed reference frame. The position and orientation trajectory dynamics may be obtained by integrating the rigid body dynamics in (30) along through

This work was supported in part by NSF CNS-1229236

the kinematic equations in (36). The inertial position can be found given the body velocities through $\dot{p}^I = v_I = Rv^B$. The euler rates can be found through the relationship $\dot{\Theta} = \Omega(\Theta)\omega_b$ in (34):

$$\dot{x}^I = c_\theta c_\psi u + (s_\theta s_\phi c_\psi - c_\phi s_\psi)v + (s_\theta c_\phi c_\psi + s_\phi s_\psi)w \tag{37}$$

$$\dot{y}^I = c_\theta c_\psi u + (c_\phi c_\psi + s_\phi s_\psi s_\theta)v + (c_\theta s_\psi s_\theta - c_\psi s_\phi)w \tag{38}$$

$$\dot{z}^I = -s_\theta u + c_\theta s_\phi v + c_\phi c_\theta x \tag{39}$$

$$\dot{\phi} = p + s_\phi t_\theta q + c_\phi t_\theta r \tag{40}$$

$$\dot{\theta} = c_\phi q - s_\phi r \tag{41}$$

$$\dot{\psi} = \frac{s_\phi}{c_\theta} q + \frac{c_\phi}{c_\theta} r \tag{42}$$

2.3 Forces and Torques

A result of the main and tail rotor rotation is the generation of thrust and torques acting on the helicopter body. Gravity is also acting on the body of the helicopter, and must be taken into account while determining the total body forces on the helicopter. The forces and torques acting on the helicopter are functions of the main rotor thrust, T_{MR}, tail rotor thrust, T_{TR}, and the main rotor cyclic angles, a_1 and b_1, [64].

2.3.1 Main Rotor Forces

The thrust generated by the main rotor results in a translational force on the helicopter. This thrust is perpendicular to the Tip-Path-Plane (TPP), Figure 10, which is the plane formed by the blade tips. This force vector can be decomposed into components along the body-frame x, y, and z axis. The magnitude of the thrust vector is represented as T_{MR}. The components of the main rotor forces as a result of the blade flapping and thrust are given as:

$$F^B_{MR} = \begin{bmatrix} X_{MR} \\ Y_{MR} \\ Z_{MR} \end{bmatrix} = \begin{bmatrix} -T_{MR} sin(a_1) \\ -T_{MR} sin(b_1) \\ -T_{MR} cos(a_1) cos(b_1) \end{bmatrix} \tag{43}$$

2.3.2 Tail Rotor Forces

Unlike the main rotor, the tail rotor generates a force perpendicular to the rotor hub. The pilot has no control of the flapping angles. As a result, the resulting force component is in the y-direction only. The components of the tail rotor thrust are given in (44):

$$F^B_{TR} = \begin{bmatrix} X_{TR} \\ Y_{TR} \\ Z_{TR} \end{bmatrix} = \begin{bmatrix} 0 \\ T_{TR} \\ 0 \end{bmatrix} \tag{44}$$

This work was supported in part by NSF CNS-1229236

2.3.3 Gravity

The gravitational force on the helicopter is represented in the inertial Earth-fixed frame in the downward direction. Thus, the gravity vector is given as $F_g^I = [0\ 0\ mg]^T$. This force may be expressed as components with respect to the body-fixed frame as given in (45), [12, 64, 102].

$$F_g^B = \begin{bmatrix} X_g \\ Y_g \\ Z_g \end{bmatrix} = R(\Theta)F_g^I = \begin{bmatrix} -sin(\theta)mg \\ sin(\phi)cos(\theta)mg \\ cos(\phi)cos(\theta)m]cdotg \end{bmatrix} \tag{45}$$

2.3.4 Torques

The torques acting on the body of the helicopter are a result of the forces being offset from the center of gravity. The relation below defines the relationship between the force (F), distance (d) and the resultant torque:

$$\tau = Fd \tag{46}$$

2.3.5 Main Rotor Torque

For the main rotor torque, the distance offset of the main rotor from the helicopter center of gravity is defined as $[l_m, y_m, h_m]^T$, [147]. The resulting torque contributed by the main rotor is given as:

$$\begin{bmatrix} L_{MR} \\ M_{MR} \\ N_{MR} \end{bmatrix} = \begin{bmatrix} Y_M R h_m - Z_{MR} y_m \\ -X_{MR} h_m - Z_{MR} l_m \\ X_{MR} y_m + Y_{MR} l_m \end{bmatrix} \tag{47}$$

2.3.6 Tail Rotor Torque

For the tail rotor torque, the distance offset of the tail rotor from the helicopter center of gravity is defined as $[l_t, 0, h_t]^T$. The resulting torque contributed by the main rotor is given by:

$$\begin{bmatrix} L_{TR} \\ M_{TR} \\ N_{TR} \end{bmatrix} = \begin{bmatrix} Y_{TR} h_t \\ 0 \\ -Y_{TR} l_t \end{bmatrix} \tag{48}$$

2.3.7 Main Rotor Drag

The main rotor generates an aerodynamic drag as it rotates. This drag results in a torque, Q_{MR}, [64, 93]. This torque is perpendicular to the TPP and it can be decomposed into components along the body frame by projecting the torque vector on to the hub plane. The resultant components are given as:

$$\begin{bmatrix} L_D \\ M_D \\ N_D \end{bmatrix} = \begin{bmatrix} Q_{MR} sin(a_1) \\ -Q_{MR} sin(b_1) \\ Q_{MR} cos(a_1) cos(b_1) \end{bmatrix} \tag{49}$$

2.4 Rotor

The helicopter receives most of its propulsive force from the main and tail rotors. The aerodynamics of the rotors, especially that of the main rotor, are highly nonlinear and complex. In order to reduce the complexity and simplify the dynamics for use in modeling and control design, a number of assumptions are considered, [12, 148, 29, 147] as follows:

- Rotor blades are rigid in both bending and torsion
- Small flapping angles
- Uniform inflow across rotor blade, no inflow dynamics used
- Effects of coning, due to flapping angles, is constant
- Forward velocity effect omitted
- Coupling ratio for pitch-flap is disregarded
- Constant rotor speed

The dynamics of the main and tail rotors are controlled by input control commands. However, they are also affected by the motion of the helicopter. These control commands are represented by $\vec{u}_c = [\delta_{lon}\ \delta_{lat}\ \delta_{ped}\ \delta_{col}]^T$. The thrust magnitudes of the main and tail rotors are controlled by the collective commands δ_{col} and δ_{ped}, respectively. The main rotor blade flapping dynamics is controlled by the cyclic inputs δ_{lon} and δ_{lat}, which control the tilt of the TPP. Control of the propulsive forces is achieved by controlling the direction and inclination of the TPP. Thrust produced by the rotor blades is perpendicular to the TPP.

The orientation of the TPP is dependent on main rotor blade flapping dynamics. During rotation, the blades exhibit a flapping motion, Figure 11, a lead-lagging motion, Figure 12 and a pitching motion of the blade, Figure 13. These motions make-up the rotor blade DoF and are denoted by β, ξ, and ζ, respectively.

2.4.1 Lift and Drag

The aerodynamic forces on the rotor blade depend on the 3-DoF orientation of the blade at any time. The blade's pitch angle, ζ, affects the lift and drag of the blade elements. The flapping angle of the blade affects the inertial forces on the blade along the direction

This work was supported in part by NSF CNS-1229236

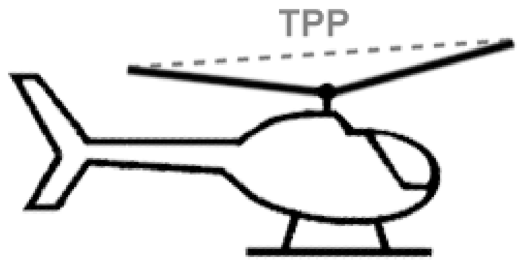

Figure 10: Helicopter Tip-Path-Plane (TPP).

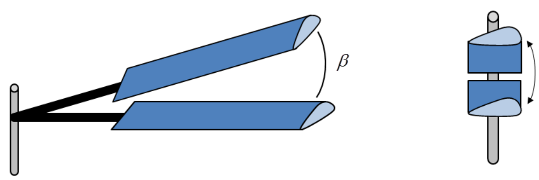

Figure 11: Helicopter blade flapping motion.

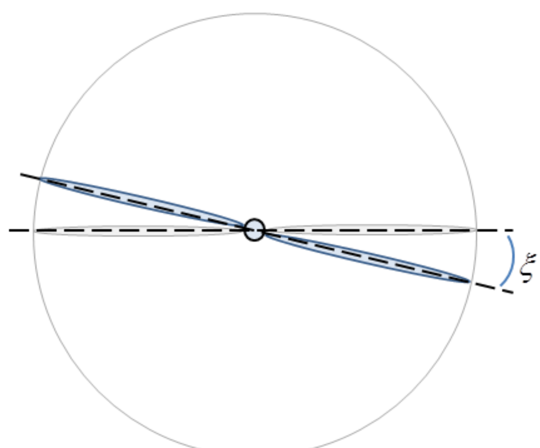

Figure 12: Helicopter blade lead-lagging motion.

This work was supported in part by NSF CNS-1229236

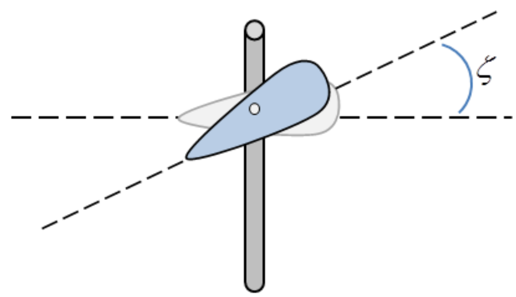

Figure 13: Helicopter blade pitching motion.

of the main rotor thrust vector. In determining the lift and drag generated by the main rotor requires consideration of the blade's flapping motion, ζ, helicopter forward velocity with respect to the air, also known as free stream velocity and denoted by V_∞, rotation of the blade about the shaft in the form of angular velocity, Ω, and also the inflow velocity of air through the rotor, [148]. This total air velocity on the blade, U, can be decomposed into three components. These components are defined in relation to the plane perpendicular to the rotor shaft, known as the hub plane. The plane hub frame is defined as $\mathcal{F}_h = O_h, \vec{i}_h, \vec{j}_h, \vec{k}_h$; where $\vec{i}_h$ points backwards towards the tail, $\vec{j}_h$ points to the right of the helicopter, and $\vec{k}_h$ points up. Two components are in the hub plane while the third is out of the plane. All three components are normal to the hub plane. The out of plane component is perpendicular to the hub plane pointing downward and is denoted by U_P, as seen in Figure 14(c). The next component, U_T, is parallel to the hub plane and tangential to the blade in the direction of the blade rotational motion as seen in Figure 14(a) and (d). The last component, U_R, lies on the hub plane and points radially pointing outward in the direction of and parallel to the blade, as seen in Figure 14(a) and (c). The total air velocity seen by the blade is given as:

$$U = \sqrt{U_T^2 + U_P^2}. \tag{50}$$

At any time during flight, the blade experiences a pitch angle, ζ, related to the angle of attack α_b of the blade with respect to the airstream U, which approaches the blade at an inflow angle ϕ_b. This relationship is given by (51), as seen in Figure 15:

$$\zeta = \alpha_b + \phi_b. \tag{51}$$

The U_T component is defined in terms of the blade angular velocity and the component of the free stream velocity in the direction parallel to the hub plane as:

$$U_T = \Omega r + V_\infty cos\alpha_{hb} sin\psi_b. \tag{52}$$

The U_P component is defined in terms of the main rotor flapping, the blade angular velocity,

This work was supported in part by NSF CNS-1229236

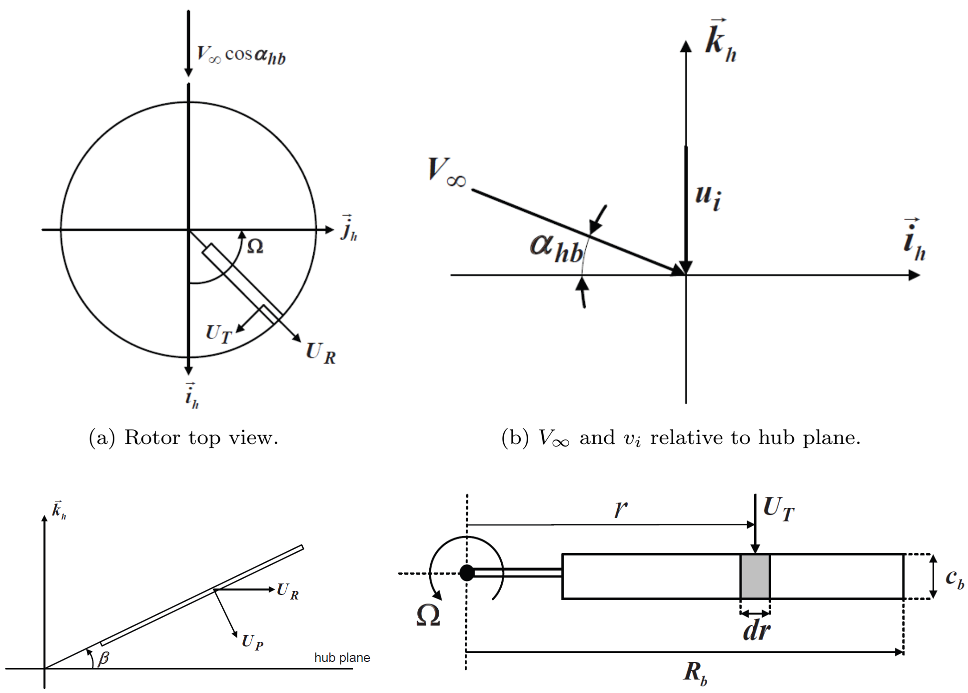

(a) Rotor top view.

(b) V_∞ and v_i relative to hub plane.

(c) Rotor side view.

(d) 2D blade element.

Figure 14: Air velocity components relative to the blade element. [148]

the free stream velocity component perpenticular to the blade, and the inflow velocity u_i, and is given as:

$$U_P = r\dot{\beta} + (V_\infty cos\alpha_{hb} sin\psi_b + \Omega r)sin\beta + V_\infty sin\alpha_{hb} cos\beta + u_i cos\beta \quad (53)$$
$$= r\dot{\beta} + V_\infty cos\alpha_{hb} sin\psi_b \beta + \Omega r\beta + V_\infty sin\alpha_{hb} + u_i. \quad (54)$$

It should be noted that here r represents the distance from the rotor shaft along the blade. It is not to be mistaken for the pitch angular rate.

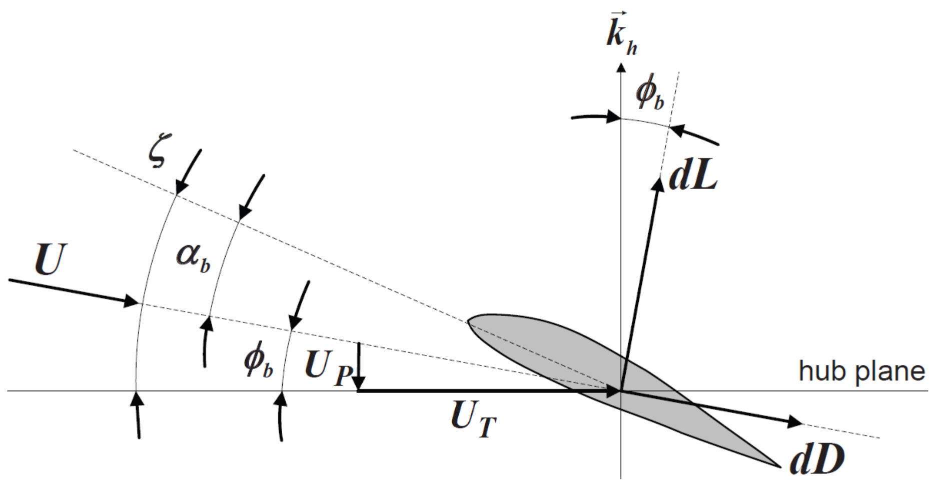

Figure 15: Helicopter blade cross-section. [148]

The lift and drag on the blade are determined through blade element analysis. By considering the blade as a two-dimensional airfoil, the lift and drag vectors at each blade element may be determined. The infinitesimal lift of the blade element dr is given as:

$$dL = 1/2\rho_a U^2 c_b C_{l\alpha} \alpha_b dr. \quad (55)$$

The infinitesimal drag of the blade element is given as:

$$dD = 1/2\rho_a U^2 c_b C_d dr. \quad (56)$$

Here, ρ_a is the air density, c_b is the blade chord, $C_{l\alpha}$ is the blade lift coefficient, C_D is the blade drag coefficient, and α_b is the blade angle of attack with respect to the air velocity U. The total lift and drag may then be derived by integrating along the distance of the blade, r, from the rotor to the end of the blade length, R_b.

The forces perpendicular and parallel to the hub plane can be expressed in terms of the lifting and drag forces. These are given in (57) and (58). Since it is assumed that the inflow angle is very small, $sin\phi_b \approx \phi_b$, $cos\phi_b \approx 1 - \frac{\phi^2}{2} \approx 1$, and $tan \approx \phi_b$. Then, the relationship between the inflow angle and the air stream velocity components, $tan\phi_b = \frac{U_P}{U_T}$, becomes $\phi_b = \frac{U_P}{U_T}$. The angle of attack can then be written as $\alpha_b = \zeta - \frac{U_P}{U_T} = \frac{\zeta U_T - U_P}{U_T}$. In addition to the small inflow angle, the rotor rotational speed is assumed to be high, making the

This work was supported in part by NSF CNS-1229236

perpendicular component of air stream significantly smaller than the tangential component, $U_T >> U_P$. This allows for simplification of the total air stream velocity to $U^2 = U_T^2$. In [12], it is stated that $C_{l\alpha}$ is usually much larger than C_D, so much so that the effect of drag in the perpendicular direction can be neglected.

Using these simplifications, the total force on the blades parallel ($F_{\|}$) and perpendicular ($F_{\perp}$) to the hub plane can be expressed in terms of the lift and drag forces as:

$$\begin{aligned} dF_{\|} &= dLsin\phi_b + dDcos\phi_b \approx \phi_b dL + dD \\ &= \frac{1}{2}\rho c_b C_{l\alpha}\alpha_b\phi_b U^2 dr + \frac{1}{2}\rho c_b C_D U^2 dr \\ &= \frac{1}{2}\rho c_b C_{l\alpha}\left(\zeta U_T U_P - U_P^2\right) dr + \frac{1}{2}\rho c_b C_D U_T^2 dr \end{aligned} \tag{57}$$

$$\begin{aligned} dF_{\perp} &= dLcos\phi_b - dDsin\phi_b \approx dL \\ &= \frac{1}{2}\rho c_b C_{l\alpha}\alpha_b U^2 dr \\ &= \frac{1}{2}\rho c_b C_{l\alpha}(\zeta U_T^2 - U_T U_P) dr \end{aligned} \tag{58}$$

Table 1: Lift and drag equations

Force parallel to the hub plane:
$dF_{\|} = \frac{1}{2}\rho c_b C_{l\alpha}\left(\zeta U_T U_P - U_P^2\right) dr + \frac{1}{2}\rho c_b C_D U_T^2 dr$
Force perpendicular to the hub plane:
$dF_{\perp} = \frac{1}{2}\rho c_b C_{l\alpha}(\zeta U_T^2 - U_T U_P) dr$
Lifting force of blade element:
$dL = 1/2\rho_a U^2 c_b C_{l\alpha}\alpha_b dr$
Drag force of blade element:
$dD = 1/2\rho_a U^2 c_b C_d dr$

2.4.2 Flapping Dynamics

The total pitch of the blade can be described as in (59), where ζ_0 is the collective pitch to control the thrust of the rotor and $\zeta_1 = A_{lon}\delta_{lon}$ and $\zeta_2 = B_{lat}\delta_{lat}$ are the linear functions of the pilot's lateral and longitudinal cyclic control stick inputs, respectively:

$$\zeta = \zeta_0 - \zeta_1 cos\psi_b - \zeta_2 sin\psi_b \tag{59}$$

As seen in Figure 16, the blade is modeled as a rigid thin plate rotating about the shaft at an anglar rate of Ω. The angular position of the blade in the hub plane is denoted as ψ_b measured from the tail axis. The blade flapping hinge is modeled as a torsional spring with stiffness K_β. The moments acting on the blade are due to the lifting force described in Section 2.4.1, weight of the blade (M_W), the inertial forces acting on the blade (M_i and M_c), and the restoring force of the spring (M_{K_β}). Equating all the moments acting on the blade results in (66). Substituting (61) – (65) into (66) results in (67), where the blade's inertia is given by:

$$\mathcal{I}_b = \int_0^{R_b} m_b r^2 dr \tag{60}$$

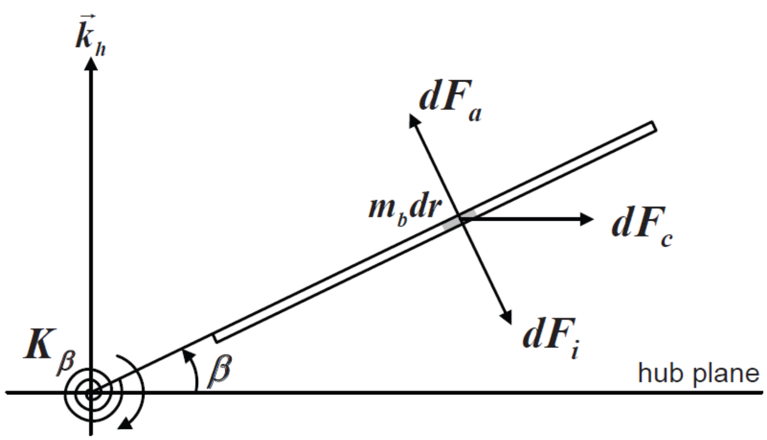

Figure 16: Blade spring model, [148].

$$M_W = \int_0^{R_b} m_b g r cos\beta dr = \frac{1}{2} m_b g R_b^2 \tag{61}$$

$$M_{K_\beta} = -K_\beta \beta \tag{62}$$

$$M_L = \int_0^{R_b} r dF_a dr = \frac{1}{2}\rho c_b C_{l\alpha} \int_0^{R_B} r(\zeta U_T^2 - U_T U_P) dr \tag{63}$$

$$M_c = \int_0^{R_b} r dF_c sin\beta = \int_0^{R_b} m_b \Omega^2 r^2 cos\beta sin\beta dr = \Omega^2 \beta \mathcal{I}_b \tag{64}$$

$$M_i = \int_0^{R_b} r dFi = \int_0^{R_b} m_b \ddot{\beta} r^2 dr = \ddot{\beta}\mathcal{I}_b \tag{65}$$

$$M_i + M_c + M_{K_\beta} + M_W = M_L \tag{66}$$

$$\ddot{\beta} + (\Omega^2 + \frac{K_\beta}{\mathcal{I}_b} + \frac{1}{2\mathcal{I}_b} m_b g R_b^2)\beta = \frac{1}{2\mathcal{I}_b}\rho c_b C_{l\alpha} \int_0^{R_B} r(\zeta U_T^2 - U_T U_P) dr \tag{67}$$

The flapping dynamics, $\beta(t)$ in (68), can be expressed as a Fourier series neglecting the higher order terms, only keeping the first order harmonics:

This work was supported in part by NSF CNS-1229236

$$\beta(t) = a_0 - a_1 cos\psi_b - b_1 sin\psi_b \tag{68}$$

Substituting (68), its first and second time derivatives, (54), and (52) into (67), the equations can then be written as a system of the form $\ddot{x} + D\dot{x} + Kx = F$. Here, the state vector $x = [a_0\ a_1\ b_1]^T$, the coning, longitudinal tilt, and lateral title angle of the TPP. The state space representation is given below in (69), where $x_1 = x$ and $x_2 = \dot{x}$:

$$\begin{bmatrix} \dot{x}_1 \\ \dot{x}_2 \end{bmatrix} = \begin{bmatrix} 0 & I \\ -K & -D \end{bmatrix} \begin{bmatrix} x_1 \\ x_2 \end{bmatrix} \tag{69}$$

The TPP dynamics are simplified, [12, 148], by assuming a constant coning angle, disregarding the hinge offset, assuming a zero pitch-flap coupling ratio, and disregarding the effects of forward velocity. The simplified dynamics are given in (70) for the longitudinal dynamics and (71) for the lateral dynamics.

$$\tau_f \dot{a} = -a - \tau_f q + A_b b + A_{lon}\delta_{lon} \tag{70}$$

$$\tau_f \dot{b} = -b - \tau_f p + B_b a + B_{lat}\delta_{lat} \tag{71}$$

Here, the time rotor constant, τ_f, is a function of the angular velocity, Ω, and the Lock number, γ.

$$\tau_f = \frac{16}{\gamma\Omega} \tag{72}$$

$$\gamma = \frac{\rho_a C_{l\alpha} R_b^4}{\mathcal{I}_b} \tag{73}$$

Additionally, A_b and B_a are the rotor cross coupling terms:

$$A_b = -B_a = \frac{8}{\gamma}(\lambda_b^2 - 1) \tag{74}$$

and λ_β is the flapping frequency ratio:

$$\lambda_\beta^2 = \frac{K_\beta}{\Omega^2 \mathcal{I}_b} + 1. \tag{75}$$

2.4.3 Main Rotor Forces

The total thrust and counter-torque produced by the main rotor is a function of the forces acting on the blades perpendicular and parallel to the hub plane. The expressions are given as:

$$T_{mr} = \frac{N_{mb}}{2\pi} \int_0^{2\pi} \int_0^{R_t} dF_{\perp,t} cos\beta d\psi_m \tag{76}$$

$$Q_{mr} = \frac{N_{mb}}{2\pi} \int_0^{2\pi} \int_0^{R_t} l dF_{\parallel,t} d\psi_m \tag{77}$$

From here, the individual body-fixed frame components may be determined following the equations in section 2.3.

This work was supported in part by NSF CNS-1229236

2.4.4 Tail Rotor

Unlike the main rotor, the tail rotor only has a collective pitch, ζ_t. The tail rotor blade experiences induced air velocity and has flow components similar to (54) and (52), but with coefficients and constants specific to the tail rotor. Additionally, the perpendicular and parallel force components resemble (57) and (58) of the main rotor. The tail rotor thrust and counter-torque can be found using (78) and (79), [12].

$$T_{tr} = \frac{N_{tb}}{2\pi} \int_0^{2\pi} \int_0^{R_t} dF_{\perp,t} d\psi_t \tag{78}$$

$$Q_{tr} = \frac{N_{tb}}{2\pi} \int_0^{2\pi} \int_0^{R_t} r dF_{\|,t} d\psi_t \tag{79}$$

This work was supported in part by NSF CNS-1229236

3 Linearization

3.1 Trim

Aircraft in steady flight must operate at some conditions where the forces and moments are in equilibrium about the center of gravity. This is when the helicopter is in what is known as trim flight, [147]. Trim conditions correspond to certain trim values of the state and input variables, given by x_0 and δ_i, respectively. The first step in determining trim values for the helicopter, is to define the equations of equilibrium and reference flight conditions. These trim values can be found both analytically, as seen in [147], or numerically, as seen in [152].

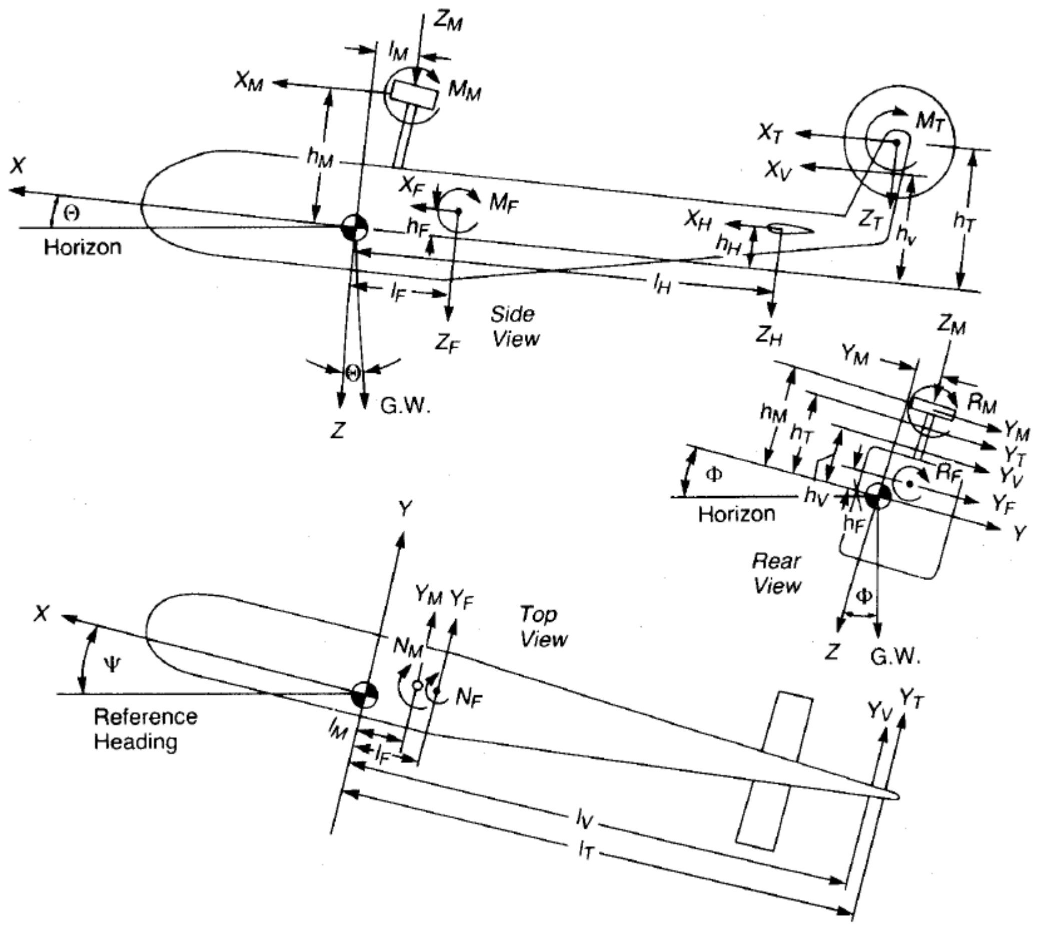

Figure 17: Forces and moments on the helicopter in trim flight, [147].

3.2 Linearization

There are two main methods to perform linearization of nonlinear dynamic equations. The first is to use Taylor series expansion about some initial condition, [64]. The second method is to follow small perturbation theory. Small perturbation theory is widely used to linearize the nonlinear helicopter dynamics about a trim flight condition, usually hover. Examples of this are seen in [39, 147, 148, 152]. In the case of the helicopter dynamics, the total force is made up of the forces and torques contributed by the various helicopter subsystems. These forces are either controlled, as a result of the pilot input, or uncontrolled, as a result of the dynamic parameters. These various forces are listed in Table 2.

Table 2: Input force categorized as controlled versus uncontrolled.

Force Type	**Notation**	**Description**
Controlled	$f_{\delta_{col}}$	Collective input
	$f_{\delta_{ped}}$	Tail rotor collective
	$f_{\delta_{lat}}$	Lateral cyclic
	$f_{\delta_{lon}}$	Longitudinal cyclic
	$f_{\delta_{thr}}$	Throttle
Uncontrolled	f_u, f_v, f_w	Translational velocities
	f_p, f_q, f_r	Angular rates
	f_ϕ, f_θ, f_ψ	Orientation angles
	f_{a_1}, f_{b_1}	Main rotor cyclic angles
	f_{c_1}, f_{d_1}	Stabilizer cyclic angles

Small perturbation analysis involves applying a small incremental force, Δf, resulting in small perturbations to the dynamics. For the helicopter, the dynamic parameters that make up the state vector are given in (80), while the dynamic inputs are given by (81).

In most cases, the engine throttle is not controlled by the pilot, but rather remains constant during flight. As a result, the engine throttle is not included in the input vector.

$$\vec{x} = [u\ v\ w\ p\ q\ r\ \phi\ \theta\ \psi\ a_1\ b_1\ c_1\ d_1\ ]^T \tag{80}$$

$$\vec{u}_c = [\delta_{col}\ \delta_{ped}\ \delta_{lat}\ \delta_{lon}]^T \tag{81}$$

In [39], the forces and moments are defined to be strictly functions of the state and input variables. This allows for the forces and moments to be defined as linear functions of the disturbed variables, Δx_i and $\Delta \delta_i$. This combination is seen in (83). Although it may be desired to retain terms of higher order derivatives or nonlinear terms for the sake of accuracy and completeness, as in [102], many times only the first order terms are considered.

This work was supported in part by NSF CNS-1229236

It is noted that for small enough motion, the effects of the nonlinear terms (e.g., $\frac{\partial^2 F}{\partial x^2}$), and derivatives of dynamic parameters, (e.g., $\dot{u}$, $\dot{q}$), are insignificant, [138]:

$$F_x = \frac{\partial f}{\partial x}|_{x_0} = \frac{f(x + \Delta x) - f(x)}{\Delta x} \tag{82}$$

$$\Delta F = \sum_{x_i \in \vec{x}} F_{x_i} \cdot \Delta x_i + \sum_{\delta_i \in \vec{u}} F_{\delta_i} \cdot \Delta \delta_i \tag{83}$$

The derivatives with respect to the controlled inputs are referred to as the *control derivatives*, while those with respect to the uncontrolled states are known as the *stability derivatives*. The notation is simplified to $\frac{\partial f}{\partial \alpha} = F_\alpha$. The derivatives are listed in Table 3.

Table 3: Control and stability derivatives.

Derivative Type	**Notation**	**Description**
Control Derivatives	$F_{\delta_{col}}$	Collective input
	$F_{\delta_{ped}}$	Tail rotor collective
	$F_{\delta_{lat}}$	Lateral cyclic
	$F_{\delta_{lon}}$	Longitudinal cyclic
	$F_{\delta_{thr}}$	Throttle
Stability Derivatives	F_u, F_v, F_w	Translational velocities
	F_p, F_q, F_r	Angular rates
	F_ϕ, F_θ, F_ψ	Orientation angles
	F_{a_1}, F_{b_1}	Main rotor cyclic angles
	F_{c_1}, F_{d_1}	Stabilizer cyclic angles

The forces and moments of the helicopter dynamics, which drive the rigid body dynamics in (30), are shown in Table 4. A small increment of each of these forces and moments is a sum of the derivatives and perturbations, as given in Table 3 and (83), and are given in (84).

$$\begin{aligned}
\Delta X &= X_u \Delta u + X_v \Delta v + \cdots + X_{\delta_{col}} \Delta \delta_{col} + \cdots \\
\Delta Y &= Y_u \Delta u + Y_v \Delta v + \cdots + Y_{\delta_{col}} \Delta \delta_{col} + \cdots \\
\Delta Z &= Z_u \Delta u + Z_v \Delta v + \cdots + Z_{\delta_{col}} \Delta \delta_{col} + \cdots \\
\Delta L &= L_u \Delta u + L_v \Delta v + \cdots + L_{\delta_{col}} \Delta \delta_{col} + \cdots \\
\Delta M &= M_u \Delta u + M_v \Delta v + \cdots + M_{\delta_{col}} \Delta \delta_{col} + \cdots \\
\Delta N &= N_u \Delta u + N_v \Delta v + \cdots + N_{\delta_{col}} \Delta \delta_{col} + \cdots
\end{aligned} \tag{84}$$

Next, small perturbations are applied to the rigid body dynamics given in (30). It is assumed that the perturbations and any derivative have very small values. As a result,

This work was supported in part by NSF CNS-1229236

Table 4: Force and moment components.

Force	X	X component force
	Y	Y component force
	Z	Z component force
Moment	L	Moment about the X-axis
	M	Moment about the Y-axis
	N	Moment about the Z-axis

the product of perturbations are subsequently very small, and negligible, [148]. These assumptions result in the following properties, shown in (86). Applying the perturbed variable in Table 5 to the the forward velocity component of the rigid body dynamics in (30) produces to (85).

$$u_0 + \Delta \dot{u} = (r_0 + \Delta r)(v_0 + \Delta v) - (q_0 + \Delta q)(w_0 + \Delta w) - sin(\theta_0 + \Delta\theta)g + \frac{X_0 + \Delta X}{m} \quad (85)$$

The perturbed dynamic equation for forward velocity can be further simplified by using the properties in (86).

$$\begin{aligned} \Delta x \Delta y &= 0 \\ cos(\Delta\theta) &= 1 \\ sin(\Delta\theta) &= \Delta\theta \\ sin(\theta_0 + \Delta\theta) &= sin\ \theta_0 + \Delta\theta\ cos\ \theta_0 \\ sin(\theta_0 + \Delta\theta) &= sin\ \theta_0 + \Delta\theta\ cos\ \theta_0 \end{aligned} \quad (86)$$

$$0 = -sin\theta_0 g + X_0/m \quad (87)$$

Table 5: Perturbed Variables

$u = \Delta u + u_0$	$p = \Delta p + p_0$	$\phi = \Delta\phi + \phi_0$
$v = \Delta v + v_0$	$q = \Delta q + q_0$	$\theta = \Delta\theta + \theta_0$
$w = \Delta w + w_0$	$r = \Delta r + r_0$	$\psi = \Delta\psi + \psi_0$

Following this same procedure, and applying the perturbed variables in Table 5 to the entire set of dynamic equations (30) and (37) – (42), along with the flapping dynamics (70) – (71) and the tail stabilizing gyro dynamics as given in [124]. The derived set of linear dynamic equations is given in Tables 6, 7, and 8. This set of dynamic equations is derived

This work was supported in part by NSF CNS-1229236

following procedures from [147, 138, 124, 148, 39]. The dynamics may further be simplified according to the assumed flight condition (i.e., hover, cruise, turn, etc.).

At trim, it is assumed that the helicopter is operating in hover conditions where, $u_0 = v_0 = w_0 = p_0 = q_0 = r_0 = 0$. Additionally, it is assumed that there are no disturbances so that $\delta u = \delta \dot{u} = \delta \theta = \delta X = \dot{u}_0 = 0$. Given these assumptions, the forward velocity dynamics in (85) becomes (87). The set of equilibrium equations are derived and given as:

$$X_0 = mgsin\theta_0 \tag{88}$$
$$Y_0 = -mgsin\phi_0 cos\theta_0 \tag{89}$$
$$Z_0 = -mgcos\theta_0 cos\phi_0 \tag{90}$$
$$L_0 = M_0 = N_0 = 0 \tag{91}$$
$$\dot{x}^I = u_0 cos\theta_0 \tag{92}$$
$$\dot{y}^I = 0 \tag{93}$$
$$\dot{z}^I = -u_0 sin\theta_0. \tag{94}$$

At level cruise, the trim conditions mimic those of hover except that the intial condition for translational velocity, usually forward, is set to a non-zero value. In the case of level forward flight, $u_0 = u_0 \neq 0$. In [134], the trim condition for a level banked turn is given using a constant forward velocity, constant yaw angle, and no sideslip.

Table 6: State Vector $\vec{x}$

$$x = \left[\begin{array}{ccc|ccc|ccc|cc|cc|c} u & v & w & p & q & r & \phi & \theta & \psi & a_1 & b_1 & c_1 & d_1 & r_{fb} \end{array}\right]^T$$

Table 7: State Space **A** Matrix

$$\left[\begin{array}{ccc|ccc|ccc|cc|cc|c}
X_u & X_v + r_0 & X_w - q_0 & X_p & X_q - w_0 & X_r + v_0 & 0 & -gc_{\theta_0} & 0 & X_{a_1} & 0 & 0 & 0 & 0 \\
Y_u - r_0 & Y_v & Y_w + p_0 & Y_p + w_0 & Y_q & Y_r - u_0 & gc_{\phi_0}c_{\theta_0} & -gs_{\phi_0}s_{\theta_0} & 0 & 0 & Y_{b_1} & 0 & 0 & 0 \\
Z_u + q_0 & Z_v - p_0 & Z_w & Z_p - v_0 & Z_q + u_0 & Z_r & -gs_{\phi_0}c_{\theta_0} & -gc_{\phi_0}s_{\theta_0} & 0 & Z_{a_1} & Z_{b_1} & 0 & 0 & 0 \\
\hdashline
L_u & L_v & L_w & L_p & L_q + J_p r_0 & L_r + J_p q_0 & 0 & 0 & 0 & 0 & L_{b_1} & 0 & 0 & 0 \\
M_u & M_v & M_w & M_p + J_q r_0 & M_q & M_r + J_q p_0 & 0 & 0 & 0 & M_{a_1} & 0 & 0 & 0 & 0 \\
N_u & N_v & N_w & N_p + J_r q_0 & N_q + J_r p_0 & N_r & 0 & 0 & 0 & 0 & 0 & 0 & 0 & N_{r_{fb}} \\
\hdashline
0 & 0 & 0 & 1 & s_{\phi_0}t_{\theta_0} & c_{\phi_0}t_{\theta_0} & 0 & \Omega/c_{\theta_0} & 0 & 0 & 0 & 0 & 0 & 0 \\
0 & 0 & 0 & 0 & c_{\theta_0} & -s_{\theta_0} & -\Omega c_{\theta_0} & 0 & 0 & 0 & 0 & 0 & 0 & 0 \\
0 & 0 & 0 & 0 & s_{\phi_0}/c_{\theta_0} & c_{\phi_0}/c_{\theta_0} & (q_0 s_{\phi_0} - r_0 c_{\phi_0})t_{\theta_0}/c_{\theta_0} & (q_0 c_{\phi_0} - r_0 s_{\phi_0})/c_{\theta_0} & 0 & 0 & 0 & 0 & 0 & 0 \\
\hdashline
0 & 0 & 0 & 0 & -1 & 0 & 0 & 0 & 0 & -1/\tau_f & A_b & A_c & 0 & 0 \\
0 & 0 & 0 & -1 & 0 & 0 & 0 & 0 & 0 & B_a & -1/\tau_f & 0 & B_d & 0 \\
\hdashline
0 & 0 & 0 & 0 & -1 & 0 & 0 & 0 & 0 & 0 & 0 & -1/\tau_s & 0 & 0 \\
0 & 0 & 0 & -1 & 0 & 0 & 0 & 0 & 0 & 0 & 0 & 0 & -1/\tau_s & 0 \\
\hdashline
0 & 0 & 0 & 0 & 0 & K_r & 0 & 0 & 0 & 0 & 0 & 0 & 0 & K_{r_{fb}}
\end{array}\right]$$

This work was supported in part by NSF CNS-1229236

This work was supported in part by NSF CNS-1229236

Table 8: State Space **B** Matrix

$$
\mathbf{B}: \left[\begin{array}{ccc|ccc|ccc|cc|cc|c}
X_{\delta_{lat}} & Y_{\delta_{lat}} & Z_{\delta_{lat}} & L_{\delta_{lat}} & M_{\delta_{lat}} & N_{\delta_{lat}} & 0 & 0 & 0 & A_{lat} & B_{lat} & 0 & D_{lat} & 0 \\
X_{\delta_{lon}} & Y_{\delta_{lon}} & Z_{\delta_{lon}} & L_{\delta_{lon}} & M_{\delta_{lon}} & N_{\delta_{lon}} & 0 & 0 & 0 & A_{lon} & B_{lon} & C_{lon} & 0 & 0 \\
X_{\delta_{ped}} & Y_{\delta_{ped}} & Z_{\delta_{ped}} & L_{\delta_{ped}} & M_{\delta_{ped}} & N_{\delta_{ped}} & 0 & 0 & 0 & 0 & 0 & 0 & 0 & 0 \\
X_{\delta_{col}} & Y_{\delta_{col}} & Z_{\delta_{col}} & L_{\delta_{col}} & M_{\delta_{col}} & N_{\delta_{col}} & 0 & 0 & 0 & 0 & 0 & 0 & 0 & 0
\end{array}\right]^T
$$

4 Control Approaches

Considerable research has already been conducted in the area of flight control for rotorcraft. The platforms used in design of flight control systems and navigational control algorithms range from full to small scale rotorcraft which can be flown with or without pilot commands and, especially in early research, may have been mounted on an experimental gimbaled stand for ease of indoor flight. Advances in both sensing and computing technology has led to increased precision and reliability as well as significantly higher update rates in necessary navigational sensors (i.e. GPS, IMUs, etc.) as well as increased processing capabilities for the flight computer. As a result, along with advancements in control theory, a number of control strategies have been implemented for various flight modes and maneuvers of the rotorcraft, validated using numerical simulations and/or experimental results.

Flight controllers typically fit in one of three main categories - linear, nonlinear, or model-free - depending on the model representation used to describe the dynamics of the rotorcraft. The dynamics of the rotorcraft are inherently nonlinear, making determination of a full and accurate model difficult. The rotorcraft is an underactuated system, since there are significantly fewer control inputs than states to be controlled. There is major dynamic coupling between the control inputs and the states, that is, each input affects multiple states and may cause unintended responses. Nonlinear models are the most difficult to identify and implement due to the complexity of the equations and often high order of polynomial or differential equation necessary to fully describe the system dynamics. Additionally, there are a number of phenomena that exist in nonlinear systems, such as the existence of multiple equilibria and modes of behavior that cannot be described by a linear model. Linear controllers use a number of assumptions in order to simplify the nonlinear dynamic models. Usually, this linearization occurs about some particular condition. They also are usually only valid in a small subset of the entire flight envelope. This limits the capability, maneuvers and flight scenarios of linear controllers. Despite their drawbacks, linear controllers are still the easiest to design and implement. Finally, model-free control designs, as the name suggests, do not require a model of the helicopter dynamics. Instead, model-free control designs utilize learning or human based algorithms. These types of controllers tend to rely heavily on pilot commanded flight testing in order to teach the algorithms to mimic the human pilot behavior and decision making.

Regardless of the type of flight controller used, the control architectures consist of a number of interconnected loops in order to control navigation, translational dynamics and attitude dynamics of the helicopter. For rotorcraft, the attitude dynamics are much faster than the translational dynamics. Typically, flight controllers are designed with at least two loops. The inner most loop controls the attitude dynamics. The next outer loop deals with translational dynamics. An additional outer-most loop may be used for navigational guidance, such as trajectory generation or tracking. A second approach to the control architecture is to separate the lateral-longitudinal dynamics from the heave-yaw dynamics. Both approaches associate the system inputs with a rigid-body dynamic state to be controlled. These states include translational positions and velocities, angular rates, and attitude angles. However, since rotorcraft are underactuated systems, there are more states than inputs to the helicopter dynamics. In order to deal with this, many of the helicopter states may be used as intermediate or virtual inputs to subsequent cascaded loops. Generally, the rotorcraft main rotor collective and throttle are associated with heave, or altitude. The tail rotor

This work was supported in part by NSF CNS-1229236

collective is associated with the yaw motion. Lastly, the main rotor lateral and longitudinal collectives are associated with the roll and pitch of the helicopter which subsequently result in lateral and longitudinal translation. A third, less frequently used, approach uses classical control analysis in order to manipulate system poles and gain or phase margins to stabilize the helicopter. However, even this structure utilizes multiple loops.

4.1 Control Architecture Structures

Depending on the type of flight maneuver desired to achieve, the design of the control loop architecture varies. This is due to the assumptions or simplifications that can be made and the type of reference input to follow. The most common types of flight controllers can be separated into the following categories: yaw or heading control, attitude or orientation control, altitude control, velocity control, position control. Each of the control structures can be designed using simplified dynamic models specific to the navigational dynamic states and particular flight mode to be controlled. These same controllers may be combined in order to achieve more advanced maneuvers, such as hover control and trajectory tracking.

4.1.1 Hover Control

Hover control is the most basic of maneuvers. Most linearizations of dynamic models are done assuming hover conditions. At hover, the goal is to keep the helicopter at a desired position, sometimes while maintaining a certain heading or yaw rate.

4.1.2 Yaw or Heading Control

The rotorcraft yaw rate or heading can be controlled using the tail rotor collective input. One important consideration for control of yaw is the possible presence of a yaw-rate gyro in RC helicopters. These gyros are used to provide stabilization in the yaw channel during piloted flight and have their own dynamics that are not described by the dynamic equations of the helicopter. It is possible to create model of the gyro dynamics through comparison of flight tests with and without the gyro. This is done in [140, 124]. The yaw dynamics are most easily decoupled for a helicopter in hover, while in translational flight a change in heading will affect the lateral-longitudinal dynamics. However, for very small changes in heading or at low enough velocities, the controller can be successful. A basic structure of a yaw controller, shown in Figure 18, may take in as a reference command a constant yaw angle or a yaw rate depending on the maneuver to be performed. The control block represents any time of control that might be used, typically a PID controller.

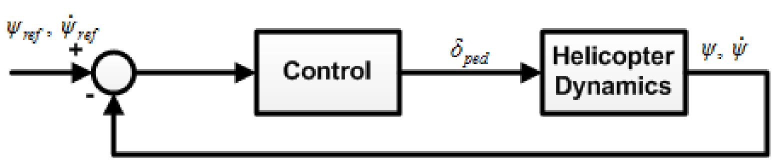

Figure 18: Yaw control block diagram.

4.1.3 Attitude or Orientation Control

Attitude control is used to stabilize the orientation of the rotorcraft. A typical attitude control architecture is shown in Figure 19. This control structure uses the rotorcraft cyclic inputs for pitch and roll and tail rotor collective for yaw stabilization. Attitude control is placed as an inner loop. Typically, an attitude controller will either regulate the pitch and roll only, the yaw only, or all three. This can depend on how the controller will be used in the FCS, whether as part of a larger control structure, such as one for hover or trajectory tracking. For a SISO control architecture, a single controller is used for each channel. However, with MIMO approaches, such as LQR and $\mathcal{H}_\infty$, a single controller may be responsible for two or more channels at once. The method of decoupling the dynamics will determine how these channels can be lumped. However, most approaches keep the pitch and roll angles together.

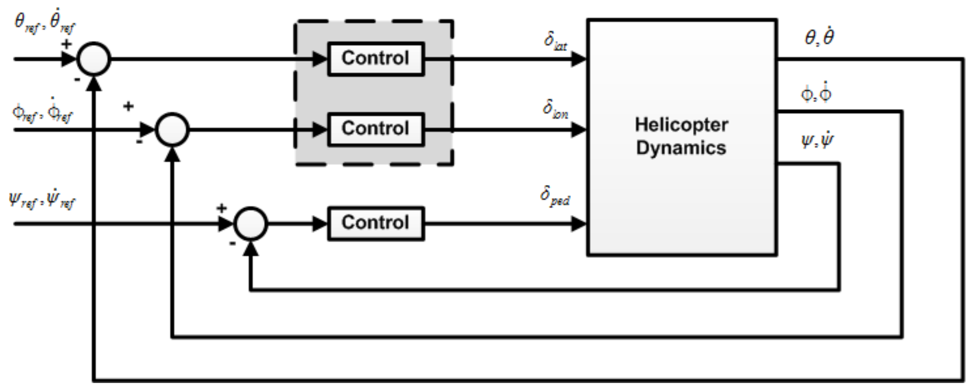

Figure 19: Attitude/orientation control block diagram.

4.1.4 Velocity Control

Velocity control is used to ensure that a particular velocity trajectory is achieved. Usually, this is used for cruise flight in parallel with a heading and attitude controller or in a trajectory tracking scheme in order to generate virtual attitude commands for the inner loop of the FCS, given desired positions or velocities. A typical architecture for velocity control is given in Figure 20. For SISO schemes, the control blocks represent individual controllers for each channel. However, a MIMO control approach can be used. In most cases, the lateral and longitudinal translational velocities u and v are controlled together. The velocity control block will generate desired roll and pitch orientation angles or rates in order to achieve the desired velocity and feed that *virtual command* to the inner loop attitude controller.

4.1.5 Altitude Control

Altitude control is used to ensure the helicopter maintains a desired height during flight. The main rotor collective and, if controllable, the engine throttle inputs are regulated in order to maintain the desired altitude. Sometimes, altitude control is coupled with the inner

This work was supported in part by NSF CNS-1229236

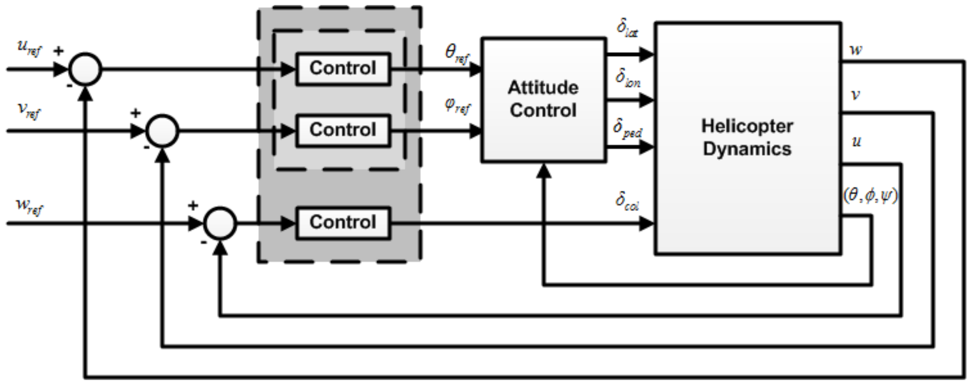

Figure 20: Velocity control block diagram.

loop attitude control and decoupled from the lateral-longitudinal dynamics. This is known as lateral-longitudinal outerloop and heave-yaw inner-loop control. In this type of structure, the outer-loop controller produces the reference roll and pitch trajectories for the inner-loop controller. One such example is given below in Figure 21.

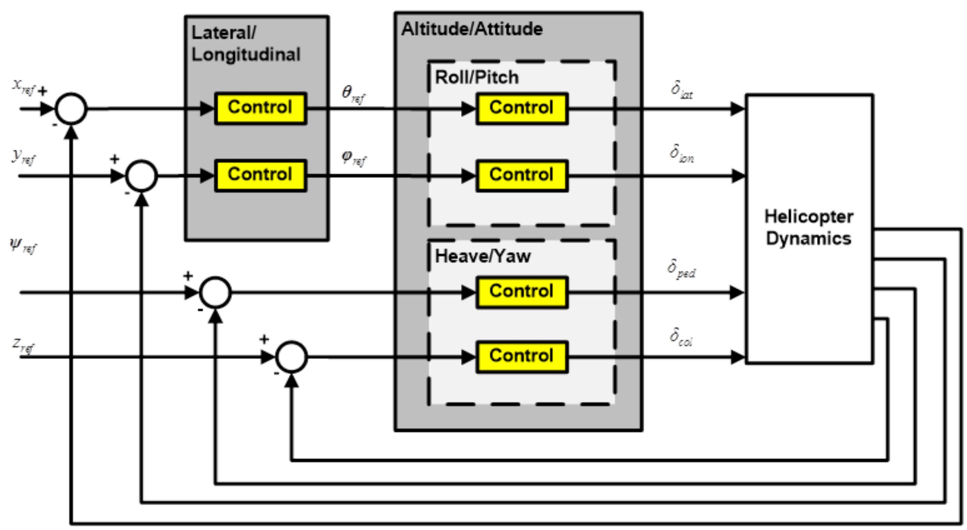

Figure 21: Lateral-longitudinal and heave-yaw control structure.

Another approach uses two individual controller to handle decoupled longitudinal-vertical and lateral-directional dynamics. This type of structure is shown below in Figure 22.

4.1.6 Position Control and Trajectory Tracking

Position control and trajectory tracking is achieved by providing a desired trajectory reference to the FCS. In order to achieve this, a combination of velocity, altitude, and orientation control must be used. This is shown in Figure 23. For position control, it may be desired

This work was supported in part by NSF CNS-1229236

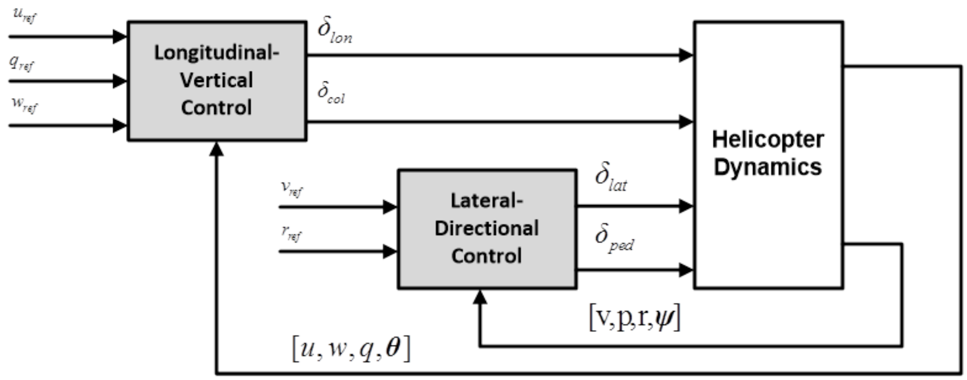

Figure 22: Longitudinal-vertical and lateral-directional control structure.

to maintain the helicopter at a particular position. This can be achieved by a two loop structure. The outermost loop takes the desired position and determined the necessary helicopter orientation in order to maintain that position. The innermost loop will then determine necessary helicopter control inputs. A three loop structure may also be used. Here the outer-most loop uses the desired trajectory in order to determine desired translational velocities. These velocities act as virtual inputs to the middle loop, which determines ideal attitude trajectories as inputs the the inner-most loop. This inner-most loop determined the necessary helicopter control inputs. Trajectory tracking may have the additional requirement of maintaining a desired heading trajectory.

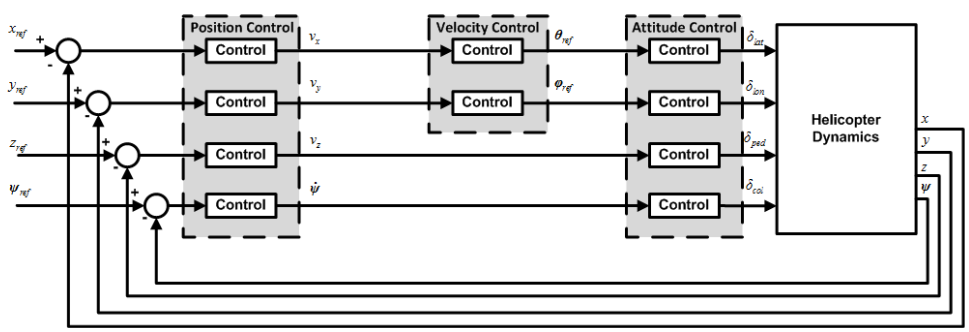

Figure 23: Block diagram for trajectory tracking.

4.2 Control Methods

In this section, two main classifications of control methods used in rotorcraft navigation and control are presented. For each classification, specific methods are presented, giving details on the theory and how they are used in the overall control architecture. For linear methods, PID, LQR/LQG, $\mathcal{H}_\infty$, and gain scheduling techniques are presented. For nonlinear methods, backstepping, adaptive, model predictive, linearization, and nested saturation techniques are presented. Table 9 summarizes the advantages and disadvantages of each approach and lists typical maneuvers that have been achieved, either in simulation or experimentally, by various groups. Lastly, a comprehensive overview of the control approaches is given in Table 10.

This work was supported in part by NSF CNS-1229236

Table 9: Comparison of Control Methods

Control Algorithm		**Advantages**	**Disadvantages**	**Maneuvers**
LINEAR	PID (SISO)	Easily implemented Assumes simplified decoupled dynamics Gains can be tuned in flight	Lacks robustness Ignores coupling of dynamics	Mostly hovered flight Attitude/Altitude control Lateral/ Longitudinal control
	LQG/ LQR	Multivariable capabilities Used to stabilize both inner and outer loops -	Limited to certain flight conditions Gain calculation is an iterative process -	Hovering Trajectory tracking -
	$\mathcal{H}_\infty$	Deals with parametric uncertainty Can handle unmodeled dynamics can be used for loop-shaping	High level of math understanding and computation Need a reasonably good system model	Hovering Trajectory tracking -
	Gain Scheduling	Larger range of flight envelope and operating conditions Can use a bank of simple controllers	Requires ability to store a number of gains and control approaches Transition between switches might be unsteady	Hovering Trajectory tracking
NONLINEAR	Back-stepping	Good technique for underactuated systems	Need a nonlinear model	Trajectory tracking
	Feedback Linearization	Can deal with nonlinearties while allowing for application of linear techniques -	Higher computational complexity Transformed variables and actual output may vary greatly	Auto take-off and landing Hovering and aggressive maneuvers
	Adaptive Control	Robust technique Can adapt to unmodeled dynamics and parametric uncertainty	Complex analysis Need good knowledge of the system	Formation flight Vision based navigation
	Model Predictive Control (MPC)	Can predict future behavior, to some extent Can place constraints on the input Tracking errors can be minimized	Prediction model must be formulated correctly - -	Target tracking - -

This work was supported in part by NSF CNS-1229236

4.2.1 Linear PID Controllers

PID controllers are a type of single-input/single-output (SISO) control structure in which one controlled input is associated with a single output. The PID algorithm consists of three gains: a proportional, integral, and derivative gain. A great advantage of the PID approach is the ease of implementation. PID controllers can be implemented without any sort of model. This method requires multiple flight tests in order to manually tune each of the gains until a desired response is obtained. While the lack of need for a model may make this approach appealing, it may become tedious and difficult to obtain desired gains, not to mention the added risk of failure or crash if improper gains are chosen.

A second approach to the PID structure is to determine a transfer function, which describes the relationship between the chosen input/output pair to be controlled. Once a satisfactory function is identified and validated, classical methods may be used to determine ideal gains for the PID controller. This can include looking at overshoot, settling or rise times, and even gain and phase margins. Once identified, these ideal gains can be tested during flight, where they may be manually fine tuned according to the observed response. These approaches, however, do not directly deal with the time scaling between the inner loop and outer loop dynamics.

Another structure using PID control requires the use of multiple loops in order to separately address the inner loop and outer loop dynamics. For this type of control structure it is necessary to create virtual inputs from outer loops to the inner control loops. Rather than pairing one of the rotorcraft outputs to a controlled input directly, the outer loops create virtual inputs to the inner loops in the form of a desired trajectory needed in order to achieve stability in the outer loop. The inner loops are then tasked to achieve the trajectory determined by the outer loop. An example is a multi-loop PID (MLPID) controller that separates the attitude and translational dynamics. In this type of structure, see Figure 20, the outer loop is tasked with achieving the desired velocity in 3-axis. Because the cyclic inputs of the helicopter affect the lateral-longitudinal motion of the helicopter most, the lateral-longitudinal velocity controllers output desired pitch and roll in order to achieve the referenced velocities. From there, the inner attitude controller will use these as virtual inputs in order to determine the necessary controlled inputs to the rotorcraft.

In [18], a cascaded control architecture is used for a 13 state linear model of an R-MAX helicopter. The proposed controller is based on a cascaded architecture with an inner and outer loop. However, rather than simply controlling the attitude (inner loop) and tracking (outer loop), this architecture looks at the poles of the dynamic model in order to stabilize the system. The helicopter model is derived from [31]. This linear dynamic model, derived at hover, consists of 14 states which include the linear velocities, angular rates, main rotor and stabilizer flapping dynamics, yaw rate feedback, main blade coning dynamics and first derivative, and the inflow. This model is augmented and then reduced for the purpose of this study to 13 states. For trajectory tracking, the body frame positions are added, rather than inertia frame which cause nonlinearities. Attitude angles are approximated by time integrals to remove nonlinearities, valid for small roll and pitch angles. Next, the states which are not directly measured are removed, except the yaw rate feedback. The final state vector includes the body frame positions, linear velocities, attitude, angular rates and yaw-rate feedback. This model is used for the purpose of control synthesis. The control architecture consists of three loops. The innermost loop uses a linear quadratic regulator (LQR) controller to stabilize right hand plane poles. A feedback linearization mid loop controller is used to decouple the input/output pairs. Then a PD controller is used for trajectory tracking. The final cascaded controller's matrices are able to be compute off-line, allowing for relatively simple implementation in real time. A simplified state estimator is used for real time implementation to track the yaw-rate feedback parameter. Lastly, guidance waypoints are transformed to the body frame by a direct cosine matrix. Simulated and experimental results are presented for a figure 8 trajectory with constant altitude.

In [82, 83], an adaptive controller is designed on a 13 state linear model of the Yamaha R-Max with decoupled translational and attitude dynamics. A PD compensator is added to each of the loops.

In [89, 88], a tracking controller is designed for a 12 state LTI model, for the Berkeley Yamaha R-Max, using a Multi-Loop PID (MLPID) 3 loop architecture. This structure is similar to that in Figure 23. The inner loop for attitude, middle loop for linear velocity and the outermost loop for position control. The group compares two control approaches for a spiral ascent maneuver. Results of a spiral ascent are compared with a Nonlinear Model Predictive Tracking Controller (NMPTC). The MLPID is able to track the trajectory with some significant errors compared to the NMPTC.

In [161], a MLPID controller is designed for an 11 states linear model using a 3 loop architecture shown in Figure 23. The three loops consist of inner attitude, mid velocity and outer position loop control. Loop gains are acquired using root locus methods for response speed and damping ratio. In this control scheme, loops may be disabled according to the flight maneuver. In cruise mode, only velocity and attitude loops are necessary, whereas in hover mode all loops are needed. Experimental results show adequate performance in hover for nearly 3 minutes with slight yet acceptable oscillatory motion. A pilot uses velocity control to take-off and put the helicopter at a necessary altitude, then engages the hover control.

Lastly, in [155], a mixed controller architecture is used for a 2 loop architecture, lateral/longitudinal and attitude/altitude control, capable of hover, positioning and forward flight at low velocities. Here, PID control is used for the innermost attitude/altitude control.

4.2.2 Linear LQG/LQR Controllers

Linear Quadratic Gaussian (LQG) and Linear Quadratic Regulators (LQR) controllers are types of optimal feedback controllers that utilize quadratic cost functions. They can be used in a SISO or multi-input/multi-output (MIMO) structure. Linear quadratic controllers use full state feedback in order to obtain an optimal input for the system. LQG controllers consists of a LQR controller and a Kalman filter, and is based on separation of control (LQR) and estimation (Kalman). LQG controllers are meant to operate in the presence of white noise. LQR controllers seek to find an optimal input that will drive the state to a desired final state by minimizing a quadratic cost, a function of both the state vector, the input vector, and two gain matrices.

Linear quadratic controllers have their drawbacks. First, if it is not possible to reach the final state from the initial state, then it becomes impossible to determine any input

This work was supported in part by NSF CNS-1229236

vector. Additionally, in the case that not all the states are observable, it becomes necessary to implement a state observer to feedback the missing measurements for full state feedback. Additionally the output limitations are not considered in the controller design, which may lead to optimal input vectors beyond the operating conditions of the system.

Despite the drawbacks, LQG and LQR controllers have been implemented in a number of UAV applications, including rotorcraft. In [16], the LQG controller is used in hover control of a gimbaled model helicopter and a 6 state linear time-invariant (LTI) model. Simulated results are presented for both a 3DOF and 6DoF model for hover with pilot commanded attitude. In [129], an LQG controller with setpoint tracking is developed using this same linear model for hover and a low velocity regime. Experimental results are presented for hover stabilization using the 3DoF stand.

In [18], an LQG controller is used on a 13-state linear model of the Yamaha RMAX for right hand plane stabilization and placed as an innermost loop.

In [53, 123], a LQR controller is used a two loop architecture where the dynamics are separated into outer longitudinal-vertical and inner lateral-directional dynamics. The outer loop structure and control design is given in detail in [53], where integrators are added to the LQR controller in order to drive the forward speed and altitude rate tracking steady-state error to zero. Because of the limitations of the controller to the operating points assumed for the purpose of linearization of the dynamics, different gains are designed for a set of forward speeds. The inner loop structure is given in detail in [123]. Here the structure follows a similar approach to the outer loop, only integrators are added to the sideways velocity and yaw rate. In both, the LQR control is augmented with feed-forward schemes and notch filters for shaping of closed-loop responses and to compensate for the slight damping of the stabilizer bar, respectively.

In [80], a Linear Quadratic Regulator (LQR) based controller of a linearized model at hover is enhanced with an Unscented Kalman Filter (UKF) for online active model error approximation between the simplified and full dynamic models. The UKF is used because of it's ability to handle nonlinear systems with fast dynamics in online applications. UKFs use nonlinear models without the need of some heavy computations that are required of Extended Kalman Filters (EKF). The linearized model consists of 12 states, (linear velocities, angular rates, attitude and position), and 4 inputs, $\vec{u}_c = [\delta_{col}\ \delta_{ped}\ \delta_{lat}\ \delta_{lon}]^T$. Results are presented for simulations comparing the UKF estimation and true model difference that show the UKF's ability to track the true model difference. Secondly, simulation results are presented that show the ability of the enhanced LQR controller to track a desired trajectory.

In [106], hovering attitude controller is developed from an 8 state linearized model using a Loop Transfer Recovery (LTR) approach, LQG/LTR.

In [196], a Linear Quadradic Guassian/ Loop Transfer Recovery (LQG/LTR) approach is used on an RC model helicopter on a mechanical stand that allows 6DoF flight in a 2 meter cube area. The helicopter is modeled as an 18 state linear time-invariant model which includes positions, linear velocities, attitude angles, angular rates, main rotor flapping angles, main rotor time constant, induced main and tail rotor velocities, and motor state (PI for constant speed). Output measurements of position and attitude. The helicopter model is then split into two seperate dynamics: 1) the heave/yaw motion and 2) the lateral/longitudinal motion. The former consists of vertical position and speed, yaw angle and rate, induced velocities, motor state, and rotor speed. The latter consist of side and forward positions and velocities, roll and pitch angles and rates, main rotor flapping angles. Additionally, a second order Padè approximation (transfer function) is used before each input to model the delay of transmitting the controller commands through the multiplexing radio. This adds 4 states to each subsystem. The controller design goals are to reject disturbances in the low-frequencies while maintaining a good robustness margin. A cascaded PD controller is used for flight in order to determine necessary model parameters. A PD controller is added to each input of the system, with a cascade on the forward/pitch and sideways/roll inputs. Next, a LQG/LTR controller is used, one for each subsystem. The results for the LQG/LTR show unsatisfactory input-output behavior despite good closed-loop behavior. This is is somewhat remedied by leading the reference signal statically to the controller output.

In [155], a mixed 2 loop controller is designed for a 6 state LTI model of an EC Ceoncept electric RC model helicopter. Here, the outer loop handles lateral-longitudinal control while the inner loop handles altitude-attitude control. A LQR is used on the inner loop for heave and yaw control. Simulated results are presented for hover and position control and in a low velocity regime.

4.2.3 Linear $\mathcal{H}_\infty$ Controllers

$\mathcal{H}_\infty$ control is a type of multi-variable robust model based control. One major advantage of $\mathcal{H}_\infty$ control is its robustness in the presence of model uncertainties and disturbances. This quality becomes very useful for highly complex systems. Since complete modeling of the rotorcraft dynamics is very difficult and a number of assumptions and simplifications are made in order to obtain a workable dynamic model.

A number of works have applied $\mathcal{H}_\infty$ controllers for both loop shaping, which uses classical control approaches, and synthesis, where a feedback gain is determined.

In [16], an $\mathcal{H}_\infty$ for a 6 state linear model, of a helicopter on a 3DoF stand, is designed for hover with piloted attitude commands. In this design, the weighting functions are specified for continuous time, and are chosen so that the yaw dynamics are faster than the pitch and roll. The controller is discretized using a bi-linear transformation. It is shown in simulated results that the $\mathcal{H}_\infty$ controller is able to decouple the modes while maintaining fast dynamics. Experimental results are done with a pilot assistance to place the helicopter in hover, then engaging the controller and finally providing attitude commands. Overall, the $\mathcal{H}_\infty$ controller responded quickly on the pitch and roll access with higher damping in the yaw access, allowing for greater and faster disturbance rejection and reduce cross coupling.

In [103], an $\mathcal{H}_\infty$ controller is designed for a 30 state linear model of the CMU Yamaha R-50 helicopter and designed for hover operation. This model includes the 9 rigid body states, 6 main rotor states, 4 stabilizer bar states, 3 states for Pitt-Peters inflow dynamics, and 2 states for each of the 4 actuators. This controller uses a 3 loop architecture, as seen in Figure 23, to perform heading and tracking control. The inner-most loop handles attitude and altitude control. The mid loop handles lateral-longitudinal velocity control. And

This work was supported in part by NSF CNS-1229236

finally, the outer-most loop handles position control in the form of a reference trajectory. The controller is implemented using four maneuvers: a forward coordinated turn, a backward coordinated turn, a nose-out pirouette, and a nose-in pirouette. In the case of the two turns the helicopter starts at hover, then the pilot commands forward velocity. Afterwards, the pilot commands the turn giving a forward velocity, v_x, and yaw rate command, $\dot{\psi}$, while maintaining zero side-ways velocity, V_y. Since the command is on v_x, the x-position loop is disengaged, however the y-position loop is engaged to drive the tracking error to zero. In the case of the pirouettes the helicopter starts at hover, then the pilot commands a side-ways velocity, v_y, until the turn is commanded. For this, the controller is given a constant v_y and $\dot{\psi}$, while maintaining zero v_x. Similar to the turns, the y-position loop is disengaged, but the x-position loop is engaged to drive the error to zero.

In [197], a robust controller that uses $\mathcal{H}_2$ and $\mathcal{H}_\infty$ methods is designed for position control at hover. The helicopter testbed and model are identical to that in [196]. This control scheme takes advantage of the fact that the interaction between vertical/yaw motion and lateral/longitudinal motion of the helicopter is weak at hover in order to design control of the two systems separately. In the $\mathcal{H}_2$ design, an augmented scheme is used and weighting matrices are presented. In the $\mathcal{H}_\infty$ design, a a 2DoF design is used for the vertical/yaw dynamics in order to deal with resonance and reference tracking. For the lateral/longitudinal dynamics, a weighting scheme is used to shape the sensitivity matrices since the number of measurements is larger than the number of control signals. Results for each controller are compared using the static gain and bandwidths. It is shown that the $\mathcal{H}_\infty$ design shows higher performance, but with the need of additional knowledge than the $\mathcal{H}_2$ design.

4.2.4 Linear Gain Scheduling Controllers

Gain scheduling is a term that describes approaches that seek to switch between various controllers designed for specific operating conditions. Since linear controllers are designed through linearization about some operating conditions, it may be necessary to determine multiple linear models, controller gains, or even control methods in order to be able to operate the helicopter in a larger flight envelope. Some of the considerations with gain scheduling is choosing which parameters and operating points will be used to determine the switching requirements as well as how the switching will occur.

In [172], a switching controller using piece-wise quadratic Lyapunov-like functions is presented based Mettler's 13 state linear model of the Yamaha R-50 model parameters identified for hover and cruise. Simulations are chosen with a simple flight scenario, allowing focus on the switching phenomena for smoothing the transition between hover and cruise.

In [53], an adaptive control scheme using neural networks, linear quadratic regulators, and notch filters, is designed for various sets of gains. Each set of gains is determined for 6 forward speed values. Switching occurs between the gains once the helicopter enters a new flight regime.

This work was supported in part by NSF CNS-1229236

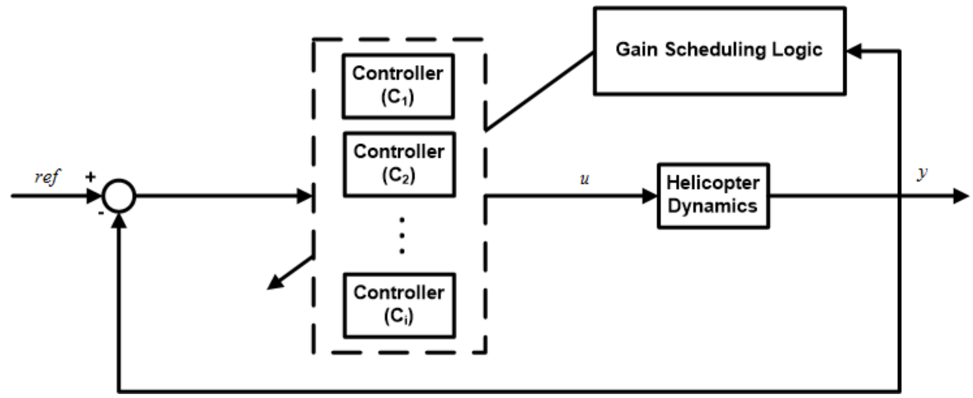

Figure 24: Gain scheduling control block diagram.

4.2.5 Nonlinear Controllers

While linear techniques have proven capable of performing maneuvers in hover or low velocity regimes, there are still a number of limitations associated with linearization and simplification of the dynamics models for the purpose of control law design. By using a nonlinear dynamic model of the helicopter, new control laws can be designed with greater capabilities to perform more complex maneuvers at higher velocities. Much of the work involving nonlinear models includes backstepping, adaptive control, feedback linearization or dynamic inversion, model predictive control, and nested saturation loops.

4.2.6 Nonlinear Backstepping Controllers

Backstepping is a recursive control method used to find a control Lyapunov function (clf) for stabilizing nonlinear systems of a lower triangle form, known pure-feedback form, [98]. Design of backstepping controllers starts with looking at creating a feedback control law and Lyapunov function to a general rigid body model of Newton Euler form with force and moments as system inputs, [54]. In order to ensure this cascaded structure, it is common practice to neglect the small parasitic, or small body, forces, [26, 150]. In [26], a controller is presented based on backstepping techniques for an Euler-Lagrange dynamic model in addition to the traditional Newton-Euler helicopter dynamic model used more commonly.

A theoretical analysis for guaranteed tracking using a Lyapunov based backstepping controller is presented in [115]. The work is continued in [116] on a nonlinear model of the Vario 23cc helicopter. Simulations show the ability of the controller to perform trajectory tracking for position adjustments while in hover and following an ascending helical trajectory.

In [42], a backstepping controller is presented with the purpose of avoiding artificial singularities that are caused by representation of the attitude angles using Euler coordinates. The controller uses an approximate model of the helicopter based on [94]. The helicopter dynamics are modeled using to states, an element matrix representing the helicopter orientation and translation vector, and an element of the Lie algebra which contains the angular and translational velocities in the body axes. The control law is designed with the objective of tracking a smooth, feasible reference trajectory. The translational dynam-

This work was supported in part by NSF CNS-1229236

ics are controlled with the use of a quadratic Lyapunov function and PD control law in order to determine desired attitude trajectories. The attitude dynamics are controlled using backstepping techniques in order to track the reference attitude trajectories and stabilize the system. Simulated results are presented helicopter undergoing 4 different maneuvers: 1) point stabilization, 2) point stabilization during inverted flight, 3) trim trajectory tracking of a climbing turn, and 4) transition to inverted flight. The first two maneuvers show similar responses. The third manever showed good results, though tracking of a time-parameterized trajectory resulted in aggressive flying and excessive control effort. The final maneuver shows the effect of going through the singularity, causing larger deviations in the second half of the maneuver. However, the results show ability to perform the maneuver.

In [144], a velocity control law based on backstepping techniques is developed for a nonlinear Newton-Euler dynamic model of a Yamaha R-MAX as part of an overall scheme to land the helicopter on a moving platform by tracking its velocity. The model includes forces and torques generated by the main and tail rotors, as well as the flapping and thrust dynamics. Simulations show the ability of the controller to track a desired velocity.

In [3], a position controller using backstepping is designed for a nonlinear model of an Eagle UAV, with tune-able parameters for position and velocity control. Again, the model is derived from Newton-Euler equations of motion and includes models of induced velocity, thrust, forces and moments, and flapping dynamics of the rotors and flybar. Simulation shows the ability of the controller to perform position and velocity control.

In [4], backstepping control is used for autonomous landing control using a tether and correction to the flapping and servo dynamics. In [32], backstepping is used to stabilize the translational and attitude dynamics for hover and trajectory tracking. Backstepping is also used to perform trajectory generation for target tracking using a discretized nonlinear controller in [158]. In [175], backstepping is used in attitude control using a nonlinear model based on quaternion feedback. Other works involving backstepping include [181, 184, 188, 202, 203].

4.2.7 Nonlinear Adaptive Control

Adaptive control is an area of control law with a wide range of techniques and algorithms. It seeks to address the issues of parameter uncertainties. This can include parametric, structural and environmental uncertainties as well as unmodeled or changes in dynamics, [76, 182]. The goal of an adaptive controller is to adapt itself to changes in these uncertainties based on a desired performance criteria. Adaptive controllers typically include some class of parameter estimator, or adaptive element, and a control law that adapts according to the estimation. The various classes of adaptive controllers result from the choice of estimator and control law, [75]. This type of control has a great potential for applicability in a much larger flight envelope than other traditional control approaches. The adaptive element or parameter estimator uses the input to the plant as well as the output in order to determine the changes to the control law gains or parameters. This type of structure is shown in Figure 25. Another type of popular controller utilizes an ideal reference model in addition to the adaptive element, or parameter estimator. This class of adaptive control is known as model reference adaptive control (MRAC). The desired system behavior is given by the reference model and is governed by the reference input. This type of architecture is shown in Figure 26.

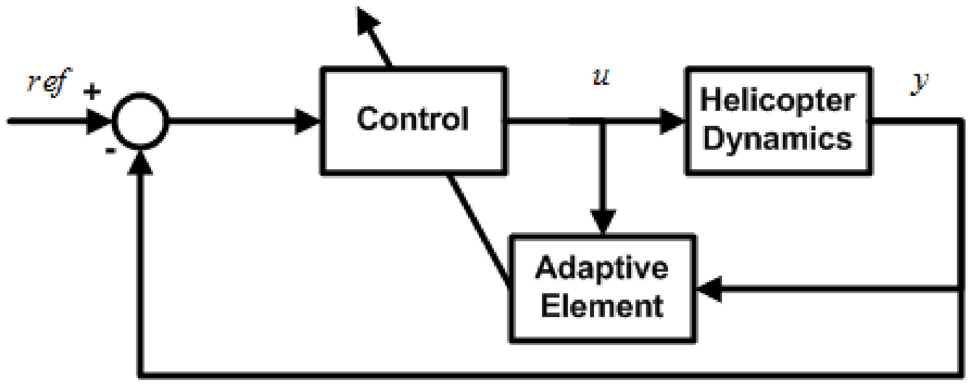

Figure 25: Adaptive control block diagram.

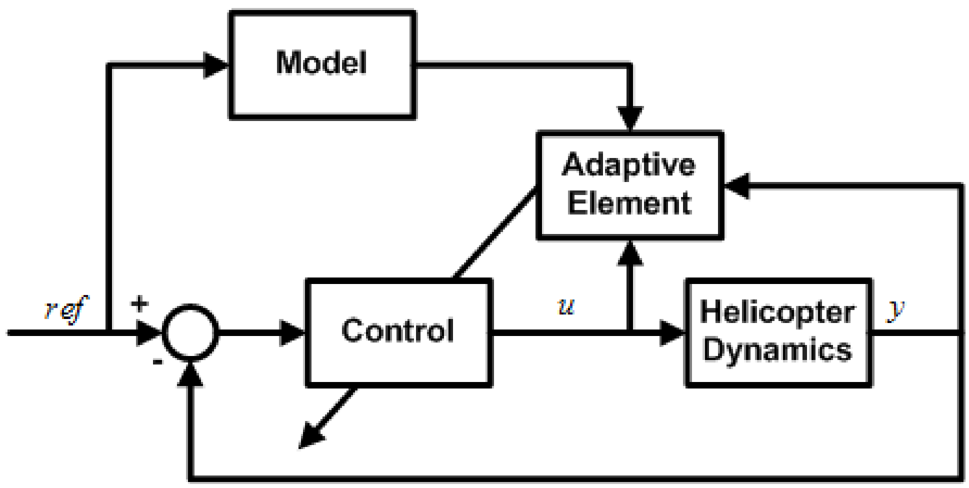

Figure 26: Model referenced adaptive control block diagram.

In [33], an adaptive nonlinear controller design, presented in [25], is implemented on a Yamaha R-50 helicopter which utilized approximate inversion linearization. The controller can be configured for each rotational access as an attitude command attitude hold (ACAH) scheme or rate command controller. The adaptive element is achieved through the use of neural networks for online adaptation and to cancel the effects of inversion errors. Real-time Hardware-in-the-Loop (HIL) testing is performed using piloted commands and visualization software. The simulations show the controller's ability for online learning and tolerance of unmodeled dynamics, noise and delays.

In [63], a high bandwidth inner loop controller for attitude and velocity stabilization is designed for a Vario X-treme helicopter using $\mathcal{L}_1$ adaptive control theory. to test the controllers robustness against uncertainties and disturbances, Von Karman wind models and

This work was supported in part by NSF CNS-1229236

gusts were implemented in simulation. The simulation trajectory included three stages: 1) sideways translation, 2) helical motion with nose pointed inward, and 3) hover.

4.2.8 Feedback Linearization Controllers

Feedback linearization, also known as Nonlinear Dynamic Inversion (NDI), is a technique used to find a feedback control law by transforming the nonlinear system dynamics into an equivalent fully or partial linear form through some algebraic transform. There exist various levels of feedback linearization, from full state feedback linearization, which yields a fully linearization, to input-output linearization, where the mapping between inputs and particular outputs of interest are linearized but the state equations are only partially linearized, [87]. This method allows the application of linear control techniques to the system.

In [10], a 3DOF reduced-order nonlinear model of a scale model helicopter mounted on an experimental platform is presented. This is in part of the development of a 7DOF nonlinear model and nonlinear control design for a VARIO Benzin-Trainer scale model helicopter. Different to this modeling method is the inclusion of the main and tail rotor dynamics in the Lagrangian equations. Additionally, the inputs are taken as the actual helicopter inputs. The aerodynamic forces and torques used in the Lagrangian equations are presented. Next, the dynamics of the helicopter mounted on the experimental platform are derived using Lagrangian dynamics. Details on the derivation of the dynamics are given in [9]. Next a linearizing control design is presented on the reduced order model. This reduced order model only considers the pilot inputs for collective pitch of the main and tail rotors. The design is split into two phases: 1) start-up and take-off, and 2) vertical flight. Simulation results show the ability of the controller to track a desired trajectory. However, it is obvious that the design of trajectory is crucial for control design and must be chosen so as not to saturate the inputs. Experimental results are also presented for stabilization of the helicopter dynamics for various values of altitude and yaw.

In [19], a theoretical stability analysis is presented for a proposed nonlinear UAV rotorcraft controller. The controller proposed is a hierarchical controller for position and attitude control using partial state feedback with time-scale separation between the translational and orientation dynamics. The proposed controller is analyzed using single perturbation theory, and is found to be stable.

In [94], output tracking control is investigated. The helicopter dynamic model is derived from Newton-Euler equations. The controller is based on input/output linearization and by neglecting coupling between roll/pitch and lateral/longitudinal forces. Positions and headings are chosen as outputs in order to ensure that the approximated system is dynamically linearizable without zero dynamics. Simulation results are shown for a control based on exact input/output linearization and the approximated input/output linearization presented here. The results show that the approximate model is able to track the trajectories without exciting oscillations in the internal model.

In [95], a control design based on differential flatness is presented. This design involves neglecting the coupling between the rolling/pitching moment and the lateral/longitudinal forces. The details of the dynamics equations used is given in [94] and are based on

This work was supported in part by NSF CNS-1229236

Newton-Euler equations. An approximate model is presented for control design followed by an modification for the exact helicopter model under trim flight conditions. The control scheme features an inner attitude control loop and outer position control loop. The outer controller consists a mapping function that utilizes the flatness of the outer loop to generate the inner trajectory. It is assumed that there is an inner controller to drive the error to zero. For the inner loop two controllers are used. One is for tracking the attitude, and the other for tracking main rotor thrust. Attitude control is based on feedback linearization. Simulations are performed in which the controllers are required to achieve hover from an initial position relatively large compared to the desired origin and turning the heading to the desired orientation. The results show the controllers ability to drive trajectory error to zero with the exact model and with the condition that the trajectory is in trim flight conditions.

In [17], dynamic feedback linearization is used for tracking the longitudinal dynamics. Feedback linearization is implemented on a Bergen Industrial Twin with compensation of small body forces in [56] and also combined with nonlinear $\mathcal{H}_\infty$ in [68] for trajectory tracking. Incremental nonlinear dynamic inversion is used on an 8 DOF nonlinear model for velocity reference tracking and attitude control in [165]. Other examples include [157, 163, 181, 184].

4.2.9 Nested Saturation Loops

In [14], a nonlinear controller is designed with the goal of asymptotically tracking a vertical, lateral and longitudinal reference while maintaining a constant yaw angle. This is done by taking advantage of techniques from [78] and modifying the control structure. The helicopter model is based on [94]. An external wrench nonlinear model is used to derive the helicopter dynamics with 5 control inputs, $u = [P_M \; P_T \; a \; b \; T_h]^T$, the main and tail rotor collective pitch, the lateral and longitudinal cyclic angles, and engine throttle control, respectively. The dynamics are divided into 4 groups: the vertical, attitude, engine, and lateral/longitudinal dynamics. Quaternions are used to describe the rotation between the body and inertial reference frames and the helicopter attitude. The controller is designed to handle large uncertainties in parameters, including vehicle mass, inertia, aerodynamic coefficients, and the engine model. The inner loop is a high-gain feedback and controls the attitude dynamics. The outer loop is designed with a nested saturation structure and controls the lateral/longitudinal dynamics. The attitude dynamics for pitch and roll are used as virtual inputs to the lateral/longitudinal dynamics and for a virtual control law which is "step back" to the actual control inputs $v = [a \; b \; T_h]^T$. The control law developed is inspired by [77]. Simulations are performed using parameters with assumed uncertainties of 30%. The chosen trajectory is created using the 3rd order spline interpolation method and must satisfy bounds on the higher order time derivatives. The trajectory has three main movements: forward/lateral movement with ascent, lateral movement with descent, and reverse movement to start position. The simulations show the ability of the controller to maintain a relatively constant yaw angle while tracking a vertical/lateral/longitudinal reference trajectory.

In [119], a nonlinear controller is presented with the objective of controlling vertical, lateral, longitudinal and yaw attitude of a helicopter along a trajectory. The control design includes a combination of feed-forward control actions, high gain feedback laws, and nested saturation feedback laws. The control structure consists of an inner loop to govern attitude

This work was supported in part by NSF CNS-1229236

dynamics, and an outer loop to govern the lateral-longitudinal dynamics. It is proposed that this control structure can achieve very aggressive maneuvers characterized by large attitude angles. In addition, it is proposed the controller is able to cope with the possibility of large uncertainties in the physical parameters. The helicopter dynamic model is derived from Newton-Euler equations of motion of a rigid body. This model includes 5 inputs, the main and tail rotor collective pitches, the lateral/longitudinal cyclic angles, and the motor throttle. The desired trajectories are defined as known time profiles with restrictions on the time derivatives dictated by functional controllability and physical constraints on the inputs. Experimental results are presented using a miniature commercial 60 series helicopter. Nominal values of controller gains are refined by trial an error. An aggressive maneuver is used to test the controller, which consists of fast forward speed with a constant desired yaw such that the maneuver required both pitch and roll aggressive attitudes. Altitude is fixed. A polynomial describing the maneuver is provided. The controller presented a small tracking error and slight fluctuations. These have been attributed to measurement precision and model uncertainty.

4.2.10 Nonlinear Model Predictive Controllers

Model predictive control (MPC) is a technique that utilizes a dynamic model of the system in order to anticipate and predict future behavior of the plant while considering constraints on states and inputs, [5] This ability to predict future behavior allows for on-line solving of an optimization problem that minimizes the error over a future horizon. MPC is also known as moving horizon or receding horizon control (RHC). [89]. The general structure of an MPC controller is shown in Figure 27.

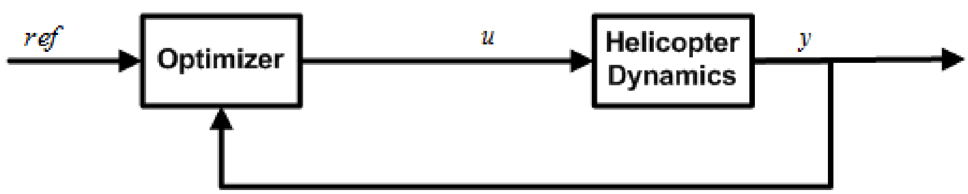

Figure 27: Model predictive control block diagram

In [89, 88], a nonlinear model predictive tracking controller (NMPTC) is designed for the Berkeley Yamaha R-MAX. The helicopter model is a 12 parameter nonlinear model of the Yamaha R-Max. The Model Predictive Controller (MPC), or Receding Horizon Controller (RHC), uses a cost minimization function with gradient descent for trajectory and tracking control. Simulations in both show the NMPTC is superior over the MLPID for a spiral ascent in the presence of heavy nonlinearities and coupling along with being robust to parameter uncertainty. This paper also presents an application to collision avoidance and vision guided landing. Experimental results are presented in [88].

In [36, 37], a nonlinear MPC is used for auto-rotation landing using a nonlinear model of the autorotation dynamics of a helicopter which includes the drop rate, altitude, engine RPM and inflow dynamics.

This work was supported in part by NSF CNS-1229236

In [40], a predictive controller with a disturbance observer is designed for a Hirobo Shuttle Plus30 helicopter. The model used is a 10 parameter attitude model. A PID controller is used for comparison of the controller performance and experimental results are presented for attitude control using a testbench.

In [110], a piecewise MPC is used on a 14 parameter nonlinear model of a Hummingbird helicopter. Simulated and experimental results are presented for a square trajectory. In [112, 113], explicit nonlinear MPC (ENMPC) is used for trajectory tracking using a Trex 250 nonlinear model for square, pirouette and figure-8 trajectories. Both simulated and experimental results are presented. Lastly, nonlinear MPC is presented in [109] for path planning.

Other examples of MPC control include [169, 168].

4.2.11 Other Nonlinear Methods

In addition to the nonlinear control methods discussed, there has been a fair amount of research introducing new or novel nonlinear techniques to helicopter navigation and stability control. One such method is sliding mode control, a robust method that forces the system behavior toward a particular trajectory, known as a sliding surface or manifold, in a finite amount of time and then maintain that behavior. Sliding mode control has been shown to be robust against uncertainties, [87]. Examples of sliding mode control include [23, 43, 166, 185].

Another approach involves using Linear Matrix Inequalities (LMI) in the design process, such as with $\mathcal{H}_\infty$ and $\mathcal{H}_2$ or optimal control techniques. This can be seen in [62, 122].

Lastly, the use of model-free or learning-based methods, such as Neural Networks and Fuzzy Control, have been used to augment model-based methods or tune gains. These approaches include [33, 36, 37**?**].

This work was supported in part by NSF CNS-1229236

This work was supported in part by NSF CNS-1229236

5 Comparison of Approaches

5.1 Linear Controllers

Table 10: Linear Control Survey

Paper	Year	Vehicle Model	Control Technique	Maneuver	Results
Ahmed: "Dynamic Compensation for Control of a Rotary wing UAV Using Positive Position Feedback" [2]	2010	2nd order linear roll and pitch model based on Hirobo "Eagle" identified at 50 Hz using frequency response	Positive Position Feedback inner loop with PI low bandwidth outer loop controller	Attitude Control for roll and pitch	Simulation
Antequera: "A Helicopter Control based on Eigenstructure Assignment" [6]	2006	9 state linear model	Eigenvalue assignment (EA) compared with LQR	Hover and low velocities	Simulation comparisons
Bai: "Control system design of a small-scale unmanned helicopter" [11]	2010	8 state linear model: $[u\ v\ p\ q\ \phi\ \theta\ a\ b]$	$\mathcal{H}_\infty$ loop-shaping for lateral and forward velocity; outer loop PD for lateral and forward velocity, inner loop PID for attitude	Forward velocity	Simulation results, summary of flight testing
Bendotti: "Robust hover control for a model helicopter" [16]	1995	EC Concept electric RC model helicopter Discretized linear time invariant model decoupled at hover with 6 states (attitude and angular rates) sampled at 50Hz, similar to [129]	$\mathcal{H}_\infty$ and LQG	Hover with pilot attitude commands	Simulation and experimental results using a model helicopter on a 3DOF and 6DOF stand

Continued on next page

This work was supported in part by NSF CNS-1229236

continued from previous page

Paper	Year	Vehicle Model	Control Technique	Maneuver	Results
Bergerman: "Cascaded position and heading control of a robotic helicopter" [18]	2007	Linear model with 13 states including position in body frame for R-Max helicopter	Cascaded position controller with inner loop to LQG for RHP stabilization, feedback linearization to decouple input/output pairs, and PD for trajectory tracking	Figure 8 with heading tangential to path, constant altitude and constant speed along path	Simulation, HIL, and flight tests
Budiyono: "Optimal Tracking Controller Design for a Small Scale Helicopter" [22]	2007	Yamaha R-50 linear model based on [123] with parameters identified at hover and cruise: $[u\ v\ p\ q\ \phi\ \theta\ a\ b\ w\ r\ r_{fb}\ c\ d]$	LQR with reference tracking and bounded control	Tracking control: square trajectory & square to circle trajectory	Simulation
Cai: "Design and Implementation of a Flight Control System for an Unmanned Rotorcraft using RPT Control Approach" [24]	2013	Helion based on Raptor 90-SE	Robust and Perfect Tracking with 3-layer control structure. Inner loop $\mathcal{H}_\infty$ attitude control and outer loop translational control	Take-off, hover, lateral/longitudinal translation, turn in place, slalom, pirouette, turn to target	HIL simulations and flight test results
Chen: "Modeling and attitude control of the miniature unmanned helicopter" [30]	2013	8 state linear model: $[u\ v\ p\ q\ \phi\ \theta\ a\ b]$, identified with PEM	$\mathcal{H}_\infty$ loop-shaping	Attitude control (roll and pitch)	Simulated step response and pilot commanded attitude reference
Datta: "Digital controller for attitude control of a rotary-winged flying robot in hover" [38]	2009	Bergen Turbine Observer Linear model from Mettler. Helicopter strapped to a platform	First order compensator for attitude control	Attitude control	Simulation

Continued on next page

continued from previous page

Paper	Year	Vehicle Model	Control Technique	Maneuver	Results
Gadewadikar: "Structured $\mathcal{H}_\infty$ Command and Control-Loop Design for Unmanned Helicopters" [44]	2008	Raptor90 SE 11 state linear model based on [126]	Position control with inner loop orientation and outer loop tracking control using $\mathcal{H}_\infty$ and L_2	Hovering, position tracking, yaw tracking	Simulated results
Gadewadikar: "$\mathcal{H}_\infty$ Static Output-feedback Control for Rotorcraft" [45]	2008	Raptor90 SE 11 state linear model based on [126]	Attitude control using $\mathcal{H}_\infty$ loop shaping	Hover and bank angles tracking pitch and roll	Simulated results with response to disturbances
Gavrilets: "Control logic for automated aerobatic flight of miniature helicopter" [50]	2002	X-Cell 60 decoupled linear model. Longitudinal/vertical $[u, a_1, w, q, z\theta]$ and Lateral/directional $[v, b, p, r, \phi]$	LQR with 6 trim points and notch filter	Roll command and Vertical ACAH	Flight test
Gavrilets: "Aggressive Maneuvering Flight Tests of a Miniature Robotic Helicopter" [53] MIT	2003	XCell 60 Helicopter Linearized decoupled longitudinal-vertical (4 state, 2 input) and lateral-directional (4 state, 2 input) dynamics based on nonlinear model in [51]	Linear quadratic regulators with feed forwards schemes to improve transient response and shape closed loop response. Notch filters are added to reduce gain margin problems on longitudinal and lateral cyclics. Gains were calculated for 6 forward speed values for switching.	Roll maneuver using human pilot inspired strategy. Pilot engages axial roll maneuver during flight	Experimental results for a roll maneuver

Continued on next page

This work was supported in part by NSF CNS-1229236

continued from previous page

Paper	Year	Vehicle Model	Control Technique	Maneuver	Results
Godbolt: "Experimental Validation of a Helicopter Autopilot Design using Model-Based PID Control" [60]	2012	Bergen Industrial Twin	PID with feedforward gravity compensation tuned in flight	Translational control	Experimental validation
Godbolt: "Model-Based Helicopter UAV Control: Experimental Results" [57]	2013	Bergen Industrial Twin	PID	Attitude Control	Experimental results
He: "Modeling, identification and robust $\mathcal{H}_\infty$ static output feedback control of lateral dynamics of a miniature helicopter" [69]	2011	Lateral dynamic linial model: $[v \quad \psi \quad p \quad b]$ and actuator dynamics	Robust $\mathcal{H}_\infty$ static output feedback (RHSOF)	Lateral speed tracking control	Simulation
Ji: "Study on dual-loop controller of helicopter based on the robust $\mathcal{H}_\infty$ loop shaping and mixed sensitivity" [79]	2011	9 state linear model	Dual loop: robust $\mathcal{H}_\infty$ inner-loop loop-shaping with outer-loop mixed sensitivity	Outer loop velocity control with inner loop ACAH	Simulation
Jiang: "Enhanced LQR Control for Unmanned Helicopter in Hover" [80]	2006	Linear 12 state model for LQR and nonlinear model for UKF	UKF enhanced LQR control	Hover	Matlab simulation
*Joelianto: "Model predictive control for autonomous unmanned helicopters" [81]	2011		MPC	Trajectory tracking at hover and cruise	

Continued on next page

continued from previous page

Paper	Year	Vehicle Model	Control Technique	Maneuver	Results
Johnson: "Adaptive flight control for an autonomous unmanned helicopter" [82]	2002	Yamaha RMax 13 state linearized model with quaternions for control design and nonlinear model for simulation	NN Adaptive Element, PD compensator, Pseudo Control Hedging and approximate inversion	Trajectory tracking and attitude control	Simulations and one step command response during flight
Kannan: "Adaptive Trajectory Control for Autonomous Helicopters" [83]	2005	GTMax (Yamaha R-MAx Variant) 13 state linearization of nonlinear model around hover	PID, Dynamic inversion, Neural networks	Trajectory and attitude control	Simulation and successful flights
Kim: "A flight control system for aerial robots: algorithms and experiments" [88]	2003	12 state LTI model for MLPID, Nonlinear model for NMPTC	Multi-Loop PID with inner/mid/outer loop, Nonlinear Model Predictive Tracking Controller (NMPTC) as a tracking layer	Spiral ascent with perturbation to system dynamics	Simulated and experimental results
Kureemun: "Helicopter Flight Control Law Design Using $\mathcal{H}_\infty$ Techniques" [99]	2005	Bell 412 9 state linear model $[u, v, w, p, q, r, \psi, \phi, \theta]$	$\mathcal{H}_\infty$ control	$\mathcal{H}_\infty$ robust stabilization & loop shaping, LQR., PI compensators	Simulated results
La Civita: "Design and flight testing of a gain-scheduled $\mathcal{H}_\infty$ loop shaping controller for wide-envelope flight of a robotic helicopter" [101] "Design and Flight Testing of a High-Bandwidth $\mathcal{H}_\infty$ Loop Shaping Controller for a Robotic Helicopter" [100]	2003	CMU Yamaha R-50 30 state nonlinear model	Gain scheduling and $\mathcal{H}_\infty$ loop shaping	-	Simulation and flight testing

Continued on next page

This work was supported in part by NSF CNS-1229236

continued from previous page

Paper	Year	Vehicle Model	Control Technique	Maneuver	Results
La Civita: "Design and Flight Testing of an $\mathcal{H}_\infty$ Controller for a Robotic Helicopter" [103]	2006	Yamaha R-50. 30 state model	$\mathcal{H}_\infty$, 3 loops for heading and tracking. Position, velocities, attitude	-	-
Lee, Bang: "Model-free linear quadratic tracking control for unmanned helicopters using reinforcement learning" [105] "Model-free LQ control for unmanned helicopters using reinforcement learning" [104]	2011	Model Free	LQR tuned with reinforcement learning	Tracking control	Simulation
Lee, Shim: "Design of hovering attitude controller for a model helicopter" [106]	1993	8 state linearized model	LQR/LTR feedback control	Hovering flight control	Simulation and experimental results on gimbal-like device
*Liang: "Combined of vector field and linear quadratic Gaussian for the path following of a small unmanned helicopter" [108]	2012	Align T-Rex 600 linear model: lateral-longitudinal $[u\ v\ \theta\ \phi\ p\ q\ a\ b]$ and heave-yaw $[w\ r\ r_{fb}]$	LQR with set-point tracking	Inner loop control	
Lungu: "Optimal control of helicopter motion" [114]	2012	Linear model from [44]: $[u\ v\ p\ q\ \psi\ \theta\ a\ b\ w\ r]$	LQR based optimal control with linear velocity and yaw rate error augmentation	Linear velocity tracking	Simulation

Continued on next page

This work was supported in part by NSF CNS-1229236

continued from previous page

Paper	Year	Vehicle Model	Control Technique	Maneuver	Results
Marantos: "Robust attitude control for an unmanned helicopter in near-hover flights" [117] "Robust $\mathcal{H}_2$ / $\mathcal{H}_\infty$ Position Tracking control of an Unmanned Helicopter for near-hover flights" [118]	2013	Family of linear models with inner-loop $[p\ q\ r\ \phi\ \theta\ \psi\ a\ b\ r_{fb}]$ and outer-loop $[x\ y\ z\ u\ v\ w]$	Robust $\mathcal{H}_\infty/\mathcal{H}_2$ methodologies	Attitude control using multi-section trajectory	Simulation
Masajedi: "Optimal Control Designing for a Discrete Model of Helicopter in Hover" [120]	2012	Yamaha R-50 discrete linear model $[u\ v\ w\ p\ q\ r\ \phi\ \theta\ \psi\ a\ b]$	LQR with integration operation and Kalman observer	Steady-state hover	Simulation
Megawati: "Robust switched linear controller for multimode helicopter models" [122]	2011	5 linearized models at trim for hover, acceleration and upward flight	Switched LMI/$\mathcal{H}_2$	Hover, acceleration, flying up	Simulation
Mettler: "Attitude control optimization for a small-scale unmanned helicopter" [127] CMU	2000	Yamaha R-50 13 state linear model w/ frequency domain identification (CIFER)	PID attitude control	Hover and forward flight	MATLAB
Mettler: "Attitude control optimization for a small-scale unmanned helicopter" [123] MIT	2002	X-Cell linear model, 4 states lateral-directional dynamics	Notch filter for dynamic compensation of stabilizer bar with PID and LQ feedback	Roll bank angle	Flight test results for a bank angle step command
Morris: "Identification and control of a model helicopter in hover" [129] Caltech	1994	EC Concept electric RC model helicopter with 6 states linear time-invariant model also used in [16]	LQG control with setpoint tracking	Hover and low velocities	Experimental result of hover using a 3DOF stand

Continued on next page

This work was supported in part by NSF CNS-1229236

This work was supported in part by NSF CNS-1229236

continued from previous page

Paper	Year	Vehicle Model	Control Technique	Maneuver	Results
*Oktay: "Simultaneous Helicopter and Control-System Design" [136]	2013	Linear model based on [138] at level cruise and hover	MPC	Trajectory tracking with discontinuous trajectories	Simulation
*Oktay: "Constrained predictive control of helicopters" [135]	2013	PUMA SA330 25 state linear model around trim detailed in [134]	LQG based Output Variance Constrained (OVC) control	Cruise, banekd turn, helical turn	Simulation
Pan: "PID Control of Miniature Unmanned Helicopter Yaw System based on RBF Neural Network" [139]	2011	Yaw dynamics 2nd order transfer function	Radial Basis Function based PID	Yaw Control	Simulation
Peng: "Comprehensive Modeling and Control of the Yaw Dynamics of a UAV Helicopter" [140]	2006	NUSIX Frequency Response Identification of Yaw Dynamics	Linear Feedback Control, Observer	Yaw Control	Simulation
Pieper: "Linear-quadratic optimal model-following control of a helicopter in hover" [142]	1994	Bell 205 linear model	LQ optimal model following control	Hover	Simulated results
Postlethwaite: "Design and flight testing of various controllers for the Bell 205 helicopter" [143]	2005	Bell 205 30 state nonlinear model simplified to 13 states	$\mathcal{H}_\infty$ frequency domain optimization		Simulation and flight test results
Pradana: "Robust MIMO Integral-Backstepping PID Controller for Hovering Control of Unmanned Model Helicopter" [145]	2011	11 state linear model: $[u\ v\ w\ \phi\ \theta\ p\ q\ r\ a\ b\ r_{fb}]$ based on [123]	Robust $\mathcal{H}_\infty$ and Integral-Backstepping PID control	Hover stabilization under parametric uncertainties	Simulated

Continued on next page

This work was supported in part by NSF CNS-1229236

continued from previous page

Paper	Year	Vehicle Model	Control Technique	Maneuver	Results
Raptis: "Velocity and heading tracking control for small-scale unmanned helicopters" [149]	2011	Raptor90 SE 11 state decoupled linear model: lateral/longitudinal and heave/yaw	Velocity and yaw tracking	Reference trajectories	X-plane simulations
*Safaee: "System identification and robust controller design for the autopilot of an unmanned helicopter" [153]	2013	Trex-600 SISO transfer functions	Robust $\mathcal{H}_2/\mathcal{H}_\infty$, mixed sensitivity	Tracking control	Piloted flight results
*Samal: "Model predictive flight controller for longitudinal and lateral cyclic control of an unmanned helicopter" [154]	2012	Vario-XLC decoupled lateral $[v\ p\ \phi\ b]$ and longitudinal $[u\ q\ \theta\ a]$ models	MPC with time delay and servo dynamic consideration	Lateral and longitudinal cyclic control	Simulation at hover with commanded x-y positions
Sanchez: "Combining fuzzy, PID and regulation control for an autonomous mini-helicopter" [155]	2007	X-Cell mini helicopter 14 state model	1)PID, Mamdani-type Fuzzy Control 2)MTFC, PID, LQR	1)Attitude/ Altitude, Lateral/ longitudinal 2)Lateral/ longitudinal, Roll/ pitch, altitude/ yaw	Simulation results for hover and position and low speeds
Shim: "A comprehensive study of control design for an autonomous helicopter" [159] Berkeley	1998	Non-linear model at hover	PID (8 state model), μ-synthesis, fuzzy logic, I/O linearization	–	Simulation results
Shim: "Control system design for rotorcraft-based unmanned aerial vehicles using time-domain system identification" [161]	2000	Kyosho Concept 60 Graphite 11 state linear model based on [126]	Multi-loop SISO PID control	Hover and low-velocity maneuvers	Experimental data for hover

Continued on next page

This work was supported in part by NSF CNS-1229236

continued from previous page

Paper	Year	Vehicle Model	Control Technique	Maneuver	Results
Shin: "Model-based optimal attitude and positioning control of small-scale unmanned helicopter" [162] Chiba University	2005	SF-40 helicopter, 8 state linear attitude model with roll, pitch, their rates, and the main and stabilizer flapping dynamics. Model adopted from Mettler's model.	MIMO attitude and trajectory controller with Kalman Filter based Linear Quadratic Integral (LQI)	Hover and reference tracking	Simulation results
*Sira-Ramirez: "A Liouvillian systems approach for the trajectory planning-based control of helicopter models" [167]	2000	Lynx heli 9 state model simplified to LTV model	Louivillan system feedback control	Trajectory Tracking	Simulation
Sun: "Application of μ / $\mathcal{H}_\infty$ Control to Modern Helicopters" [171]	1994	10 state model	Hybrid $\mu/\mathcal{H}_\infty$	-	Simulation results
Sutarto: "Switched Linear Control of a Model Helicopter" [172]	2006	Yamaha R-50, follows Mettler for EOM (13 states)	Switched control	Hover, cruise	Simulation results
Tang: "Static $\mathcal{H}_\infty$ Loop-Shaping Control for Unmanned Helicopter" [179]	2012	AF25B 10 state linear model at hover: $[\ v\ w\ p\ q\ r\ \phi\ \theta\ a\ b]$	Static $\mathcal{H}_\infty$ loop-shaping output feedback (OPFB) control with inner loop ACAH	Hover	Simulation
*Teimoori: "Planar trajectory tracking controller for a small-sized helicopter considering servos and delay constraints" [183]	2011	Vario-XLC linear model [154]	LQR with Integral action (LQI)and LQI with feed forward (LQIFF) control	Trajectory tracking of circular trajectory	Simulated comparison of LQI and LQIFF

Continued on next page

This work was supported in part by NSF CNS-1229236

continued from previous page

Paper	Year	Vehicle Model	Control Technique	Maneuver	Results
Wang: "A gust-attenuation robust $\mathcal{H}_\infty$ output-feedback control design for unmanned autonomous helicopters" [191]	2012	Linear model of inner-loop $[p\ q\ a\ b\ \delta_{lat}\ \delta_{lon}]$ and outer-loop $[x\ y\ u\ v\ p\ q\ \phi\ \theta]$ dynamics	Robust $\mathcal{H}_\infty$ OPFB control	Trajectory Tracking with position tracking of a helical ascent	Simulation
*Wang: "Robust flight control of small-scale unmanned helicopter" [193] "Robust attitude tracking control of small-scale unmanned helicopter" [192]	2013	THeli 260 roll and pitch linear SISO models with frequency response SID and time-domain validation	PD with robust compensation	Hover and attitude control with trajectory tracking	Flight test at hover and tracking square trajectory with constant heading
Weilenmann: "Test bench for rotorcraft hover control" [196]	1994	Graupner Avant Garde RC model helicopter. 18 state linear model angles.	Channelwise PD,LQG/Loop Transfer Recovery (LTR), Modal controllers	Hover and flight with low velocities	-
Weilenmann: "Robust helicopter position control at hover" [197]	1994	Graupner Avant Garde RC model helicopter. 18 state linear model angles. [196]	$\mathcal{H}_2$ and $\mathcal{H}_\infty$	Position control	-
*Xia: "Finite-horizon optimal linear control for autonomous soft landing of small-scale helicopter" [198]	2010	12 state linear model $[u\ v\ p\ q\ \phi\ \theta\ \psi\ q\ r\ x\ y\ h]$	LQR with two-point boundary value problem using: 1) Riccati equation and 2) transition matrix	Trajectory tracking and landing	Simulation

This work was supported in part by NSF CNS-1229236

5.2 Nonlinear Controllers

Table 11: Nonlinear Control Survey

Paper	Year	Vehicle Model	Control Technique	Maneuver	Results
Ahmed: "Flight control of a rotary wing UAV using backstepping" [4]	2009	Tethered Eagle RUAV	Backstepping	Autonomous landing	High fidelity simulation
Avila-Vilchis: "Nonlinear modelling and control of helicopters" [10]	2003	VARIO Benzin-Trainer Scale Model 3DOF Nonlinear model	Linearizing controller design	Altitude and yaw stabilization	Simulation for trajectory tracking in altitude and yaw, experimentation for stabilization of altitude and yaw.
Bejar: "Robust Vertical/Lateral/Longitudinal Control of a Helicopter with Constant Yaw-Attitude" [14]	2005	Helicopter model parameters from [94] Nonlinear external wrench model with 5 inputs including engine throttle.	Nonlinear controller with high feedback gain inner attitude control loop and nested saturation structure for the outer lateral/longitudinal control loop.	vertical, lateral/longitudinal control with constant yaw.	Simulations with given maneuver with reference trajectories satisfying bounds on higher order time derivatives.
Benitez-Morales: "A static feedback stabilizer for the longitudinal dynamics of a small scale helicopter including the rotor dynamics with stabilizer bar" [17]	2013	Longitudinal dynamic model: $[u\ w\ q]$	Dynamic Feedback Linearization with Differential Flatness	Trajectory tracking (longitudinal dynamics)	Simulation

Continued on next page

continued from previous page

Paper	Year	Vehicle Model	Control Technique	Maneuver	Results
Bertrand: "Stability analysis of an UAV controller using singular perturbation theory" [19]	2008	Nonlinear dynamics with forces and torques as inputs.	Nonlinear partial state feedback control with time-scale separation between translational and orientation dynamics.	Position and attitude control.	Theoretical stability analysis is performed. No numerical results.
Butt: "Robust altitude tracking of a helicopter using sliding mode control structure" [23]	2012	Heave-yaw dynamic model: $[z\ w\ \dot{\Omega}\ \beta\ \dot{\beta}]$	Lyapunov stability analysis and Sliding Mode control	Altitude tracking	Simulation at hover
Chingozha: "Low cost controller for small scale helicopter" [32]	2013	Translational/attitude dynamic loops	Backstepping	Take-off and hover	Simulated and experimental results
Corban: "Implementation of adaptive nonlinear control for flight test on an unmanned helicopter" [33]	1998	Yamaha R-50 Nonlinear Model with approximate inversion linearization.	Adaptive Nonlinear Control with Neural Networks and approximate inversion.	Attitude hold, rate command.	HIL simulations with pilot commands.
Cunha: "A path following controller for model-scale helicopters" [35]	2003	Vario X-treme non-linear model	Gain scheduling and D-methodology	Path following	Simlation at level flight, climbing helix and ascending ramp

Continued on next page

This work was supported in part by NSF CNS-1229236

This work was supported in part by NSF CNS-1229236

continued from previous page

Paper	Year	Vehicle Model	Control Technique	Maneuver	Results
Dalamagkidis: "Autonomous Autorotation of Unmanned Rotorcraft using Nonlinear Model Predictive Control" [36] "Nonlinear Model Predictive Control With Neural Network Optimization for Autonomous Autorotation of Small Unmanned Helicopters" [37]	2009, 2011	Thundertiger Raptor 30v2 Vertical autorotation model: $[v_H \ z \ \Omega \ u_i]$	Nonlinear MPC with Neural Networks	Autorotation landing	Simulation with hardware testing
Fan: "Nonlinear predictive attitude control with a disturbance observer of an unmanned helicopter on the test bench" [40]	2011	Hirobo Shuttle Plus 30 attitude model: $[\phi \ \theta \ \psi \ p \ q \ r \ a \ b \ c \ d]$	Nonlinear Predictive Controller with disturbance observer and PID comparison	Attitude control on a testbench	Experimental
Frazzoli: "Trajectory tracking control design for autonomous helicopters using a backstepping algorithm" [42] MIT	2000	Approximate model based on [94]. New coordinates defined to deal with singularities.	Backstepping, PD control law.	Trajectory tracking.	Simulation for point stabilization with regular and inverted flight, trim trajectory tracking for a turning climb and transition to inverted flight.

Continued on next page

This work was supported in part by NSF CNS-1229236

continued from previous page

Paper	**Year**	**Vehicle Model**	**Control Technique**	**Maneuver**	**Results**
Fu: "Sliding mode control for a miniature helicopter" [43]	2011	Trex-250 with offboard flight controller	Sliding Mode with uni-directional auxiliary surfaces and PID comparison using 3 nested loops for position, velocity and attitude control and open-loop rotor dynamic controller	Position Tracking for take-off and landing	Experimental reslts
Godbolt: "A novel cascade controller for a helicopter UAV with small body force compensation" [55]	2013	Bergen Industrial Twin [60]	Feedback linearization with small body force compensation	Trajectory tracking of a figure-8 trajectory	Simulation
Guerreiro: "Trajectory tracking $\mathcal{H}_2$ controller for autonomous helicopters: An application to industrial chimney inspection" [62]	2007	Vario X-treme nonlinear model from Cunha's 2005 thesis (don't have citation)	$\mathcal{H}_2$ synthesis with LMI for parameter varying systems	Trajectory tracking of a helical climb	Simulation
Guerreiro: "$\mathcal{L}_1$ adaptive control for autonomous rotorcraft" [63]	2009	Vario X-treme linear time-variant model.	$\mathcal{L}_1$ Adaptive Control for inner loop velocity and attitude stabilization.	Velocity and attitude control.	Simulation with sideways translation, helical maneuver and hover.
He: "Acceleration-Feedback-Enhanced Robust Control of an Unmanned Helicopter" [68]	2010	Nonlinear	Feedback linearization with nonlinear $\mathcal{H}_\infty$ and acceleration feedback	Tracking	Simulation

Continued on next page

This work was supported in part by NSF CNS-1229236

continued from previous page

Paper	**Year**	**Vehicle Model**	**Control Technique**	**Maneuver**	**Results**
Isidori: "Robust nonlinear motion control of a helicopter" [78]	2003	Nonlinear based on Newton-Euler, Vario X-Treme.	$\mathcal{L}_1$ Adaptive Control: high bandwidth inner loop.	Attitude and velocity stabilization.	Simulation results for sideways translation, helical climb, hover.
Kim: "Nonlinear model predictive tracking control for rotorcraft-based unmanned aerial vehicles" [89]	2002	12 state LTI model for MLPID, Nonlinear model for NMPTC	NMPTC and MPLPID	Trajectory tracking and heading control	Simulation of a spiral ascent
Koo: "Output tracking control design of a helicopter model based on approximate linearization" [94]	1998	Nonlinear model based on Newton-Euler equations	Input Output linearization	Position and heading tracking	Simulated results
Koo: "Differential flatness based full authority helicopter control design" [95]	1999	Nonlinear model based on [94]	Differential flatness and feedback linearization	Position and attitude tracking	Simulated results
Leonard: "Robust Nonlinear Controls of Model-Scale Helicopters Under Lateral and Vertical Wind Gusts" [107]	2012	7 DOF Lagrangian model using Tiny CP3 Helicopter based on Vario Benzin Trainer	Robust Feedback linearization and active disturbance rejection control (ADJC) based on extended state observer (ESO)	Lateral and vertical gust attenuation	Simulation of hover with 2 position set points and vertical helix. Experimental of a 5 DOF $[\phi \;\; \theta \;\; \psi \;\; z \;\; \gamma]$ stand with wind gusts
Liu: "Piecewise constant model predictive control for autonomous helicopters" [110]	2011	Hummingbird heli with 14 state model: $[x\, y\, z\, u\, v\, w\, p\, q\, r\, \phi\, \theta\, \psi\, a\, b]$	Piece-wise MPC	Square trajectory	Simulation and flight-test

Continued on next page

This work was supported in part by NSF CNS-1229236

continued from previous page

Paper	Year	Vehicle Model	Control Technique	Maneuver	Results
Liu: “Explicit non-linear model predictive control for autonomous helicopters” [112]	2011	Trex 250	Explicit nonlinear MPC (ENMPC)	Trajectory Tracking	Simulation of a square trajectory with parameter uncertainties. Experimental of square and figure 8 trajectories.
Liu: “Tracking control of small-scale helicopters using explicit nonlinear MPC augmented with disturbance observers” [111]	2012	Trex 250	ENMPC with disturbance observer	Trajectory tracking square and pirouette	Simulations and flight tests
Liu: “Hierarchical path planning and flight control of small autonomous helicopters using MPC techniques” [109]	2013	Lateral-longitudinal and heave-yaw decoupled dynamics	Hierarchical MPC. Linear for tracking control. Nonlinear for path planning.	Path planning	Experimental
Mahony: “Hover control via Lyapunov control for an autonomous model helicopter” [115]	1999	Vario 23cc	Lyapunov based control using backstepping	Analysis for guaranteed tracking	Theoretical analysis
Mahony: “Robust trajectory tracking for a scale model autonomous helicopter” [116]	2004	Vario 23cc	Continued from [115] (Lyapunov based control using backstepping)	Trajectory tracking of ascending helix and position adjustments	Simulation
Marconi: “Robust full degree-of-freedom tracking control of a helicopter” [119]	2007	60 series helicopter, nonlinear model based on Newton-Euler equations	feedforward, high gain feedback, nested saturation feedback	vertical, lateral/longitudinal, yaw attitude	Experimental results

Continued on next page

This work was supported in part by NSF CNS-1229236

continued from previous page

Paper	Year	Vehicle Model	Control Technique	Maneuver	Results
Nodland: "Neural Network-Based Optimal Adaptive Output Feedback Control of a Helicopter UAV" [133]	2013	Nonlinear 6DOF model	Neural Networks, Backstepping and Lyapunov-based methods	Trajectory tracking	Simulation of take-off and circular trajectory
Peng: "Design and Implementation of a Fully Autonomous Flight Control System for a UAV Helicopter" [141]	2007	HeLion, 12 State linearized model	Dynamic Inversion, Pole Placement, Composite Nonlinear Feedback (CNF)	Full Envelope	Experimental results for take-off, landing, hover and pirouette
Pota: "Velocity Control of a UAV using Backstepping Control" [144]	2006	Yamaha R-Max Nonlinear model based on Newton Euler	Backstepping	Velocity control	Simulated results
Pota: "Rotary wing UAV position control using backstepping" [3]	2007	Nonlinear model for an Eagle UAV	Backstepping	Position and Velocity control	Simulation for hover stabilization
Sandino: "Improving hovering performance of tethered unmanned helicopters with nonlinear control strategies" [157]	2013	Tethered helicopter nonlinear model	Model inversion, PID and feedforward techniques	Tethered Hover	Simulation
Sconyers: "Rotorcraft control and trajectory generation for target tracking" [158]	2011	Discretized nonlinear model	Backstepping	Trajectory generation for target tracking	Simulation

Continued on next page

This work was supported in part by NSF CNS-1229236

continued from previous page

Paper	Year	Vehicle Model	Control Technique	Maneuver	Results
Sieberling: "Robust Flight Control Using Incremental Nonlinear Dynamic Inversion and Angular Acceleration Prediction" [163]	2010	Nonlinear model of a T-tail helicopter	Incremental Nonlinear Dynamic Inversion (INDI) and Angular Acceleration Prediction	Trajectory generation for target tracking	Simulations
Simplicio: "An acceleration measurements-based approach for helicopter nonlinear flight control using Incremental Nonlinear Dynamic Inversion" [165]	2013	8 DOF Nonlinear Helicopter Model	Incremental nonlinear dynamic inversion with pseudo control hedging, see [163]	Velocity reference tracking and attitude control	Simlation of heave and pirouette
Sira-Ramirez: "Dynamical sliding mode control approach for vertical flight regulation in helicopters" [166]	1994	Xcell 50 on a stand (parameters from Pallet, "Realtime Helicopter Flight Control Tested"), NL model at hover	Dynamical Sliding Model control	Altitude control	Simulations
*Song: "Active model based predictive control for unmanned helicopter in full flight envelope" [169]	2010	ServoHeli-20	Active MPC, Generilized Predictive Control (GPC), and Active Model Based Stationary Increment Predictive Control (AMSIPC)	Hover to cruise flight mode change	Flight experiments

Continued on next page

continued from previous page

Paper	**Year**	**Vehicle Model**	**Control Technique**	**Maneuver**	**Results**
Song: "Active Model-Based Predictive Control and Experimental Investigation on Unmanned Helicopters in Full Flight Envelope" [168]	2013	ServoHeli-40 Semi-decoupled linear model in hover: longitudinal, lateral, and heave-yaw dynamics	Active MPC, see [169]	Tracking	Flight tests
Suzuki: "Attitude Control of Small Electric Helicopter by Using Quaternion Feedback" [175]	2011	Nonlinear model using quaternion derivatives, Euler based rotation equation and flapping dynamics.	Backstepping with quaternion feedback compared with Euler based SISO LQR	Attitude control	Simulations and Experiments
Taamallah: "Optimal Control For Power-Off Landing Of A Small-Scale Helicopter A Pseudospectral Approach" [177]	2012	13 state nonlinear model: $[x\ y\ z\ u\ v\ w\ p\ q\ r\ \phi\ \theta\ \psi\ \Omega]$	Direct Optimal control and pseudospectral discretization	Autorotation landing	Simulation
Tang: "Adaptive height and attitude control of small-scale unmanned helicopter" [181]	2013	AF25B Nonlinear model	Adaptive feedback linearization and backstepping	Height and attitude control	Simulation
Teimoori: "Helicopter flight control using inverse optimal control and backstepping" [184]	2012	Vario XLC Carrier Nonlinear model	Inverse optimal control and backstepping attitude, velocity and position control inner/outerloop structure with input delay consideration	Trajectory Tracking	Simulation

Continued on next page

This work was supported in part by NSF CNS-1229236

This work was supported in part by NSF CNS-1229236

continued from previous page

Paper	**Year**	**Vehicle Model**	**Control Technique**	**Maneuver**	**Results**
Teimoori: "Attitude control of a miniature helicopter using optimal sliding mode control" [185]	2012	Nonlinear model with normalized quaternions (Cayley-Rodrigues parameters)	Optimal sliding mode	Attitude control	Simulation in hover
Tsai: "Intelligent adaptive trajectory tracking control using fuzzy basis function networks for an autonomous small-scale helicopter" [188]	2011	Nonlinear model based on [49]	Fuzzy basis Fuzzy Networks (FBFN) augmented adaptive backstepping	Intelligent adaptive trajectory tracking	Simulation of a helical trajectory with performance index comparisons
Yang: "Nonlinear $\mathcal{H}_\infty$ Decoupling Hover Control Of Helicopter With Parameter Uncertainties" [199]	2003	6DOF hover, 3DOF decoupled translational and rotational dynamics at hover	Nonlinear $\mathcal{H}_\infty$ decoupling using quaternions	6DOF hover control compared to 3DOF attitude and velocity control	Theoretical analysis
Zhang: "Nonlinear control design and stability analysis of a small-scale unmanned helicopter" [202]	2013	Orientation inner-loop and translational outer-loop with flapping dynamics	Backstepping	Simultaneous inner/outer-loop control	Simulation
Zhu: "Adaptive backstepping control for a miniature autonomous helicopter" [203]	2011	Nonlinear model and parameters from [49]	Adaptive Backstepping	3D Trajectory Tracking	Simulation

5.3 Model-Free Controllers

Table 12: Model-free Control Survey

Paper	Year	Vehicle Model	Control Technique	Maneuver	Results
Abeel: "An application of reinforcement learning to aerobatic helicopter flight" [1] Stanford	2007	XCell Tempest Model-free	Model free reinforcement learning using differential dynamic programming (DDP)	Acrobatic maneuvers	Successful flights
Prasad: "Adaptive nonlinear controller synthesis and flight test evaluation on an unmanned helicopter" [146] GaTech	1999	Yamaha R-50 [33] Approximate linear model	Inner Loop Rate-Command/Attitude-Hold (RCAH): PD, First order command filter, NN adaptive element, approximate inversion. Outer loop trajectory tracking.	Take-off, anding, vertical climb, hover, forward & sideways flight, elliptical turn	Simulation of various maneuvers, Experimental RCAH with and without NN.

This work was supported in part by NSF CNS-1229236

6 References

[1] Pieter Abbeel and Adam Coates. An application of reinforcement learning to aerobatic helicopter flight. *Advances in Neural Information Processing Systems*, 19:1–8, 2007.

[2] Bilal Ahmed and Hemanshu R. Pota. Dynamic Compensation for Control of a Rotary wing UAV Using Positive Position Feedback. *Journal of Intelligent & Robotic Systems*, 61(1-4):43–56, October 2010.

[3] Bilal Ahmed, Hemanshu R. Pota, and Matt Garratt. Rotary wing UAV position control using backstepping. *2007 46th IEEE Conference on Decision and Control*, pages 1957–1962, 2007.

[4] Bilal Ahmed, Hemanshu R. Pota, and Matt Garratt. Flight control of a rotary wing UAV using backstepping. *International Journal of Robust and Nonlinear Control*, 2009.

[5] Frank Allgower, Rolf Findeisen, and Zoltan K. Nagy. Nonlinear model predictive control: From theory to application. *Journal of Chinese Institute of Chemical Engineers*, 35(3):299–315, 2004.

[6] N. Antequera, M. Santos, and J.M. de la Cruz. A Helicopter Control based on Eigenstructure Assignment. *2006 IEEE Conference on Emerging Technologies and Factory Automation*, pages 719–724, September 2006.

[7] M.C. Arlinghaus. *Autopilot Development for an RC Helicopter*. Master of science, Wright State University, 2009.

[8] Giulio Avanzini, Douglas Thomson, and Alberto Torasso. Model Predictive Control Architecture for Rotorcraft Inverse Simulation. *Journal of Guidance, Control, and Dynamics*, 36(1):207–217, January 2013.

[9] J.C. Avila Vilchis. *Modélisation et commande d'hélicoptère*. Phd thesis, INGP, 2001.

[10] J.C. Avila Vilchis, B. Brogliato, A. Dzul, and R. Lozano. Nonlinear modelling and control of helicopters. *Automatica*, 39(9):1583–1596, September 2003.

[11] Zhiqiang Bai, Peizhi Liu, Jinhua Wang, Xiongwen Hu, and Xinxin Zhao. Control system design of a small-scale unmanned helicopter. In *2010 IEEE International Conference on Control and Automation*, pages 1414–1417, June 2010.

[12] Martin Barczyk. *Nonlinear State Estimation and Modeling of a Helicopter UAV*. Phd thesis, University of Alberta, 2012.

[13] Martin Barczyk and A.F. Lynch. Control-oriented modeling of a helicopter UAV with a Bell-Hiller stabilizer mechanism. *American Control Conference (ACC)*, pages 313–320, 2013.

[14] M. Bejar, A. Isidori, L. Marconi, and R. Naldi. Robust Vertical/Lateral/Longitudinal Control of a Helicopter with Constant Yaw-Attitude. In *Proceedings of the 44th IEEE Conference on Decision and Control*, pages 6192–6197, 2005.

[15] Manuel Béjar, Anibal Ollero, and Federico Cuesta. Modeling and control of autonomous helicopters. *Advances in Control Theory and Applications*, 353/2007:1–29, 2007.

[16] Pascale Bendotti and J.C. Morris. Robust hover control for a model helicopter. In *Proceedings of 1995 American Control Conference*, volume 1, pages 682–687, 1995.

[17] J. G. Benitez-Morales, H. Rodriguez-Cortes, and R. Castro-Linares. A static feedback stabilizer for the longitudinal dynamics of a small scale helicopter including the rotor dynamics with stabilizer bar. *2013 International Conference on Unmanned Aircraft Systems (ICUAS)*, pages 634–641, May 2013.

[18] Marcel Bergerman, Omead Amidi, James Ryan Miller, Nicholas Vallidis, and Todd Dudek. Cascaded position and heading control of a robotic helicopter. In *2007 IEEE/RSJ International Conference on Intelligent Robots and Systems*, pages 135–140, October 2007.

[19] S. Bertrand, T. Hamel, and H. Piet-Lahanier. Stability analysis of an UAV controller using singular perturbation theory. In *Proceedings of the 17th World Congress The International Federation of Automatic Control*, pages 5706–5711, Seoul, Korea, 2008.

[20] Morten Bisgaard. *Modeling , Estimation , and Control of Helicopter Slung Load System*. Phd thesis, Aalborg University, 2007.

[21] A. R. S. Bramwell, David Balmford, and George Done. *Bramwell's helicopter dynamics*. Butterworth-Heinemann, 2nd edition, 2001.

[22] Agus Budiyono and Singgih S. Wibowo. Optimal Tracking Controller Design for a Small Scale Helicopter. *Journal of Bionic Engineering*, 4(4):271–280, December 2007.

[23] Yasir Awais Butt and Aamer Iqbal Bhatti. Robust altitude tracking of a helicopter using sliding mode control structure. *2012 International Conference on Emerging Technologies*, pages 1–7, October 2012.

[24] Guowei Cai, Biao Wang, Ben M. Chen, and Tong H. Lee. Design and Implementation of a Flight Control System for an Unmanned Rotorcraft using RPT Control Approach. *Asian Journal of Control*, 15(1):95–119, January 2013.

[25] A.J. Calise and R.T. Rysdyk. Nonlinear adaptive flight control using neural networks. *IEEE Control Systems Magazine*, 18(6):14–25, 1998.

[26] Pedro Castillo, Rogelio Lozano, and A.E. Dzul. *Modelling and Control of Mini-Flying Machines*. Springer, 2005.

[27] HaiYang Chao, YongCan Cao, and YangQuan Chen. Autopilots for small unmanned aerial vehicles: A survey. *International Journal of Control, Automation and Systems*, 8(1):36–44, February 2010.

[28] Robert T. N. Chen. A simplified rotor system mathematical model for piloted flight dynamics simulation. Technical Report A-7538; NASA-TM-78575, NASA, May 1979.

[29] Robert T. N. Chen. Effects of primary rotor parameters on flapping dynamics. Technical Report A-7777; NASA-TP-1431, NASA, January 1980.

This work was supported in part by NSF CNS-1229236

[30] Xianxiang Chen, Ying Liu, and Xiongwen Hu. Modeling and attitude control of the miniature unmanned helicopter. *Control Conference (CCC2013 32nd Chinese*, pages 2723–2726, 2013.

[31] R.P. Cheng, M.B. Tischler, and G.J. Schulein. RMAX Helicopter State-Spaec Model Identification fo Hober and Forward-Flight. *Journal of the American Helicopter Society*, pages 202–210, April 2006.

[32] Tinashe Chingozha, Otis Nyandoro, and Ayushi Malani. Low cost controller for small scale helicopter. *2013 IEEE 8th Conference on Industrial Electronics and Applications*, pages 439–444, June 2013.

[33] J.E. Corban, A.J. Calise, and J.V.R. Prasad. Implementation of adaptive nonlinear control for flight test on an unmanned helicopter. In *Proceedings of the 37th IEEE Conference on Decision and Control*, volume 4, pages 3641–3646, December 1998.

[34] John C. Craig. *Introduction to Robotics: Mechanics and Control*. Prentice Hall, 3rd edition, 2004.

[35] R. Cunha, C. Silvestre, and A. Pascoal. A path following controller for model-scale helicopters. *Proceedings of European Control Conference*, 2003.

[36] Konstantinos Dalamagkidis, Kimon P. Valavanis, and Les A. Piegl. Autonomous Autorotation of Unmanned Rotorcraft using Nonlinear Model Predictive Control. *Journal of Intelligent and Robotic Systems*, 57(1-4):351–369, September 2009.

[37] Konstantinos Dalamagkidis, Kimon P. Valavanis, and Les A. Piegl. Nonlinear Model Predictive Control With Neural Network Optimization for Autonomous Autorotation of Small Unmanned Helicopters. *IEEE Transactions on Control Systems Technology*, 19(4):818–831, July 2011.

[38] S. Datta, U.S. Patkar, and S. Majumder. Digital controller for attitude control of a rotary-winged flying robot in hover. *2009 IEEE International Symposium on Industrial Electronics*, pages 390–395, July 2009.

[39] Bernard Etkin and Lloyd Duff Reid. *Dynamics of Flight: Stability and Control*. John Wiley & Sons, Inc., 3rd edition, 1996.

[40] Caizhi Fan, Shengpeng Guo, Dongxu Li, and Yunhui Liu. Nonlinear predictive attitude control with a disturbance observer of an unmanned helicopter on the test bench. *2011 IEEE 5th International Conference on Robotics, Automation and Mechatronics (RAM)*, pages 304–309, September 2011.

[41] Jay A. Farrell. *Aided Navigation: GPS with High Rate Sensors*. McGraw-Hill, 2008.

[42] Emilio Frazzoli, M.A. Dahleh, and E. Feron. Trajectory tracking control design for autonomous helicopters using a backstepping algorithm. In *Proceedings of the 2000 American Control Conference*, volume 6, pages 4102–4107. American Autom. Control Council, June 2000.

[43] Jian Fu, W.H. Chen, and Qing-xian Wu. Sliding mode control for a miniature helicopter. *Automation and Computing (ICAC), 2011 17th International Conference on*, pages 98–103, 2011.

[44] Jyotirmay Gadewadikar, Frank Lewis, Kamesh Subbarao, and Ben M. Chen. Structured $\mathcal{H}_\infty$ Command and Control-Loop Design for Unmanned Helicopters. *Journal of Guidance, Control, and Dynamics*, 31(4):1093–1102, July 2008.

[45] Jyotirmay Gadewadikar, Frank L. Lewis, Kamesh Subbarao, Kemao Peng, and Ben M. Chen. $\mathcal{H}_\infty$ Static Output-feedback Control for Rotorcraft. *Journal of Intelligent and Robotic Systems*, 54(4):629–646, August 2008.

[46] Richard D. Garcia. *Designing an Autonomous Helicopter Testbed: From Conception Through Implementation.* Phd thesis, University of South Florida, 2008.

[47] Matt Garratt, Bilal Ahmed, and Hemanshu R. Pota. Platform Enhancements and System Identification for Control of an Unmanned Helicopter. In *2006 9th International Conference on Control, Automation, Robotics and Vision*, pages 1–6. IEEE, December 2006.

[48] Matthew Garratt and Sreenatha Anavatti. Non-linear Control of Heave for an Unmanned Helicopter Using a Neural Network. *Journal of Intelligent & Robotic Systems*, 66(4):495–504, September 2011.

[49] V Gavrilets. *Autonomous aerobatic maneuvering of miniature helicopters.* Phd thesis, Massachusetts Institute of Technology, 2003.

[50] V. Gavrilets, I. Martinos, B. Mettler, and E. Feron. Control logic for automated aerobatic flight of miniature helicopter. In *AIAA Guidance, Navigation, and Control Conference and Exhibit*, pages 1–8, Monterey, California, 2002.

[51] V. Gavrilets, B. Mettler, and E. Feron. Nonlinear model for a small-size acrobatic helicopter. *AIAA Guidance, Navigation, and Control Conference*, 2001.

[52] V. Gavrilets, B. Mettler, and E. Feron. Dynamic model for a miniature aerobatic helicopter. *Massachusetts Institute of Technology*, pages 1–22, 2003.

[53] Vladislav Gavrilets, Ioannis Martinos, Bernard Mettler, and Eric Feron. Aggressive Maneuvering Flight Tests of a Miniature Robotic Helicopter. In Bruno Siciliano and Paolo Dario, editors, *Experimental Robotics VIII*, volume 5 of *Springer Tracts in Advanced Robotics*, pages 456–465. Springer Berlin Heidelberg, June 2003.

[54] S.T. Glad and O. Harkegard. Backstepping control of a rigid body. In *Proceedings of the 41st IEEE Conference on Decision and Control, 2002.*, volume 4, pages 3944–3945. IEEE, 2002.

[55] Bryan Godbolt and A.F. Lynch. A novel cascade controller for a helicopter UAV with small body force compensation. *American Control Conference (ACC), 2013*, (2):1–6, 2013.

[56] Bryan Godbolt and Alan F. Lynch. Control-Oriented Physical Input Modelling for a Helicopter UAV. *Journal of Intelligent & Robotic Systems*, 73(1-4):209–217, October 2013.

[57] Bryan Godbolt and Alan F. Lynch. Model-Based Helicopter UAV Control: Experimental Results. *Journal of Intelligent & Robotic Systems*, 73(1-4):19–31, October 2013.

[58] Bryan Godbolt and Alan F. Lynch. Physical input modelling and identification for a helicopter UAV. *2013 International Conference on Unmanned Aircraft Systems (ICUAS)*, pages 890–896, May 2013.

[59] Bryan Godbolt, Nikolaos Vitzilaios, Chris Bergen, and Alan F. Lynch. Experimental validation of a helicopter autopilot: Time-varying trajectory tracking. *2013 International Conference on Unmanned Aircraft Systems (ICUAS)*, pages 392–397, May 2013.

[60] Bryan Godbolt, Nikolaos I. Vitzilaios, and Alan F. Lynch. Experimental Validation of a Helicopter Autopilot Design using Model-Based PID Control. *Journal of Intelligent & Robotic Systems*, 70(1-4):385–399, August 2012.

[61] Wolfgang von Grünhagen, Gerd Bouwer, Heinz-Jürgen Pausder, Fromhut enschel, and Jürgen Kaletka. A high bandwidth control system for a helicopter in-flight simulator. *International Journal of Control*, 59(1):239–261, January 1994.

[62] B.J. Guerreiro. Trajectory tracking $\mathcal{H}_2$ controller for autonomous helicopters: An application to industrial chimney inspection. *Automatic Control in Aerospace*, 17(1):431–436, June 2007.

[63] B.J. Guerreiro, C. Silvestre, R. Cunha, C. Cao, and N. Hovakimyan. $\mathcal{L}_1$ adaptive control for autonomous rotorcraft. In *American Control Conference, 2009. ACC '09.*, pages 3250–3255, 2009.

[64] Ulrik B. Hald and Mikkel V. Hesselbæk. Autonomous Helicopter Modelling and Control. Technical report, Aalborg University, 2005.

[65] Johnnie A. Ham, Charles K. Gardner, and Mark B. Tischler. Flight-Testing and Frequency-Domain Analysis for Rotorcraft Handling Qualities. *Journal of the American Helicopter Society*, 40(2):28, 1995.

[66] Peter G. Hamel and Jürgen Kaletka. Advances in rotorcraft system identification. *Progress in Aerospace Sciences*, 33(3-4):259–284, March 1997.

[67] Raymond S. Hansen. Toward a Better Understanding of Helicopter Stability Derivatives. *Journal of the American Helicopter Society*, 29(1):15, 1984.

[68] Y. Q. He and J. D. Han. Acceleration-Feedback-Enhanced Robust Control of an Unmanned Helicopter. *Journal of Guidance, Control, and Dynamics*, 33(4):1236–1250, July 2010.

[69] Yuebang He, Hailong Pei, Tairen Sun, and Hongbo Zhou. Modeling, identification and robust $\mathcal{H}_\infty$ static output feedback control of lateral dynamics of a miniature helicopter. *2011 IEEE 5th International Conference on Robotics, Automation and Mechatronics (RAM)*, pages 310–315, September 2011.

[70] R.K. Heffley and M.A. Mnich. Minimum-complexity helicopter simulation math model. Technical report, NASA, 1988.

[71] Robert K. Heffley. A Compilation and Analysis of Helicopter Handling Qualities Data: Volume Two, Data Analysis. Technical Report NASA-CR-3145; TR-1087-2, NASA, Aug 1979.

[72] Robert K. Heffley, Simon M. Bourne, Howard C. Curtiss, Jr., William S. Hindson, and Ronald A. Hess. Study of Helicopter Roll Control Effectiveness Criteria. Technical report, NASA, 1986.

[73] Robert K. Heffley, Wayne F. Jewell, John M. Lehman, and Richard A. Van Winkle. A Compilation and Analysis of Helicopter Handling Qualities Data: Volume 1, Data compilation. Technical Report NASA-CR-3144; TR-1087-1, NASA, August 1979.

[74] K.H. Hohenemser. Hingeless rotorcraft flight dynamics. 1974.

[75] P.A. Ioannou and Baris Fidan. *Adaptive Control Tutorial (Advances in Design and Control)*. SIAM, Society for Industrial and Applied Mathematics, 2006.

[76] P.A. Ioannou and J Sun. *Robust adaptive control*. Prentice Hall, 1996.

[77] A. Isidori, L. Marconi, and A. Serrani. *Robust Autonomous Guidance*. Springer US, Boston, MA, 2003.

[78] A. Isidori, L. Marconi, and A. Serrani. Robust nonlinear motion control of a helicopter. *IEEE Transactions on Automatic Control*, 48(3):413–426, March 2003.

[79] Shiyong Ji and Aiguo Wu. Study on dual-loop controller of helicopter based on the robust $\mathcal{H}_\infty$ loop shaping and mixed sensitivity. *2011 International Conference on Electrical and Control Engineering*, (2):1291–1294, September 2011.

[80] Zhe Jiang, Jianda Han, Yuechao Wang, and Qi Song. Enhanced LQR Control for Unmanned Helicopter in Hover. *2006 1st International Symposium on Systems and Control in Aerospace and Astronautics*, pages 1438–1443, 2006.

[81] Endra Joelianto, Edwina Maryami Sumarjono, Agus Budiyono, and Dini Retnaning Penggalih. Model predictive control for autonomous unmanned helicopters. *Aircraft Engineering and Aerospace Technology*, 83(6):375–387, 2011.

[82] E.N. Johnson and S.K. Kannan. Adaptive flight control for an autonomous unmanned helicopter. In *AIAA Guidance, Navigation, and Control Conference and Exhibit*, August 2002.

[83] Eric N. Johnson and Suresh K. Kannan. Adaptive Trajectory Control for Autonomous Helicopters. *Journal of Guidance, Control, and Dynamics*, 28(3):524–538, May 2005.

[84] B. Kadmiry and D. Driankov. A fuzzy flight controller combining linguistic and model-based fuzzy control. *Fuzzy Sets and Systems*, 146(3):313–347, September 2004.

[85] S.K. Kannan and E.N. Johnson. Adaptive trajectory based control for autonomous helicopters. In *Proceedings. The 21st Digital Avionics Systems Conference*, volume 2, pages 8D1–1 – 8D1–12. IEEE, 2002.

[86] Farid Kendoul. Survey of advances in guidance, navigation, and control of unmanned rotorcraft systems. *Journal of Field Robotics*, 29(2):315–378, 2012.

[87] Hassan L. Khalil. *Nonlinear Systems*. Prentice Hall, 3rd edition edition, 2001.

[88] H. Kim and D.H. Shim. A flight control system for aerial robots: algorithms and experiments. *Control Engineering Practice*, 11(12):1389–1400, December 2003.

[89] H.J. Kim, D.H. Shim, and S. Sastry. Nonlinear model predictive tracking control for rotorcraft-based unmanned aerial vehicles. In *Proceedings of the 2002 American Control Conference*, volume 5, pages 3576–3581, 2002.

[90] S.K. Kim. *Modeling, identification, and trajectory planning for a model-scale helicopter*. Phd thesis, The University of Michigan, 2001.

[91] S.K. Kim and D.M. Tilbury. Mathematical Modeling and Experimental Identification of a Model Helicopter. *AIAA Guidance, Navigation and Control Conference*, 1998.

[92] S.K. Kim and D.M. Tilbury. Mathematical Modeling and Experimental Identification of an Unmanned Helicopter Robot with Flybar Dynamics. *Journal of Robotic Systems*, 21(3):95–116, March 2004.

[93] T.J. Koo, Y. Ma, and S.S. Sastry. Nonlinear control of a helicopter based unmanned aerial vehicle model. Technical report, 2001.

[94] T.J. Koo and Shankar Sastry. Output tracking control design of a helicopter model based on approximate linearization. In *Proceedings of the 37th IEEE Conference on Decision and Control*, volume 4, pages 3635–3640. IEEE, December 1998.

[95] T.J. Koo and Shankar Sastry. Differential flatness based full authority helicopter control design. In *Proceedings of the 38th IEEE Conference on Decision and Control*, volume 2, pages 1982–1987. IEEE, December 1999.

[96] Markus Koslowski, Amr A. Kandil, and Essameddin Badreddin. Modeling and identification of a small-scale unmanned autonomous helicopter. *2012 IEEE/RSJ International Conference on Intelligent Robots and Systems*, pages 2160–2165, October 2012.

[97] Markus Koslowski, Amr A. Kandil, and Essameddin Badreddin. Platform description and system modelling for control of an unmanned helicopter. In *2012 6th IEEE INTERNATIONAL CONFERENCE INTELLIGENT SYSTEMS*, pages 391–396, September 2012.

[98] Kenallakopoulos Krstć, Mirslav, Ioannis, and Petar Kokotovic. *Nonlinear and Adaptive Control Design*. John Wiley & Sons, 1995.

[99] R. Kureeemun, D.J. Walker, B. Manimala, and M. Voskuijl. Helicopter Flight Control Law Design Using $\mathcal{H}_\infty$ Techniques. In *Proceedings of the 44th IEEE Conference on Decision and Control*, pages 1307–1312. IEEE, 2005.

[100] M. La Civita, G. papageorgiou, W.C. Messner, and T. Kanade. Design and Flight Testing of a High-Bandwidth $\mathcal{H}_\infty$ Loop Shaping Controller for a Robotic Helicopter. In *AIAA Guidance, Navigation, and Control Conference*, August 2002.

[101] M. La Civita, George Papageorgiou, W.C. Messner, and T. Kanade. Design and flight testing of a gain-scheduled $\mathcal{H}_\infty$ loop shaping controller for wide-envelope flight of a robotic helicopter. In *Proceedings of the 2003 American Control Conference, 2003.*, volume 5, pages 4195–4200. IEEE, 2003.

[102] Marco La Civita. *Integrated modeling and robust control for full-envelope flight of robotic helicopters*. Phd thesis, Carnegie Mellon Universiy, 2002.

[103] Marco La Civita. Design and Flight Testing of an $\mathcal{H}_\infty$ Controller for a Robotic Helicopter. *Journal of Guidance, Control and Dynamics*, 29(2):485 – 494, 2006.

[104] Dong Jin Lee and Hyochoong Bang. Model-free LQ control for unmanned helicopters using reinforcement learning. *Control, Automation and Systems (ICCAS), 2011 11th International Conference on*, (6):117–120, 2011.

[105] Dongjin Lee, Mooncheon Choi, and Hyochoong Bang. Model-free linear quadratic tracking control for unmanned helicopters using reinforcement learning. *The 5th International Conference on Automation, Robotics and Applications*, (3):19–22, December 2011.

[106] E.H. Lee, H. Shim, H. Park, and K.I. Lee. Design of hovering attitude controller for a model helicopter. *Proceedings of Society of Instrument and Control Engineers*, pages 1385–1389, 1993.

[107] F. Leonard, Adnan Martini, and Gabriel Abba. Robust Nonlinear Controls of Model-Scale Helicopters Under Lateral and Vertical Wind Gusts. *IEEE Transactions on Control Systems Technology*, 20(1):154–163, January 2012.

[108] J. Liang, T. Wang, C. Wang, Y. Zhang, and Y. Chen. Combined of vector field and linear quadratic Gaussian for the path following of a small unmanned helicopter. *IET Control Theory & Applications*, 6(17):2696–2703, November 2012.

[109] Cunjia Liu and Wen-Hua Chen. Hierarchical path planning and flight control of small autonomous helicopters using MPC techniques. In *2013 IEEE Intelligent Vehicles Symposium (IV)*, number Iv, pages 417–422, June 2013.

[110] Cunjia Liu, Wen-Hua Chen, and John Andrews. Piecewise constant model predictive control for autonomous helicopters. *Robotics and Autonomous Systems*, 59(7-8):571–579, July 2011.

[111] Cunjia Liu, Wen-Hua Chen, and John Andrews. Tracking control of small-scale helicopters using explicit nonlinear MPC augmented with disturbance observers. *Control Engineering Practice*, 20(3):258–268, March 2012.

[112] Cunjia Liu, W.H. Chen, and John Andrews. Explicit non-linear model predictive control for autonomous helicopters. *Proceedings of the Institution of Mechanical Engineers, Part G: Journal of Aerospace Engineering*, 226(9):1171–1182, November 2011.

[113] Lijun Liu, Yi Shen, and Earl H. Dowell. Integrated Adaptive Fault-Tolerant $mathcal H_\infty$ Output Feedback Control with Adaptive Fault Identification. *Journal of Guidance, Control, and Dynamics*, 35(3):881–889, May 2012.

[114] Romulus Lungu, Stefan Ispas, Mihaela Iancu, and Mihai Lungu. Optimal control of helicopter motion. *2012 International Conference on Applied and Theoretical Electricity (ICATE)*, (4):1–5, October 2012.

[115] R. Mahony, T. Hamel, and A. Dzul. Hover control via Lyapunov control for an autonomous model helicopter. In *Proceedings of the 38th IEEE Conference on Decision and Control*, volume 4, pages 3490–3495. IEEE, 1999.

This work was supported in part by NSF CNS-1229236

[116] Robert Mahony and Tarek Hamel. Robust trajectory tracking for a scale model autonomous helicopter. *International Journal of Robust and Nonlinear Control*, 14(12):1035–1059, August 2004.

[117] Panos Marantos, Leonidas Dritsas, and Kostas J. Kyriakopolos. Robust attitude control for an unmanned helicopter in near-hover flights. *2013 European Control Conference (ECC)*, pages 347–352, 2013.

[118] Panos Marantos, Leonidas Dritsas, and Kostas J. Kyriakopoulos. Robust $\mathcal{H}_2$ / $\mathcal{H}_\infty$ Position Tracking control of an Unmanned Helicopter for near-hover flights. *21st Mediterranean Conference on Control and Automation*, pages 161–166, June 2013.

[119] Lorenzo Marconi and Roberto Naldi. Robust full degree-of-freedom tracking control of a helicopter. *Automatica*, 43(11):1909–1920, nov 2007.

[120] Pedram Masajedi, Afshin Ghanbarzadeh, and Mohammad Shishesaz. Optimal Control Designing for a Discrete Model of Helicopter in Hover. *2012 International Conference on Control Engineering and Communication Technology*, pages 407–412, December 2012.

[121] Matthew D Mcewen, Russ Duren, E Roberts Wood, S Author, and D Matthew. *Dynamic System Identification and Modeling of a Rotary Wing UAV for Stability.* Master of science, Naval Postgraduate School, June 1998.

[122] Noorma Yulia Megawati, Salham Solikhatun, Endra Joelianto, and Agus Budiyono. Robust switched linear controller for multimode helicopter models. In *2011 2nd International Conference on Instrumentation Control and Automation*, number November, pages 152–156, November 2011.

[123] B. Mettler, V. Gavrilets, E. Feron, and T. Kanade. Dynamic compensation for high-bandwidth control of small-scale helicopter. *American Helicopter Society Specialist Meeting*, 2002.

[124] Bernard Mettler. *Identification Modeling and Characteristics of Miniature Rotorcraft.* Springer US, Boston, MA, 2003.

[125] Bernard Mettler, Takeo Kanade, and M.B. Tischler. System identification modeling of a model-scale helicopter. *Journal of the American Helicopter Society*, pages 1–25, 2000.

[126] Bernard Mettler, Mark B. Tischler, and Takeo Kanade. System identification of small-size unmanned helicopter dynamics. *Presented at the American Helicopter Society 55th Forum*, 1999.

[127] Bernard Mettler and M.B. Tischler. Attitude control optimization for a small-scale unmanned helicopter. In *AIAA Guidance, Navigation, and Control Conference and Exhibit*, 2000.

[128] Manfred Morari. Model predictive control: Multivariable control technique of choise in the 1990s? In *Advances in Model-Based Predictive Control.*

This work was supported in part by NSF CNS-1229236

[129] J.C. Morris, M. van Nieuwstadt, and P. Bendotti. Identification and control of a model helicopter in hover. In *Proceedings of 1994 American Control Conference*, volume 2, pages 1238–1242, 1994.

[130] Roberto Naldi. *Prototyping , Modeling and Control of a Class of VTOL Aerial Robots*. PhD thesis, University of Bologna, 2008.

[131] Arbab Nighat Khizer, Dai Yaping, Syed Amjad Ali, and Xu Xiang Yang. Takagi-Sugeno Fuzzy Model Identification for Small Scale Unmanned Helicopter. *TELKOMNIKA Indonesian Journal of Electrical Engineering*, 12(1), January 2014.

[132] Parviz E. Nikravesh. *Computer-Aided Analysis of Mechanical Systems*. Prentice Hall, 1988.

[133] David Nodland, Hassan Zargarzadeh, and Sarangapani Jagannathan. Neural Network-Based Optimal Adaptive Output Feedback Control of a Helicopter UAV. *IEEE Transactions on Neural Networks and Learning Systems*, 24(7):1061–1073, July 2013.

[134] T. Oktay. *Constrained control of complex helicopter models*. Phd thesis, Virginia Polytechnic Institute and State University, 2012.

[135] Tugrul Oktay and Cornel Sultan. Constrained predictive control of helicopters. *Aircraft Engineering and Aerospace Technology*, 85(1):32–47, 2013.

[136] Tugrul Oktay and Cornel Sultan. Simultaneous Helicopter and Control-System Design. *Journal of Aircraft*, 50(3):911–925, May 2013.

[137] Aníbal Ollero and Luís Merino. Control and perception techniques for aerial robotics. *Annual Reviews in Control*, 28(2):167–178, January 2004.

[138] Gareth D Padfield. *Helicopter Flight Dynamics*. Blackwell Publishing Ltd, Oxford, UK, January 2007.

[139] Yue Pan, Ping Song, and Kejie Li. PID Control of Miniature Unmanned Helicopter Yaw System based on RBF Neural Network. *Intelligent computing and Information Science*, pages 308–313, 2011.

[140] Kemao Peng, Guowei Cai, Ben M. Chen, Miaobo Dong, and Tong Lee. Comprehensive Modeling and Control of the Yaw Dynamics of a UAV Helicopter. *2006 Chinese Control Conference*, pages 2087–2092, August 2006.

[141] Kemao Peng, Dong Miaobo, Ben M. Chen, Guowei Cai, Lum Kai-Yew, and Tong H. Lee. Design and Implementation of a Fully Autonomous Flight Control System for a UAV Helicopter. *2007 Chinese Control Conference*, pages 662–667, July 2007.

[142] J.K. Pieper, S. Baillie, and K.R. Goheen. Linear-quadratic optimal model-following control of a helicopter in hover. In *Proceedings of 1994 American Control Conference - ACC '94*, volume 3, pages 3470–3474, June 1994.

[143] Ian Postlethwaite, Emmanuel Prempain, Ercument Turkoglu, Matthew C. Turner, Kris Ellis, and A.W. Gubbels. Design and flight testing of various controllers for the Bell 205 helicopter. *Control Engineering Practice*, 13(3):383–398, March 2005.

[144] Hemanshu R. Pota, Bilal Ahmed, and Matt Garratt. Velocity Control of a UAV using Backstepping Control. *Proceedings of the 45th IEEE Conference on Decision and Control*, pages 5894–5899, 2006.

[145] Wisnu Adi Pradana, Endra Joelianto, Agus Budiyono, and Widyawardana Adiprawita. Robust MIMO Integral-Backstepping PID Controller for Hovering Control of Unmanned Model Helicopter. *Journal of Aerospace Engineering*, 24(4):454–462, October 2011.

[146] J.V.R. Prasad, A.J. Calise, Y. Pei, and J.E. Corban. Adaptive nonlinear controller synthesis and flight test evaluation on an unmanned helicopter. *Proceedings of the 1999 IEEE International Conference on Control Applications*, 1:137–142, 1999.

[147] Raymond W. Prouty. *Helicopter Performance, Stability and Control*. Krieger Publishing Company, 1995.

[148] Ioannis A. Raptis and Kimon P. Valavanis. *Linear and nonlinear control of small-scale unmanned helicopters*. Intelligent Systems, Control and Automation: Science and Engineering. Springer Netherlands, 2011.

[149] Ioannis A. Raptis and Kimon P. Valavanis. Velocity and heading tracking control for small-scale unmanned helicopters. In *American Control Conference (ACC), 2011*, pages 1579–1586, 2011.

[150] Ioannis A. Raptis, Kimon P. Valavanis, and Wilfrido A. Moreno. System Identification and Discrete Nonlinear Control of Miniature Helicopters Using Backstepping. *Journal of Intelligent and Robotic Systems*, 55(2-3):223–243, December 2008.

[151] Ioannis A. Raptis, Kimon P. Valavanis, and George J. Vachtsevanos. Linear Tracking Control for Small-Scale Unmanned Helicopters. *IEEE Transactions on Control Systems Technology*, 20(4):995–1010, July 2012.

[152] Beibei Ren, Shuzhi Sam Ge, Chang Chen, Cheng-Heng Fua, and Tong Heng Lee. *Modeling, Control and Coordination of Helicopter Systems*. Springer New York, 2012.

[153] Ahmad Safaee and Hamid D. Taghirad. System identification and robust controller design for the autopilot of an unmanned helicopter. *2013 9th Asian Control Conference (ASCC)*, pages 1–6, June 2013.

[154] Mahendra Kumar Samal, Matthew Garratt, Hemanshu Pota, and Hamid Teimoori. Model predictive flight controller for longitudinal and lateral cyclic control of an unmanned helicopter. *2012 2nd Asutralian Control Conference*, (November):386–391, 2012.

[155] Edgar N. Sanchez, Hector M. Becerra, and Carlos M. Velez. Combining fuzzy, PID and regulation control for an autonomous mini-helicopter. *Information Sciences*, 177(10):1999–2022, May 2007.

[156] C.P. Sanders, P.A. DeBitetto, E. Feron, H.F. Vuong, and N. Leveson. Hierarchical control of small autonomous helicopters. In *Proceedings of the 37th IEEE Conference on Decision and Control*, volume 4, pages 3629–3634, 1998.

[157] Luis A. Sandino, Manuel Bejar, Konstantin Kondak, and Anibal Ollero. Improving hovering performance of tethered unmanned helicopters with nonlinear control strategies. *2013 International Conference on Unmanned Aircraft Systems (ICUAS)*, pages 443–452, May 2013.

[158] Christopher Sconyers, Ioannis A. Raptis, and George J. Vachtsevanos. Rotorcraft control and trajectory generation for target tracking. In *2011 19th Mediterranean Conference on Control & Automation (MED)*, pages 1235–1240, June 2011.

[159] H. Shim, T.J. Koo, F. Hoffmann, and S. Sastry. A comprehensive study of control design for an autonomous helicopter. In *Proceedings of the 37th IEEE Conference on Decision and Control*, volume 4, pages 3653–3658, 1998.

[160] Hyunchul D. Shim. *Hierarchical Flight Control System Synthesis for Rotorcraft-based Unmanned Aerial Vehicles*. Phd thesis, University of California, Berkeley, 2000.

[161] Hyunchul D. Shim and S. Sastry. Control system design for rotorcraft-based unmanned aerial vehicles using time-domain system identification. In *Proceedings of the 2000. IEEE International Conference on Control Applications. Conference Proceedings*, pages 808–813. IEEE, 2000.

[162] Jinok Shin, Kenzo Nonami, Daigo Fujiwara, and Kensaku Hazawa. Model-based optimal attitude and positioning control of small-scale unmanned helicopter. *Robotica*, 23(1):51–63, January 2005.

[163] S. Sieberling, Q. P. Chu, and J. A. Mulder. Robust Flight Control Using Incremental Nonlinear Dynamic Inversion and Angular Acceleration Prediction. *Journal of Guidance, Control, and Dynamics*, 33(6):1732–1742, November 2010.

[164] Simone, Duranti. In-flight identification of the augmented flight dynamics of the RMAX unmanned helicopter. In Houria, Siguerdidjane, editor, *17th IFAC Symposium on Automatic Control in Aerospace*, pages 217–222, June 2007.

[165] P. Simplício, M.D. Pavel, E. van Kampen, and Q.P. Chu. An acceleration measurements-based approach for helicopter nonlinear flight control using Incremental Nonlinear Dynamic Inversion. *Control Engineering Practice*, 21(8):1065–1077, August 2013.

[166] H. Sira-Ramirez. Dynamical sliding mode control approach for vertical flight regulation in helicopters. In *IEEE Proceedings - Control Theory and Applications*, volume 141, page 19, 1994.

[167] Hebertt Sira-Ramirez, Rafael Castro-Linares, and Eduardo Liceaga-Castro. A Liouvillian systems approach for the trajectory planning-based control of helicopter models. *International Journal of Robust and Nonlinear Control*, 10(4):301–320, April 2000.

[168] Dalei Song, Jianda Han, and Guangjun Liu. Active Model-Based Predictive Control and Experimental Investigation on Unmanned Helicopters in Full Flight Envelope. *IEEE Transactions on Control Systems Technology*, 21(4):1502–1509, July 2013.

[169] Dalei Song, Juntong Qi, Jianda Han, and Guangjun Liu. Active model based predictive control for unmanned helicopter in full flight envelope. *2010 IEEE/RSJ International Conference on Intelligent Robots and Systems*, pages 616–621, October 2010.

[170] Mark W. Spong, Seth Hutchinson, and M. Vidyasagar. *Robot Modeling and Control*. Wiley, 2005.

[171] X-D. Sun and T. Clarke. Application of μ / $\mathcal{H}_\infty$ Control to Modern Helicopters. In *International Conference on Control '94*, pages 1532–1537. IEEE, 1994.

[172] H.Y. Sutarto, Agus Budiyono, Endra Joelianto, and Go Tiauw Hiong. Switched Linear Control of a Model Helicopter. *2006 9th International Conference on Control, Automation, Robotics and Vision*, pages 1–8, 2006.

[173] Satoshi Suzuki. Low accuracy sensor-based navigation and fully autonomous guidance control of small electric helicopter. *2011 IEEE International Conference on Robotics and Automation*, pages 4442–4448, May 2011.

[174] Satoshi Suzuki. Automatic Take-Off and Landing Control for Small Unmanned Helicopter. In *Robot Intelligence Technology and Applications 2012*, volume 208 of *Advances in Intelligent Systems and Computing*, pages 155–167. Springer Berlin Heidelberg, 2013.

[175] Satoshi Suzuki, Daisuke Nakazawa, Kenzo Nonami, and Makoto Tawara. Attitude Control of Small Electric Helicopter by Using Quaternion Feedback. *Journal of System Design and Dynamics*, 5(2):231–247, 2011.

[176] M. Svanfeldt. *Design of the hardware platform for the flight control system in an unmanned aerial vehicle*. PhD thesis, Linköping University, 2010.

[177] Skander Taamallah, Xavier Bombois, and Paul Van Den Hof. Optimal Control For Power-Off Landing Of A Small-Scale Helicopter A Pseudospectral Approach. *2012 American Control Conference*, pages 914–919, 2012.

[178] P.D. Talbot, B.E. Tinling, W.A. Decker, and R.T.N. Chen. A mathematical model of a single main rotor helicopter for piloted simulation. (September), 1982.

[179] Jie Tang, Chen Wei, and Fan Yang. Static $\mathcal{H}_\infty$ Loop-Shaping Control for Unmanned Helicopter. *Proceedings of the 10th World Congress on Intelligent Control and Automation*, pages 2882–2886, 2012.

[180] K. Tang, B. Wang, W. Kang, and B. Chen. Minimum time control of helicopter UAVs using computational dynamic optimization. *2011 9th IEEE International Conference on Control and Automation (ICCA)*, pages 848–852, December 2011.

[181] Shuai Tang, Li Zhang, and ZhiQiang Zheng. Adaptive height and attitude control of small-scale unmanned helicopter. *2013 25th Chinese Control and Decision Conference (CCDC)*, pages 1–6, May 2013.

[182] Gang Tao. *Adaptive Control Design and Analysis*. Wiley-IEEE Press, 2003.

[183] Hamid Teimoori, Hemanshu R. Pota, Matt Garratt, and Mahendra K. Samal. Planar trajectory tracking controller for a small-sized helicopter considering servos and delay constraints. *IECON 2011 - 37th Annual Conference of the IEEE Industrial Electronics Society*, pages 681–686, November 2011.

[184] Hamid Teimoori, Hemanshu R. Pota, Matt Garratt, and Mahendra K. Samal. Helicopter flight control using inverse optimal control and backstepping. In *2012 12th International Conference on Control Automation Robotics & Vision (ICARCV)*, volume 2012, pages 978–983, December 2012.

[185] Hamid Teimoori and H.R. Pota. Attitude control of a miniature helicopter using optimal sliding mode control. *2012 2nd Australian Control Conference*, (November):295–300, 2012.

[186] M.B. Tischler. System identification methods for aircraft flight control development and validation. *Advances in Aircraft Flight Control*, 1996.

[187] M.B. Tischler and M.G. Cauffman. Frequency-response method for rotorcraft system identification: Flight applications to BO 105 coupled rotor/fuselage dynamics. *Journal of the American Helicopter Society*, 37(3 July):3–17, 1992.

[188] Ching-Chih Tsai, Chi-Tai Lee, and Kao-Shing Hwang. Intelligent adaptive trajectory tracking control using fuzzy basis function networks for an autonomous small-scale helicopter. *2011 IEEE International Conference on Systems, Man, and Cybernetics*, pages 2255–2260, October 2011.

[189] Vincent Verdult, Marco Lovera, and Michel Verhaegen. Identification of linear parameter-varying state-space models with application to helicopter rotor dynamics. *International Journal of Control*, 77(13):1149–1159, September 2004.

[190] Guanlin Wang, Jihong Zhu, Chengxu Yang, and H Xia. System identification for helicopter yaw dynamic modelling. In *2011 3rd International Conference on Computer Research and Development*, pages 54–57, March 2011.

[191] Jun Wang, Hailong Pei, Weizhou Su, and Yuebang He. A gust-attenuation robust $\mathcal{H}_\infty$ output-feedback control design for unmanned autonomous helicopters. *American Control Conference (ACC), 2012*, pages 3260–3265, 2012.

[192] Xiafu Wang, You Chen, Geng Lu, and Yisheng Zhong. Robust attitude tracking control of small-scale unmanned helicopter. *International Journal of Systems Science*, 00(0):1–14, August 2013.

[193] Xiafu Wang, You Chen, Geng Lu, and Yisheng Zhong. Robust flight control of small-scale unmanned helicopter. *Control Conference (CCC), 2013 32nd Chinese*, pages 2700–2705, 2013.

[194] Xiaodong Wang and Xiaoguang Zhao. A practical survey on the flight control system of small-scale unmanned helicopter. *2008 7th World Congress on Intelligent Control and Automation*, pages 364–369, 2008.

[195] Xiaoyan Wang, Xinmin Wang, and Congchao Yao. Design of hovering altitude holding control system for helicopter. In *2012 IEEE International Conference on Information and Automation*, number June, pages 180–183, June 2012.

[196] Martin F. Weilenmann and Hans P. Geering. Test bench for rotorcraft hover control. *Journal of Guidance, Control, and Dynamics*, 17(4):729–736, July 1994.

[197] M.F. Weilenmann, U. Christen, and H.P. Geering. Robust helicopter position control at hover. In *Proceedings of 1994 American Control Conference - ACC '94*, volume 3, pages 2491–2495. IEEE, 1994.

[198] Xiaohu Xia and Yunjian Ge. Finite-horizon optimal linear control for autonomous soft landing of small-scale helicopter. In *The 2010 IEEE International Conference on Information and Automation*, pages 1160–1164, June 2010.

[199] Ciann-dong Yang and Wen-hsiung Liu. Nonlinear $\mathcal{H}_\infty$ Decoupling Hover Control Of Helicopter With Parameter Uncertainties. *Proceedings of the American Control Conference*, pages 3454–3459, 2003.

[200] Xilin Yang, Matt Garratt, and Hemanshu Pota. Flight validation of a feedforward gust-attenuation controller for an autonomous helicopter. *Robotics and Autonomous Systems*, 59(12):1070–1079, December 2011.

[201] Ilkay Yavrucuk and J.V.R. Prasad. Online Dynamic Trim and Control Limit Estimation. *Journal of Guidance, Control, and Dynamics*, 35(5):1647–1656, September 2012.

[202] Lin Zhang and Zhengtao Ding. Nonlinear control design and stability analysis of a small-scale unmanned helicopter. In *2013 10th IEEE International Conference on Control and Automation (ICCA)*, pages 1662–1667, June 2013.

[203] Bing Zhu and Wei Huo. Adaptive backstepping control for a miniature autonomous helicopter. *IEEE Conference on Decision and Control and European Control Conference*, (1):5413–5418, December 2011.